ABSOLUTE INFRARED INTENSITIES OF THE CYANATE ION IN KCl, KBr and KI LATTICE ENVIRONMENT

by

KALKUNTE SRINIVASA IYENGAR SESHADRI

A THESIS

submitted to

OREGON STATE COLLEGE

in partial fulfillment of
the requirements for the
degree of

DOCTOR OF PHILOSOPHY

June 1960

APPROVED:

Redacted for Privacy

Professor of Chemistry

In Charge of Major

Redacted for Privacy

Chairman of Department of Chemistry

Redacted for Privacy

Chairman of School Graduate Committee

Redacted for Privacy

Dean of Graduate School

Date thesis is presented Nov 6, 1959.

Typed by Lilah N. Potter

ACKNOWLEDGMENT

I am highly indebted to Dr. J. C. Decius for his cordial and illuminating guidance throughout this work, without which this work would not have been possible.

My warm thanks are due to Dr. E. C. Gilbert for his keen interest in me during my graduate study.

I am grateful to my fellow graduate students for their cooperation and above all for their brotherly affection which made my stay in this country extremely pleasant. I will be failing in my duty if I do not make special mention of Dr. A. Maki for placing at my disposal a large number of single crystals; Dr. D. N. Montan, Mr. J. V. Martinez, Mr. Wayne Woodmansee and Dr. Otto Kalman for their helpful discussion.

This work in part was supported by Sloane Foundation, which is gratefully acknowledged.

My sincere thanks are due to Mrs. L. Potter for her careful typing.

TABLE OF CONTENTS

		Page
I	INTRODUCTION	1
II	THEORY	4
	Law of Absorption	4
	Light and Matter	5
	Shape and Intensity of Infrared Bands	17
	Normal Coordinate Calculations: GF Matrix	34
	Fermi Resonance	48
	Electrostatic Phenomena in a Dielectric	52
III	PREVIOUS INTENSITY WORK	58
IV	SPECTRUM OF CYANATE ION	71
V	EXPERIMENTAL PROCEDURE AND RESULTS	74
	Spectrophotometry	74
	Analysis of Crystals	76
	Integrated Intensity	84
	Wilson-Wells Extrapolation Method	87
	Triangular Slit Transform Method	87
	Zero Slit Extrapolation Method	93
	Bending Mode	94
	CO Stretch (Fermi Doublet)	94
	CN Stretch	100
	Dipole Moment and its Derivatives	106
	Dipole Moment Derivative with Respect to Q_3	107
	Dipole Moment Derivative with Respect to Q_1	107
	Dipole Moment Derivative with Respect to Internal Coordinates	112
VI	DISCUSSION	122
	BIBLIOGRAPHY	149
	APPENDIX I	154
	APPENDIX II	158
	APPENDIX III	174

LISTS OF FIGURES

	Page
Figure 1	30
Figure 2	134
Figure 3	135
Figure 4	136
Figure 5	137
Figure 6	138
Figure 7	139
Figure 8	140
Figure 9	141
Figure 10	142
Figure 11	143
Figure 12	144
Figure 13	145
Figure 14	146
Figure 15	147
Figure 16	148
Figure 17	125

LIST OF TABLES

Table 1	62
Table 2	63
Table 3	63
Table 4	65
Table 5	65
Table 6	67
Table 7	73
Table 8	85
Table 9	91
Table 10	95
Table 11	97
Table 12	98
Table 13	101

LIST OF TABLES - Cont.

	Page
Table 14	104a
Table 15	106
Table 16	107
Table 17	111
Table 18	112
Table 19	113
Table 20	118
Table 21	121
Table 22	133
Table 23	171
Table 24	173

ABSOLUTE INFRARED INTENSITIES OF THE CYANATE ION IN KCl, KBr, AND KI LATTICE ENVIRONMENT

I. INTRODUCTION

In the early part of this century rapid developments in the field of quantum mechanics led to the study of intensities of spectral lines in atomic systems. It was realized by E. C. Kemble at about 1927 that similar studies could be done in molecular systems too and thus originated a new branch in the domain of molecular spectroscopy. During this period three papers appeared, which are purely of historical interest. But, unfortunately further progress was checked, perhaps due to the unavailability of high resolving power instrument and lack of clear understanding of the subject.

This situation continued till the publication of the classical paper by Wilson and Wells (49), in which is enunciated an extrapolation theorem (Appendix I) which gave an impetus for further development. Since then considerable amount of work has been done and in a short period of thirteen years it has reached its adolescence.

The applications of this field are many in number. One of the simple applications is in quantitative analysis. Analytical chemists usually use the

peak intensity in their quantitative analysis by optical methods, which is conditioned by instrumental factors and which does not take into account the structural features of the molecule. But true integrated band intensity is free from instrumental errors and is dependent on structural features of the molecule.

Accurate knowledge of molecular properties of gases in the atmosphere is becoming increasingly important. Their abundance and the heat transfer that takes place between them and the atmosphere can be obtained by the study of absolute intensities. Unfortunately Wilson's method is not applicable to the study of gases at atmospheric pressure, since his extrapolation theorem presupposes that the gas should be at elevated pressure. But using high dispersion spectrometer, the intensity of individual rotational lines can be measured. Such work has been carried out by Leo Golberg et al. and Goody and Wormel (8, 10). Study of the intensity of $2\nu_3$ band of methane at 1·666μ and that of nitrous oxide with dry air as foreign gas at 7.8 and 8.6μ has been carried out.

It is to be pointed out here that absolute intensity data cannot be obtained theoretically. Theoretical values can only be relative and resort to experimental method is necessary to get absolute values.

More important than these two applications is the determination of polar properties of the molecule. The intensity of absorption is determined by the change in dipole moment with respect to displacement of atoms during vibration. If the intensities of all normal modes are studied, the dipole-moment of the molecule and the derivative with respect to internal coordinate can be evaluated. In addition if the same study is made with isotopic molecule, the band moments can be evaluated. This has been at present the chief aim of this field.

Most of the work that has been done is in the gaseous phase. Recently it has been extended to the condensed phase, mainly liquids. This is one of the early works in which the study has been extended to solid phase.

II. THEORY

a) Law of Absorption

For a monochromatic light the law of absorption is given by the relation

$$\alpha(\omega) = \frac{1}{nl} \cdot \ln \frac{I_o}{I} (\omega)$$

where $\alpha(\omega)$ is the absorption coefficient which is a function of frequency of radiation, nl is molar concentration/cm^2, I_o and I are the intensities of incident and transmitted light respectively. A quantity A', called absolute integrated molar absorption coefficient, is defined as

$$A' = \int \alpha(\omega) d \ln \omega$$

$$= \frac{1}{nl} \int \ln \frac{I_o}{I} d \ln \omega \qquad (1)$$

In actual practice, the instrument does not measure the true intensity of incident and transmitted radiation, but something less. If T_o and T represent the actual values of intensity of incident and transmitted radiation, a different quantity B', called apparent integrated molar absorption coefficient is defined as

$$B' = \frac{1}{nl} \int \ln \frac{T_o}{T} \, d\ln \omega$$

It is shown in Appendix I that $B' \rightarrow A'$ as $nl \rightarrow 0$. So from a series of experimental measurements of B at different values of nl and by extrapolating to zero nl, the quantity A' can be obtained.

b) Light and Matter

To relate A' to the polar properties of the molecule, the interaction of light and matter on the basis of quantum mechanics has to be considered.

Let $\Psi_0^0, \Psi_1^0, \Psi_2^0 \text{----} \Psi_n^0$ represent the wave function of the stationary states in an unperturbed molecular system. If it is subjected to the perturbation of electromagnetic radiation, the electric field acting on the molecule, which is the same in all directions since the wave length of radiation is large compared to the size of the molecule, is

$$E_x = 2E_o(\nu) \cos \omega t$$

If H^o is the Hamiltonian for the unperturbed system, the Hamiltonian for the actual system is

$$H + H'$$

where

$$H' = E_x \sum_j e_j x_j$$

where e_j is the charge on the jth particle and x_j is the x component of the jth particle.

The wave function of the perturbed system can be expressed as a linear combination of unperturbed wave functions

$$\Psi = \sum_n a_n(t) \Psi_n^o$$

where both Ψ and Ψ^o's are coordinate and time dependent while the coefficients are only time dependent. The coefficients are such that they satisfy the wave equation

$$(H^o + H')\Psi = -\frac{h}{2\pi i} \frac{\partial \Psi}{\partial t} \qquad \text{and}$$

$$\sum_n a_n^* a_n = 1$$

By quantum mechanical procedure it can be shown that (33, p. 303)

$$a_m(t) = (\mu_x)_{n'n''} E^o{}_x(\nu) \left[\frac{1-e^{2\pi i(\nu_{n'n''}+\nu)t}}{2\pi(\nu_{n'n''}+\nu)} - \frac{1-e^{2\pi i(\nu_{n'n''}-\nu)}}{2\pi(\nu_{n'n''}-\nu)} \right] \qquad (2)$$

where ν is the frequency of radiation, $\nu_{n'n''}$ is the natural frequency of molecular system, and $(\mu_x)_{n'n''}$ is the matrix element of dipole moment. In the case of absorption, it is the second term that is important, while in the case of induced emission the first term plays the same rule. So the probability of transition is obtained by multiplying equation (2) without the first term by its complex conjugate and utilizing the relationship

$$\cos x = \frac{e^{ix} + e^{-ix}}{2}$$

$$a_m{}^*(t)\, a_m(t) = 4(\mu_x)^2_{n'n''} \left| E_x(\nu) \right|^2 \frac{\sin^2 \pi(\nu_{n'n''}-\nu)t}{(\nu_{n'n''}-\nu)^2}$$

This expression takes into consideration only single frequency and it is necessary, to be in conformity with actual practice, to integrate this over a frequency interval, usually between $+\infty$ and $-\infty$. $E^o{}_x(\nu)$ can be

replaced by $E^{o}_{x}(\nu_{n'n''})$, since most of the contribution to the integrand comes from the frequency interval near the central frequency.

$$\int_{-\infty}^{\infty} \frac{\sin^2 x}{x^2}\, dx = \pi$$

So

$$a_m^*(t)\, a_m(t) = \frac{4\pi^2}{h^2} (\mu_x)^2_{n'n''} \left| E^{o}_{x} (\nu_{n'n''}) \right|^2 t$$

But

$$\left| E^{o}_{x} (\nu_{n'n''}) \right|^2 = \frac{4\pi \rho(\nu)}{6}$$

where $\rho(\nu)$ is energy density. So the transition probability per unit time becomes

$$\frac{8\pi^3}{3h^2} (\mu_x)^2_{n'n''} \rho(\nu)$$

Since radiation passes through the molecule in all directions, expressions for y and z directions have also to be considered which are similar. So

$$a_m^*(t)\, a_m(t) = \frac{8\pi^3}{3h^2} \left[(\mu_x)^2_{n'n''} + (\mu_y)^2_{n'n''} + (\mu_z)^2_{n'n''} \right] \rho\,(\nu)$$

and Einstein transition probability is

$$B_{n'\to n''} = \frac{8\pi^3}{3h^2} \left[(\mu_x)^2_{n'n''} + (\mu_y)^2_{n'n''} + (\mu_z)^2_{n'n''} \right] \qquad (3)$$

Since $(\mu_x)_{n'n''}$ is an element of a Hermitian matrix,

$$B_{n'\to n''} = B_{n''\to n'}$$

ie, Einstein probability of absorption is the same as Einstein probability of induced emission.

The decrease in the intensity of radiation per unit area and per unit time traversing a path length l of absorbing material is (50, p. 162)

$$-dI = \alpha\, I\, dl \qquad (4)$$

This can be expressed in terms of Einstein transition probability and a relationship between integrated intensity and $(\partial\mu/\partial Q)$ can be arrived at.

It is seen above that $B_{n'n''}\rho(\nu_{n'n''})$ is transition probability for the transition between levels n" and n', when the molecule is perturbed by radiation of density $\rho(\nu_{n'n''})$. If $N_{n'}$ and $N_{n''}$ are the population in states n' and n" respectively, the net rate of transition is

$$(B_{n''n'} N_{n''} - B_{n'n''} N_{n'}) \rho(\nu_{n'n''})$$
$$= B_{n'n''} (N_{n''} - N_{n'}) \rho(\nu_{n'n''})$$

Consequently the decrease in intensity per an infinitesimal path length is

$$-dI = B_{n'n''} (N_{n''} - N_{n'}) \rho(\nu_{n'n''}) h\nu_{n'n''} dl$$

Comparing this with equation (4) and making use of the relation (3)

$$\alpha = \frac{8\pi^3}{3hc} \nu_{n'n''} (N_{n''} - N_{n'}) \left[|\mu_x|^2 + |\mu_y|^2 + |\mu_z|^2 \right]$$

Since absorption of radiation extends over a frequency range, it is more realistic to replace α by $\int \alpha(\nu)\, d\nu$ so

$$\int \alpha(\nu)\, d\nu = \frac{8\pi^3}{3hc}\, \nu_{n'n''}\, (N_{n''} - N_{n'}) \sum_F |\mu_F|^2$$

$$F = x, y, z$$

Absorption of radiation by the molecule results in the change of both rotational and vibrational quantum number and so it is necessary to sum the intensity over all such transitions. The total wave function of the molecule can be separated into vibrational and rotational parts

$$\psi = \psi_v \psi_R$$

$$\sum_F |\mu_F|^2 = \sum_F \left| \int \psi_{v'} \psi_{R'} \mu_F \psi_{v''} \psi_{R''} d\tau \right|^2$$

$$u_F = \sum_g \mu_g \Phi_{Fg}$$

$$\sum_F (\mu_F)_{v'R'v''R''} = \sum_F \int \psi_{v'} \psi_{R'} \sum_g \mu_g \Phi_{Fg} \psi_{v''}$$

$$\psi_{R''} \, d\tau$$

$$= \sum_F \int \psi_{v'} \sum_g \mu_g \psi_{v''} \, d\tau_v$$

$$\int \psi_{R'} \sum_g \Phi_{Fg} \psi_{R''} \, d\tau_R$$

$$= \sum_F \sum_g \int \psi_{v'} \mu_g \psi_{v''} \, d\tau_v$$

$$\int \psi_{R'} \Phi_{Fg} \psi_{R''} \, d\tau_R$$

$$= \sum_F \sum_g (\mu_g)_{v'v''} (\Phi_{Fg})_{R'R''}$$

$$\sum_{F} |\mu_F|^2_{v'R',\ v''R''}$$

$$= \sum_{F} \sum_{g} \sum_{g'} (\mu_{g^*})_{v'v''} (\mu_{g'})_{v'v''} (\Phi_{Fg^*})_{R'R''} (\Phi_{Fg'})_{R'R''}$$

Further reduction of the expression for the integrated intensity which would be obtained upon substitution of the above result in the formula at the top of page 11, requires some assuptions about the summation over all rotational lines (R' → R") in the given vibration-rotation band. It has been shown (50, p. 164) that on account of the nearly classical nature of the distribution of molecules amongst the rotational states, the integrated intensity after summation over all rotational transitions effectively allows one to replace the sum of squares of components of μ in laboratory axes by

$$\sum_{g} (\mu_g)^2_{v'v''}$$

This derivation, which is applicable to a gas, is also applicable to solid phase. Details are discussed in Appendix II.

$$\int \alpha(\nu)\, d\nu = \frac{8\pi^3}{3hc}(N_{n''} - N_{n'}) \sum_g (\mu_g)^2_{v'v''}$$

$\vec{\mu_g}$ is a function of normal coordinates and can be expanded in terms of normal coordinate in a Taylor series.

$$\vec{\mu_g} = \mu_g(Q_1, Q_2, \text{----} Q_k \text{----})$$

$$\vec{\mu_g} = (\vec{\mu_o})_g + \sum_k \left(\frac{\partial \vec{\mu_g}}{\partial Q_k}\right)_o Q_k + \frac{1}{2} \sum_k \sum_l \left(\frac{\partial^2 \vec{\mu_g}}{\partial Q_k \partial Q_l}\right)_o$$

$$Q_k Q_l + \text{----}$$

If electrical anharmonicity is neglected, terms beyond the second in the above expansion can be neglected. So

$$(\mu_g)_{v'v''} = \int \psi_{v'} \left((\vec{\mu_o})_g + \sum_k \left(\frac{\partial \vec{\mu_g}}{\partial Q_k}\right)_o Q_k \right) \psi_{v''}\, d\tau$$

$$= (\vec{\mu_o})_g \int \psi_{v'} \psi_{v''}\, d\tau + \left(\frac{\partial \vec{\mu_g}}{\partial Q_k}\right)_o \int \psi_{v''}$$

$$Q_k \psi_{v'}\, d\tau$$

Assuming v' and v" differ by 1

$$(\mu_g)_{v'v''} = \left(\frac{\partial \vec{\mu_g}}{\partial Q_k}\right)_o \cdot \left(\frac{h}{8\pi^2 \nu_{v'v''}}\right)^{1/2} (v'' + 1)$$

$$\int \alpha(\nu)d\nu = \frac{\pi}{3c} (N_{v''} - N_{v'}) (v' + 1) \sum_g \left(\frac{\partial \vec{u_g}}{\partial Q_k}\right)^2$$

If v' and v" differ by 1, the frequency of all other transitions , pertaining to the same normal coordinate k, differing in quantum number by 1, fall in the same position because of harmonic oscillator approximation. So the expression for intensity has to be summed over all such transitions.

$$N_{v''} = \frac{N}{a} e^{-h\nu_1/kT\, v''}$$

Where ν_1 is the frequency of transition from 0 → v"

$$N_{v'} = \frac{N}{a} e^{-h\nu_1/kT(v'' + 1)}$$

$$N_{v''} - N_{v'} = \frac{N}{a} \left\{ e^{-h\nu_1/kT\, v''} - e^{-h\nu_1/kT(v'' + 1)} \right\}$$

$$\int_{\text{band}} \alpha(\nu)d\nu = \frac{\pi}{3c} \sum_{g} \left| \frac{\partial \vec{\mu}_g}{\partial Q_k} \right|^2 \frac{N}{Q} \sum_{v''=0}^{\infty} \left\{ e^{-h\nu_1/kT v''} - e^{-h\nu_1/kT(v''+1)} \right\} (v''+1)$$

$$= \frac{\pi N}{3c} \sum_{g} \left| \frac{\partial \vec{\mu}_g}{\partial Q_k} \right|^2 \qquad (5)$$

If A' is as defined as in equation (1)

$$\int_{\text{band}} \alpha(\nu) \frac{d\nu}{\nu} = \frac{\pi N}{3c\nu_{v'v''}} \sum_{g} \left| \frac{\partial \vec{\mu}_g}{\partial Q_k} \right|^2 \qquad (6)$$

It was pointed out in the introduction that from the intensity measurement the dipole moment derivative with respect to internal coordinate can be obtained. With the aid of equation (5) $\frac{\partial \mu}{\partial Q}$ values can be obtained and from them $\frac{\partial \mu}{\partial r}$ values can be derived.

Normal and internal coordinates are related by the linear transformation

$$Q_k = \sum_{t} (L^{-1})_{k_t} r_t$$

$$\frac{\partial \mu_g}{\partial r_t} = \sum_{k} \frac{\partial \mu_g}{\partial Q_k} \cdot \frac{\partial Q_k}{\partial r_t}$$

But $\frac{\partial Q_k}{\partial r_t} = L^{-1}_{kt}$ so

$$\frac{\partial \mu_g}{\partial r_t} = \sum_k \frac{\partial \mu_g}{\partial Q_k} L^{-1}_{kt}$$

So to derive $\frac{\partial \mu}{\partial r}$ values from $\frac{\partial \mu}{\partial Q}$ it is necessary to know the elements of L^{-1} matrix and in a later section it is discussed how they are computed.

Unfortunately the correlation of this quantity $\frac{\partial \mu}{\partial r}$ with known molecular properties has been very unsatisfactory. It has not been possible to interpret $\frac{\partial \mu}{\partial r}$ values on the basis of fixed electronic charge on the nucleus and interatomic distance.

c) Shape and Intensity of Infrared Bands

It is experimentally observed that spectral lines in the infrared have a finite width. Sharp and narrow lines can only be expected in the case of an isolated undisturbed molecule, which is an ideal case. The broadening is caused by (1) Doppler effect, (2) radiation damping, and (3) collision with the neighboring molecules.

Doppler effect occurs when a molecule is moving parallel to the direction of propagation of radiation

and gives rise to a frequency shift. Doppler half intensity breadth is given by (46, p. 420)

$$\delta^{\omega} = 1.67 \frac{\omega_o}{c} \sqrt{\frac{2RT}{\mu}}$$

where ω_o is central frequency in cm^{-1} and μ is gram molecular weight of absorbing material. Assuming ω_o to be 630 cm^{-1} and μ to be 80 g $mole^{-1}$, δ^{ω} works out to be $10^{-3} cm^{-1}$.

Natural line width, i.e. the width due to radiation dumping, arises because the energy levels of a molecule are not sharp but diffuse. If a transition between two energy levels E_1 and E_2 is considered, since these energy levels have a finite width ΔE_1 and ΔE_2, the corresponding spectral line will have a finite width. The half intensity width of the line is the sum of the half intensity breadths of states E_1 and E_2. If the molecule stays in energy level E_1 for an average time t_1, according to the uncertainty principle

$$t_1 \Delta E_1 = \hbar$$

$\frac{1}{t_1}$ can be looked upon as the rate of spontaneous transition from state E_1 to any lower state E_k.

$$\frac{1}{t_1} = \frac{8\pi^2 e^2}{mc^3} \sum_k \nu_{1k}^2 f_{ik}$$

where ν_{ik} is the frequency and f_{ik} is the oscillator strength for the transition $1 \rightarrow k$. $\frac{1}{t_1} \alpha \Delta E_1$ and similarly $\frac{1}{t_2} \alpha \Delta E_2$. So the half intensity width of the line should be

$$\Delta\nu_{1/2} = \frac{4\pi^2 e^2}{mc^3} \sum_k \nu_{1k}^2 f_{1k} + \sum_k \nu_{21}^2 f_{21}$$

where 1 is a state lower in energy than E_2. From this equation it is estimated that half intensity width due to radiation damping is 10^{-4} Å (14, p. 1022). Remembering the equation

$$\frac{\Delta\lambda}{\lambda} = \frac{\Delta\omega}{\omega}$$

for a band of 630 cm^{-1}, this can be converted to cm^{-1}, which is $10^{-7} cm^{-1}$.

So the width of a line due to Doppler Shift and Radiation damping is negligible compared to the observed width, which in this work has varied from 4 to 20 cm^{-1}.

The most important source of broadening in the infrared region is due to collision or expressed

otherwise, perturbation due to neighboring molecules. Lorentz's theory of line broadening (20) which was developed to explain the absorption of radiation by oscillating electrons, can be applied to a harmonic oscillator. It has been assumed by Lorentz that the orientation of the molecule after each collision is random. But actually the molecules are oriented in such a way as to have low energy in the field. Van-Vleck and Weiskopf (44) have taken this into consideration and have derived a slightly different expression for the line shape. Nevertheless, the Lorentz line shape faithfully describes the energy distribution in the visible and infrared region where the natural frequency is large compared to the line width.

Lorentz Line Shape. Let ω be the applied circular frequency and ω_o the natural frequency of the oscillator. If e and m are the charge and mass of the oscillator, its motion can be described by a second order differential equation

$$m(\ddot{x} + \omega_o^2 x) = e E \cos \omega t$$

When x is averaged over all the molecules, it will have the value

$$\bar{x} = a E \operatorname{Exp}(i \omega t) + i_b E \operatorname{Exp}(i \omega t) \qquad (7)$$

For the differential equation the following solution can be assumed

$$x = c_1 \operatorname{Exp}(i\omega t) + c_2 \operatorname{Exp}(i\omega_o t) + c_3 \operatorname{Exp}(-i\omega_o t) \tag{8}$$

Suppose at a time $(t - \theta)$ the oscillator has experienced a collision, the amplitude after collision is determined by the values of x and $\dot{x}$ immediately after collision. Position and velocity of each oscillator after collision are different and can assume all possible values. So $\dot{x} = x = 0$, which are actually the averaged values, averaged in space.

$$\dot{x} = \omega c_1 \operatorname{Exp}(i\omega t) + \omega_o c_2 \operatorname{Exp}(i\omega_o t) - \omega_o c_3 \operatorname{Exp}(-i\omega_o t) = 0$$

$$x = c_1 \operatorname{Exp}(i\omega t) + c_2 \operatorname{Exp}(i\omega_o t) + c_3 \operatorname{Exp}(-i\omega_o t) = 0$$

Subject to the above boundary condition at $t = t - \theta$, the coefficients c_2 and c_3 are computed.

$$c_2 = -c_1 \operatorname{Exp}\left\{ i(\omega - \omega_o)t \right\} \frac{\omega + \omega_o}{2\omega_o}$$

$$c_3 = c_1 \operatorname{Exp}\left\{ i(\omega + \omega_o)t \right. \frac{\omega - \omega_o}{2\omega_o}$$

Substituting in equation (8)

$$x = c_1 \operatorname{Exp}(i\omega t) - c_1 \operatorname{Exp}\left\{ i(\omega-\omega_o)(t-\theta)\right\} \operatorname{Exp}(i\omega_o t)$$

$$\frac{\omega_+\omega_o}{2\ \ o} + c_1 \operatorname{Exp}\left\{ i(\omega+\omega_o)(t-\theta)\right\}$$

$$\operatorname{Exp}(-i\omega_o t)\ \frac{\omega-\omega_o}{2\omega_o} \qquad (9)$$

This expression has to be averaged over times of last collision. The distribution of collision in time is given

$$n(t) = \frac{1}{\tau}\ e^{-\theta/\tau}\ d\theta$$

where n(t) is the probability that a molecule after it has made a collision will make another collision after a lapse of time θ and τ is the mean time between collisions. So if the expression (9) has to be averaged over all the time of last collision, it has to be multiplied by the probability factor and integrated from 0 to ∞. Equation (9) can be rewritten as

$$x = c_1\left[1 - \frac{\omega-\omega_o}{2\omega_o}\left\{ \cos\ (\omega_o+\omega)\theta - i \sin\ (\omega_o+\omega)\theta\right\} - \frac{\omega+\omega_o}{2\omega_o}\left\{ \cos\ (\omega_o-\omega)\theta + i \sin\ (\omega_o+\omega)\right\}\right]$$

where

$$c = c_1 \operatorname{Exp}(i\omega t)$$

$$\bar{x} = c\left[1 - \frac{\omega-\omega_o}{2\omega_o}\left\{\frac{1}{\tau}\left(\frac{\frac{1}{\tau}}{(\omega_o+\omega)^2+\left(\frac{1}{\tau}\right)^2} - \frac{i}{\tau}\left(\frac{\omega_o+\omega}{(\omega_o+\omega)^2+\frac{1}{\tau}^2}\right)\right)\right\} - \frac{\omega+\omega_o}{2\omega_o}\left\{\frac{1}{\tau}\left(\frac{\frac{1}{\tau}}{(\omega_o-\omega)^2+\frac{1}{\tau}^2}\right) + \frac{i}{\tau}\left(\frac{\omega_o-\omega}{(\omega_o-\omega)^2+\frac{1}{\tau}^2}\right)\right\}\right] \quad (10)$$

The average value of x has also been expressed in a different form in equation (7), in which the coefficient of the real part is the amplitude of oscillation moving in phase with the light wave and the coefficient of imaginary part is the amplitude of out of phase oscillation. Oscillation induces a dipole moment in the molecule and the in phase and out of phase components of dipole are, respectively, æ and be.

So the imaginary part of equation (10) multiplied by e gives the out of phase component of induced dipole moment. The imaginary part is

$$Ee^{i\omega t}\left[\frac{e}{2\omega_o m}\left\{\frac{\frac{1}{\tau}}{(\omega_o+\omega)^2+\left(\frac{1}{\tau}\right)^2} - \frac{\frac{1}{\tau}}{(\omega_o-\omega)^2+\left(\frac{1}{\tau}\right)^2}\right\}\right]$$

α', the out of phase component of polarizability is

$$\alpha' = \frac{b_e}{E}$$

$$= \frac{e^2}{2\omega_o mE} \left. \frac{\frac{1}{\tau}}{(\omega_o+\omega)^2 + \left(\frac{1}{\tau}\right)^2} - \frac{\frac{1}{\tau}}{(\omega_o-\omega)^2 + \left(\frac{1}{\tau}\right)^2} \right\}$$

The absorption coefficient can be shown to be equal to

$$\alpha = \frac{4\pi n\omega}{c} \alpha' E$$

$$= \frac{2\pi ne^2}{mc} \frac{\omega}{\omega_o} \left. \frac{\frac{1}{\tau}}{(\omega_o-\omega)^2 + \left(\frac{1}{\tau}\right)^2} - \frac{\frac{1}{\tau}}{(\omega_o+\omega)^2 + \left(\frac{1}{\tau}\right)^2} \right\}$$

This expression has been derived for a classical oscillator and to adopt this to quantum mechanical case e^2/m has to be replaced by $\frac{8\pi^2}{3h} |\mu_{ij}|^2 \nu_{ij}$ where μ_{ij} is the matrix element of the transition moment.

$$\alpha = \frac{8\pi^2(N_i-N_j)}{3hc} |\mu_{ij}|^2 \nu \left[\frac{\frac{1}{2\pi\tau}}{(\nu_{ij}-\nu)^2 + \left(\frac{1}{2\pi\tau}\right)^2} - \frac{\frac{1}{2\pi\tau}}{(\nu_{ij}+\nu)^2 + \left(\frac{1}{2\pi\tau}\right)^2} \right]$$

where circular frequency has been replaced by

natural frequency. In the case of infrared absorption bands where the half intensity width is small compared to natural frequency (i.e., $\frac{1}{2\pi\tau} << \nu_{ij}$), the second term can be neglected. If j = i + 1

$$\left| u_{ij} \right|^2 = \frac{h}{8\pi^2 \nu_{ij}} \cdot \left(\frac{\partial \mu}{\partial Q} \right)^2 (v_{i+1})$$

$$\alpha = \frac{(N_i - N_j)}{3c} \left(\frac{\partial \mu}{\partial Q} \right)^2 (v_{i+1}) \frac{\nu}{\nu_{ij}} f_{ij} \qquad (11)$$

where

$$f_{ij} = \frac{\Delta \nu}{(\nu_{ij} - \nu)^2 + \Delta \nu^2}$$

is the shape factor. The expression used by Ramsay for Lorentz line shape is

$$\ln \frac{I_o}{I} = \frac{a}{(\nu_{ij} - \nu)^2 + b^2}$$

where 'a' and 'b' are constants. Comparison of these two expressions indicate that 'b' can be related to $\frac{1}{2\pi\tau}$ while 'a' includes a frequency factor and is related to 'b'. Integrating equation (11) between $+\infty$ and $-\infty$

$$A = \frac{N_i - N_j}{3c} \left(\frac{\partial \mu}{\partial Q}\right)^2 (v_{i+1}) \int_{-\infty}^{+\infty} \frac{\nu}{\nu_{ij}} f_{ij} \, d\nu$$

$$= \frac{\pi (N_i - N_j)}{3c} \left(\frac{\partial \mu}{\partial Q}\right)^2 (v_i + 1)$$

It is to be remembered that this expression has to be summed over all transitions, pertaining to a normal coordinate, in which i and j differ by 1 and the resulting expression will be the same as equation (5).

<u>Van-Vleck and Weiskopf Line Shape</u>. As has already been pointed out, Van-Vleck and Weiskopf do not assume that the polarization of the molecule after collision is random, but oriented such that their energy in the field is minimum, in accordance with Boltzmann distribution law.

The energy of the system is given by

$$H = \frac{m}{2} (\dot{x})^2 + \frac{m}{2} (\omega_o x)^2 - e_x E \cos \omega t$$

So the average value of x subject to the above condition is

$$\bar{x} = \frac{\iint x \, \mathrm{Exp}(-H/kT) \, dx \, d\dot{x}}{\iint \mathrm{Exp}(-H/kT) \, dx \, d\dot{x}} = \frac{E_e \cos \omega t}{m \omega_o^2}$$

So the expression for $\bar{x}$ will have an additional term.

$$\bar{x} = aEe^{i\omega t} + ibe^{i\omega t} + \frac{eE\cos\omega t}{m\omega_o^2}$$

By a similar procedure an expression for 'b' can be derived and consequently for α.

$$\alpha = \frac{8\pi^2(N_i-N_j)}{3hc}\,\nu_{ij}\,\left|\mu_{ij}\right|^2\left(\frac{\nu}{\nu_{ij}}\right)^2\left[\frac{\Delta\nu}{(\nu_{ij}-\nu)^2+\Delta\nu^2}\right]$$

If i and j differ by 1

$$\left|u_{ij}\right|^2 = \frac{h}{8\pi^2\nu_{ij}}\left(\frac{\partial\mu}{\partial Q}\right)^2(v_i+1)$$

$$\alpha = \frac{N_i-N_j}{3c}\left(\frac{\partial\mu}{\partial Q}\right)^2(v_i+1)\left(\frac{\nu}{\nu_{ij}}\right)^2\left[\frac{\Delta\nu}{(\nu_{ij}-\nu)^2+\Delta\nu^2}\right]$$

If integrated absorption coefficient is defined as

$$A' = \int \alpha \frac{d\nu}{\nu} = \frac{N_i - N_j}{3c}\left(\frac{\partial \mu}{\partial Q}\right)^2 (v_i+1) \int_{-\infty}^{+\infty} \frac{\nu^2}{\nu_{ij}^2} \cdot$$

$$\frac{\Delta\nu}{(\nu_{ij}-\nu)^2 + \Delta\nu^2} \cdot \frac{d\nu}{\nu}$$

$$= \frac{N_i - N_j}{3c}\left(\frac{\partial \mu}{\partial Q}\right)^2 \frac{v_i+1}{\nu_{ij}}$$

$$\int_{-\infty}^{+\infty} \frac{\nu\Delta\nu}{\nu_{ij}\left\{(\nu_{ij}-\nu)^2 + \Delta\nu^2\right\}}$$

$$= \frac{(N_i - N_j)}{3c\nu_{ij}}\left(\frac{\partial \mu}{\partial Q}\right)^2 (v_i+1)$$

which when summed over all transitions differing by 1 quantum number lead to the usual equation

$$A = \frac{\pi N}{3c\nu_{ij}}\left(\frac{\partial \mu}{\partial Q}\right)^2.$$

If Lorentian line shape is assumed, the true absorption is given by

$$\log \frac{I_o}{I} = \frac{a}{(\nu_o - \nu)^2 + b^2}$$

where 'a' and 'b' are constants. This would be the case if the resolution of the spectrograph is infinite. But due to the finite resolving power of the instrument, i.e., finite slit width, the true absorption band is modified.

When a spectrometer is set to transmit a radiation of frequency ν', it actually transmits a frequency band instead of a single frequency. The shape and width of this band depends on the width of the entrance and exit slit. If the slits are infinitely narrow, the energy distribution in the transmitted radiation is given by the diffraction function. But in the infrared region the slits are wide and are of equal width. In addition the energy of the source per frequency interval varies slowly and so a triangular slit function faithfully represents the energy distribution over the slit. Sometimes Gaussian error function has also been assumed.

Figure 1 represents the energy distribution over the slit, where S is the spectral slit width, which is the sum of two factors, one determined by mechanical slit width and the other by limiting resolving power of the instrument. For a given frequency and for a given mechanical slit width, it is given by (47, p. 151)

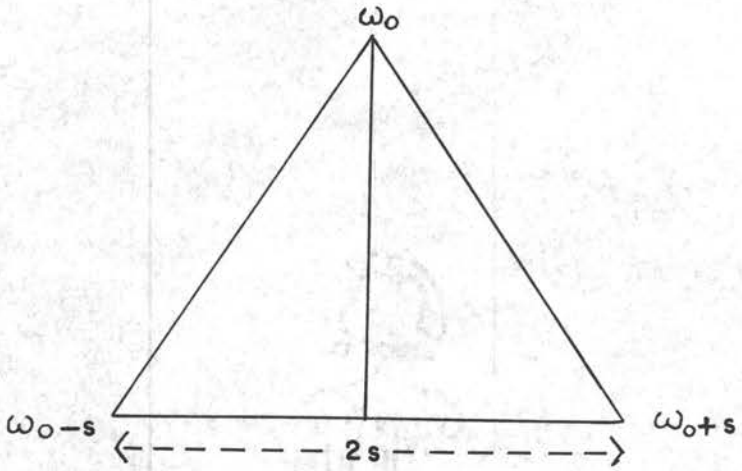

Figure 1

Energy Distribution Over the Slit (Exit) of a Spectrometer Set at a Frequency ω_o.

$$\Delta\nu\ (cm^{-1}) = \nu^2 \frac{\left[1-n^2 \sin^2 \alpha/2\right]^{1/2}}{8 \sin(\alpha/2) \frac{dn}{d\lambda}} \frac{S_1 + S_2}{f} + F(s) \frac{\nu}{2b \frac{dn}{d\lambda}}$$

ν = frequency in cm^{-1}

n = refractive index at frequency

α = prism apex angle

$\frac{dn}{d\lambda}$ = dispersion of prism material

S_1, S_2 = slit width

f = focal length

b = prism base

F(s) is a function varying from about 0.9 for S = 0 to 0.5 for S cm^{-1} = $\nu/\left[2b(dn/d\lambda)\right]$

More conveniently, the spectral slit width can be obtained by

$$\overline{\Delta\lambda} = \overline{\Delta\lambda}_p + \overline{\Delta\lambda}_{0.1} \times \frac{\text{Mechanical slit width in mm}}{0.1}$$

The values of $\overline{\Delta\lambda}_p$ and $\overline{\Delta\lambda}_{0.1}$ are read from the graph in the instruction manual provided by Perkin-Elmer Corporation (31, Figure C5).

The energy distribution over the slit is an even function of $\omega_o - \omega$ and so it can be represented as $f(|\omega_o - \omega|, s)$ and it has the following properties:

$$f(|\omega_o - \omega|, s) = \begin{cases} 0 \text{ when } \omega \leq \omega_o - s \\ 0 \text{ when } \omega \geq \omega_o + s \\ \dfrac{(\omega - \omega_o + s)\, f(0,s)}{s} \text{ when } \omega_o - s \leq \omega \leq \omega_o \\ \dfrac{(\omega_o - \omega + s)\, f(0,s)}{s} \text{ when } \omega_o + s \leq \omega \leq \omega_o \end{cases}$$

If T_o and T represent the apparent intensity of incident and transmitted radiation

$$T_o = \int_{\text{Slit}} S_\lambda \; f(|\omega_o - \omega|, s)\, d\lambda$$

$$T = \int_{\text{Slit}} S_{\omega} \, \mathrm{Exp}(-\alpha_{nl}) \, f(|\omega_o - \omega|, s) \, d\omega$$

where S_{ω} is the energy of the source, which is constant over the narrow frequency range admitted by the slit. Consequently the transmittance is

$$\frac{T}{T_o} = \frac{\int_{\text{Slit}} \mathrm{Exp}(-\alpha_{nl}) \, f(|\omega_o - \omega|, s) \, d\omega}{\int_{\text{Slit}} f(|\omega_o - \omega|, s) \, d\omega}$$

In the case of a triangular slit function the denominator is nothing but the area of the triangle which is equal to sf(o,s)

If a Lorentian line shape is accepted

$$-\alpha_{nl} = \ln \frac{I}{I_o} = - \frac{a}{(\omega - \omega_o)^2 + b^2}$$

So

$$\frac{T}{T_o} = \frac{\mathrm{Exp}\left(- \frac{a}{(\omega - \omega_o)^2 + b^2}\right. \quad f(|\omega - \omega_o|, s) \, d\omega}{\int f(|\omega - \omega_o|, s) \, d\omega} \qquad (12)$$

This equation indicates that from the 'true' absorption band, the apparent absorption band can be constructed. Assuming suitable values of a, b, and s, by numerical integration the value for T/T_o at a particular frequency can be computed. Repeating the calculation for the frequency range covered by the band, the apparent band can be constructed.

If an absorption band is studied at various slit widths, it is noticed that the peak intensity decreases and the apparent half intensity width increases as the slit width is increased. So an absorption band, whether true or apparent, can be described by these two parameters for a given slit width. For an apparent band corresponds a true band which are related by equation (12) through the slit function. So, for a given slit width, there are four interrelated quantities, the true and apparent peak intensity ($\ln (I_o/I)_{max}$, $\ln (T_o/T)_{max}$) and true and apparent half intensity widths ($\Delta\nu^a_{1/2}$ and $\Delta\nu^t_{1/2}$). Assuming a true peak intensity and half intensity width for a given slit, by the help of equation (12), the apparent band is constructed, from which $\ln (T_o/T)_{max}$ and $\Delta\nu^a_{1/2}$ can be read. Ramsay (34) has carried out such calculations and has tabulated for different values of $S/\Delta\nu^a_{1/2}$ ranging from 0 to 0.65 and for different values of

log $(T_o/T)_{max}$ ranging from 0.2 to 2.0, the ratio of true peak intensity to apparent peak intensity and also the ratio of apparent half intensity width to true half intensity width. These tables are helpful in finding the absolute integrated intensity and some new methods have been developed by Ramsay. One of them is discussed in Appendix I.

d) Normal Coordinate Calculations: GF Matrix

One of the objects of molecular spectroscopy is the computation of force constants. Absorption of radiation by a molecule takes place during its oscillatory motion and consequently to obtain force constants secular determinants have to be solved. The size of the determinant depends on the size of the molecule and their solution is extremely complicated and tedious in the case of complex molecules. A simpler technique has been developed by Wilson (48) in which group theory is employed. Cartesian coordinates which augment the size of the determinant are dispensed with and internal coordinates, i.e., the band distances and band angles, which are fewer in number are introduced. A knowledge of Wilson's method is essential in calculating normal coordinates.

Before proceeding to this novel method, it is necessary to consider briefly the classical method. It defines some of the concepts later used and at the same time systematizes the development of subject matter.

A molecule consisting of N atoms has 3N degrees of freedom. A set of coordinates q_1, q_2 ---- q_{3N}, called mass weighted coordinates, can be chosen which give the displacement of atoms from their equilibrium position. They are related to Cartesian displacement coordinates by

$$q_1 = \sqrt{m_1}\, x_1 \qquad q_2 = \sqrt{m_1}\, x_2 \qquad \ldots\ldots$$

Consequently kinetic energy is

$$2T = \sum_{i=1}^{3N} \dot{q}_i^{\,2} \tag{13}$$

Potential energy is a function of displacements and can be expanded in Taylor's series in terms of q's.

$$2V = 2V_o + 2\sum_{i=1}^{3N} \frac{\partial v}{\partial q_i}\, q_i + \sum_{ij=1}^{3N} \frac{\partial^2 v}{\partial q_i \partial q_j}\, q_i q_j + \text{---}$$

Assuming the energy of the molecule at equilibrium position is zero and neglecting mechanical anharmonicity

$$2V = \sum_{ij}^{3N} f_{ij}\, q_i\, q_j \qquad \text{where} \qquad f_{ij} = \frac{\partial^2 v}{\partial q_i \partial q_j}$$

Lagrangian equation of motion describing the oscillatory motion is

$$\frac{d}{dt}\ \frac{\partial T}{\partial \dot{q}_j} + \frac{\partial v}{\partial q_j} = 0 \qquad (14)$$

Substituting for T and v, yields

$$\ddot{q}_j + \sum_{i=1}^{3N} f_{ij}\, q_j = 0 \qquad (15)$$

For these second order simultaneous differential equations a solution of the form

$$q_j = A_j \cos\left(\lambda^{1/2} t + \epsilon\right) \qquad (16)$$

can be assumed where $\lambda = 4\pi^2 \nu^2$. Substituting for q_j in equation (15) a set of simultaneous equations are obtained

$$\sum_{i=1}^{3N} (f_{ij} - \delta_{ij}\lambda)A_i = 0$$

Since the amplitude should have nontrivial solution the determinant of its coefficients should be zero. This condition gives rise to the following secular determinant, the solution of which gives the force constants

$$\begin{vmatrix} f_{11} - \lambda & f_{12} & f_{13} \cdots\cdots & f_{13N} \\ f_{21} & f_{22} - \lambda & \cdots\cdots\cdots\cdots & f_{23N} \\ \vdots & & & \\ f_{3N1} & f_{3N2} & \cdots\cdots\cdots\cdots & f_{3N3N} - \lambda \end{vmatrix} = 0$$

To eliminate all cross terms in the expression for kinetic and potential energy, a new set of coordinates called normal coordinates are introduced. It is always possible to make a linear transformation of mass weighted coordinate to normal coordinate.

$$q_i = \sum_{K}^{3N} l'_{iK} Q_K$$

$$q_i q_j = \sum_{Kl} l'_{iK} l'_{jl} Q_K Q_l$$

The coefficients are chosen such that

$$\sum_{i} l'_{iK} l'_{il} = \delta_{Kl} \quad \text{where } \delta_{Kl} \begin{cases} = 0 \text{ when } K \neq l \\ = 1 \text{ when } K = l \end{cases}$$

So

$$2T = \sum_{K=1}^{3N} \dot{Q}_K^2$$

$$2V = \sum_{K=1}^{3N} \lambda'_K Q_K$$

Substitution of these new expressions for kinetic and potential energy in Lagrangian equation of motion results in

$$\ddot{Q}_K + \lambda' Q_K = 0$$

for which a solution of the form can be assumed

$$Q_K = K'_K \cos(\lambda'^{1/2}_K + \epsilon'_K) \qquad (17)$$

λ'_K is the same as λ used in equation (16).

In the above treatment potential energy has been expressed in terms of either mass weighted or normal coordinates which are essentially displacement coordinates. But to express potential energy in terms of internal coordinates is more meaningful and the force constants derived thereby have a better physical significance. But kinetic energy as usual can be conveniently expressed in terms of Cartesian displacements.

$$2T = \sum_{i=1}^{3N} m_i \dot{x}_i^2$$

By a linear transformation internal coordinates (R_K) can be related to Cartesian displacement coordinates

$$R_K = \sum_{i=1}^{3N} B_{Ki} x_i \qquad K = 1 \ldots\ldots 3N-6$$

A set of quantities G_{Kl} are defined as follows

$$G_{Kl} = \sum_{i=1}^{3N} B_{Ki}\, B_{li}\, m_i^{-1}$$

It can be shown that the kinetic energy is related to internal coordinates through this quantity G_{Kl}. To show this, a new matrix D is defined

$$D = \left\| B_{Ki}\, m_i^{-1/2} \right\|$$

It is already defined that

$$q_i = m_i^{1/2}\, x_i \qquad \text{or} \qquad \dot{q}_i = m_i^{1/2}\, \dot{x}_i$$

Rendering it in matrix language

$$\dot{q} = \left\| m^{1/2}\, \dot{x} \right\|$$

where this will be a column matrix and the transpose of it will be a row matrix and the product of these two will be just the internal product which is nothing but twice the kinetic energy.

$$2T = \left\| \dot{q} \right\|' \left\| \dot{q} \right\|$$

$$R_k = \sum_{i=1}^{3N} B_{ki}\, x_i$$

$$R_k = \sum_{i=1}^{3N} B_{ki}\, m_i^{-1/2}\, q_i$$

$$k = 1,2,3, \ldots. (3N-6)$$

$$= \sum_{i=1}^{3N} d_{ki}\, q_i$$

where d_{ki} are the elements of the matrix D or

$$\|R\| = \|Dq\|$$

Matrix D written out in extended form

$$D = \begin{Vmatrix} B_{11}\mu_1 & B_{12}\mu_1 & \cdots\cdots\cdots\cdots & B_{13N}\mu_N \\ B_{21}\mu_1 & B_{22}\mu_1 & \cdots\cdots\cdots\cdots & B_{23N}\mu_N \\ \vdots & & & \\ B_{3N-6\ 1}\mu_1 & B_{3N-6\ 2}\mu_1 & \cdots\cdots & B_{3N-6\ N}\mu_N \end{Vmatrix}$$

Apparently D is (3N, 3N-6) rectangular matrix and it can be augmented to (3N, 3N) square matrix by introducing 6 conditions of vanishing linear and angular momentum.

$$\mathcal{D} = \left\| \begin{array}{cccc} B_{11}\mu_1 & B_{12}\mu_1 & \cdots\cdots\cdots & B_{13N}\mu_N \\ \vdots & & & \\ B_{3N-6\ 1}\mu_1 & B_{3N-6\ 2}\mu_1 & \cdots\cdots & B_{3N-6\ 3N}\mu_N \\ \hline B_{3N-5\ 1}\mu_1 & B_{3N-5\ 2}\mu_1 & \cdots\cdots & B_{3N-5\ 3N}\mu_N \\ \vdots & & & \\ B_{3N\ 1}\mu_1 & B_{3N\ 2}\mu_1 & \cdots\cdots\cdots & B_{3N\ 3N}\mu_N \end{array} \right\|$$

which can be partitioned as shown above. Representing the lower part by D_o, D can be abbreviated as

$$\mathcal{D} = \frac{D}{D_o} \qquad\qquad \mathcal{D}^{-1} = \frac{Q}{Q_o}$$

If γ represents $D_o q = 0$, a new quantity $\mathcal{R}$ can be defined as partioned matrix

$$\mathcal{R} = \frac{R}{\gamma}$$

So $$q = \mathcal{D}^{-1}\mathcal{R}$$

$$2T = \|\dot{q}\|' \|\dot{q}\| = (\mathcal{D}^{-1}\dot{\mathcal{R}})'(\mathcal{D}^{-1}\dot{\mathcal{R}})$$

$$= \dot{\mathcal{R}}'\mathcal{D}^{-1\prime}\mathcal{D}^{-1}\dot{\mathcal{R}} \qquad (19)$$

Remembering the way in which $\mathcal{R}$, $\mathcal{D}$ and $\mathcal{D}^{-1}$ are expressed

the matrix product (19) can be expanded into

$$= R'Q'QR + {}'Q_o{}'QR' + R'Q'Q_o + {}'Q_o{}'Q_o$$

$$= R'Q'QR \qquad \text{since} \qquad \dot{\gamma} = \gamma = 0$$

$$(DD^{-1}) = E$$

So

$$\left(\frac{D}{D_o}\right)\left(\frac{Q}{Q_o}\right) = E$$

$$QD + Q^oD^o = E$$

and also $$(QD)' + (Q^oD^o)' = E$$

$$D'Q' + D^{o\prime}Q^{o\prime} = E \tag{20}$$

Premultiplying each term of (20) by D and post multiplying by Q gives

$$DD'Q'Q + DD_o{}'Q^{o\prime}Q = E$$

Since $D_o = 0$

$$DD'Q'Q = E$$

$$Q'Q = (DD')^{-1}$$

Since $$D = \sum B_{ki}\, m_i^{-1/2}$$

$$DD' = \sum B_{ki}\, B_{il}\, m_i^{-1} = \sum_{kl} G_{kl}\, m_i^{-1}$$

$$(DD')^{-1} = (G_{kl})^{-1}$$

$$2T = \dot{R}' \, G^{-1} \, \dot{R}'$$

So kinetic energy in terms of internal coordinates is

$$2T = \sum_{kl} (G^{-1})_{kl} \, \dot{R}_k \, \dot{R}_l$$

and potential energy as usual is

$$2V = \sum_{kl} F_{kl} \, R_k \, R_l$$

Substituting these expressions in the Lagrangian equation of motion yields

$$\sum_{kl=1}^{3N-6} (G^{-1})_{kl} \, \ddot{R}_l + \sum_{kl=1}^{3N-6} F_{kl} \, R_l = 0$$

This is second order differential equation and is similar to those derived using other systems of coordinates, and a similar solution can be assumed. The result is

$$\left[\sum_{kl=1}^{3N-6} F_{kl} - \sum_{kl=1}^{3N-6} (G^{-1})_{kl}\lambda\right] A_k = 0 \qquad (21)$$

and this gives rise to the secular determinant

$$\begin{vmatrix} F_{11}-(G^{-1})_{11}\lambda & F_{12}-(G^{-1})_{12}\lambda & \cdots\cdots \\ F_{21}-(G^{-1})_{21}\lambda & F_{21}-(G^{-1})_{21}\lambda & \cdots\cdots \\ \cdots\cdots & \cdots\cdots & \cdots\cdots \\ \cdots\cdots & \cdots\cdots & \cdots\cdots \end{vmatrix} = 0$$

Computation of inverse G matrix is more complicated than G matrix itself and so to make the above form more convenient to operate, it is multiplied by the determinant whose elements are G_{kl}. Since

$$\sum_{t'} G_{tt'}\left(G^{-1}_{t't''}\right) = \delta_{tt''}$$

the off diagonal λ's vanish, leaving the above determinant in a simpler form. In abbreviated form

$$\| GF - E\lambda \| = 0$$

Reverting to (21)

$$\sum_{kl} (F_{kl} - (G^{-1})_{kl}\lambda\ )\ A_k = 0$$

Which in expanded form will be

$$\left[F_{11}-(G^{-1})_{11}\lambda\right]A_1 + \left[F_{12}-(G^{-1})_{12}\lambda\right]A_2 + \cdots\cdots$$

$$\cdots\ \left[F_{1n}-(G^{-1})_{1n}\lambda\right]A_n = 0$$

$$\left[F_{21}-(G^{-1})_{21}\lambda\right]A_1 + \left[F_{22}-(G^{-1})_{22}\lambda\right]A_2 + \cdots\cdots$$

$$\cdots\ \left[F_{2n}-(G^{-1})_{2n}\lambda\right]A_n = 0$$

$$\begin{array}{ccc} \cdot & \cdot & \cdot \\ \cdot & \cdot & \cdot \\ \cdot & \cdot & \cdot \end{array}$$

$$\left[F_{n1}-(G^{-1})_{n1}\lambda\right]A_1 + \left[F_{n2}-(G^{-1})_{n2}\lambda\right]A_2 + \cdots\cdots$$

$$\cdots\ \left[F_{nn}-(G^{-1})_{nn}\lambda\right]A_n = 0$$

Comparing these equations with (16) and (17), it can be inferred that these amplitudes with a constant are the coefficients which transform internal coordinates to normal coordinates. The above simultaneous equations can be cast in a more convenient form by multiplying by the determinant whose elements are $G_{tt'}$. The result is

$$\left(\sum G_{1t'}F_{t'1} - \lambda\right) L_{1k} + \left(\sum G_{1t'}F_{t'2}\right)$$

$$L_{2k} + \ldots\ldots\ldots = 0$$

$$\left(\sum G_{2t'}F_{t'1}\right) L_{1k} + \left(\sum G_{2t'}F_{t'2} - \lambda\right)$$

$$L_{2k} + \ldots\ldots\ldots = 0$$

where $(L)_{tk}$ are the quantities which transform normal coordinates to interval coordinates. So solving the above set of simultaneous equations for $(L)_{tk}$ and normalizing them gives the required transformation matrix.

If inverse transformation is required, the following simultaneous equations have to be solved.

$$\sum (F_{1t'}G_{t'1} - \lambda_k)(L^{-1})_{k1} +$$

$$\sum (F_{it'}G_{t'2})(L^{-1})_{k2} + \ldots\ldots = 0$$

$$\sum (F_{2t'}G_{t'1})(L^{-1})_{k1} + \sum (F_{2t'}G_{t'2} - \lambda_k)(L^{-1})_{k2} + \ldots\ldots = 0$$

$$\vdots \qquad \vdots \qquad \vdots$$

The elements of $(L^{-1})'_{kt}$ matrix, as it has been already pointed out, are required to transform $\partial u/\partial Q$ values to $\partial u/\partial r$ values. But they cannot be uniquely determined by solving the above set of simultaneous equations. The normalizing condition which aids in evaluating them uniquely is (50, p. 310)

$$\| (L^{-1}) \|' \, \| (L^{-1}) \| = G^{-1}$$

e) <u>Fermi Resonance</u>

In the case of polyatomic molecules, two vibrational levels or combinations of them can be degenerate. Under such conditions, the two energy levels perturb each other and two new energy levels are created and the actual transition observed will be from the ground state to these two new levels. The classical example is carbon dioxide in which the frequency of the symmetric stretching mode (λ_1 = 1322 cm^{-1}) is almost

exactly twice that of bending mode (ν_2 = 668 cm^{-1}) and so resonance between a fundamental and the first overtone occurs and these two levels are pushed apart and the actual transitions are observed in Raman spectrum. This type of resonance was first suggested by Fermi and is commonly known as Fermi Resonance (7).

Before going into the details, one of the important conditions to be satisfied for Fermi resonance to occur should be considered. The matrix element of the perturbation function is

$$W_{ij} = \int \psi_i \, v_{anh} \, \psi_j \, d\tau$$

where v_{anh} = anharmonic perturbing potential, is independent of θ, ϕ, x, i.e. spatial orientation of the molecule. So it has full symmetry of the molecule and so if the above integrand has to be different from zero ψ_i and ψ_j should belong to the same symmetry species.

If molecular vibration were purely harmonic, the potential energy could be written

$$V = \frac{K_1}{2} Q_1^2 + \frac{K_2}{2} Q_2^2 + \frac{K_3}{2} Q_1 Q_2$$

Since interaction between energy levels has been noticed, interaction terms have to be included in the

potential function and it is enough if cubic terms are included to treat the interaction between ν_1 and $2\nu_2$.

$$V_{anh} = K_{113}Q_1^2Q_3 + K_{133}Q_1Q_3^2 + K_{122}Q_1Q_2^2 + K_{322}Q_3Q_2^2$$

With the aid of second order perturbation method it should be possible to derive the energy and wave function of the perturbed levels. The expression for the second order perturbation energy works out to be

$$W_k'' = \sum_l \frac{H'_{kl}\, H'_{lk}}{W^o_k - W^o_l} + H''_{kk}$$

For a degenerate case wherein $W_k^o = W^o_l$, the first term becomes infinite and so the second order perturbation method breaks down and cannot be profitably applied to Fermi resonance. So the problem is treated by linear variation method. By solving the following two by two secular determinant, the energy and wave function of the perturbed levels can be computed.

$$\begin{vmatrix} W_1^o - W & W_{12} \\ W_{21} & W_2^o - W \end{vmatrix} = 0$$

where W_1^o and W_2^o are the energies of the unperturbed levels and $W_\pm$ is the energy of the two perturbed levels and

$$W_{12} = \int \psi_1 \, v_{anh} \, \psi_2 \, d\tau = W_{21}$$

Solving the determinant

$$W_+ = \frac{1}{2}\left(W_1^o + W_2^o + \sqrt{\Delta_o^2 + \Delta_1^2}\right)$$

$$\Delta_o = W_1^o - W_2^o$$

$$\Delta_1 = 2W_{12}$$

$$W_- = \frac{1}{2}\left(W_1^o + W_2^o - \sqrt{\Delta_o^2 + \Delta_1^2}\right)$$

So the difference between the perturbed levels is

$$\Delta = \sqrt{\Delta_o^2 + \Delta_1^2}$$

$$a(W_1^o - W) + bW_{12} = 0$$

$$aW_{21} + b(W_2^o - W) = 0$$

Since $W_\pm$ and W_{12} are known in terms of Δ and Δ_o, 'a' and 'b' can be expressed in terms of Δ and Δ_o.

$$a = \pm \left(\frac{\Delta + \Delta_o}{2\Delta}\right)^{1/2} \qquad b = \pm \left(\frac{\Delta - \Delta_o}{2\Delta}\right)^{1/2}$$

The wave function for the perturbed levels are

$$\psi_I = a\psi_{10^00} + b\psi_{02^00}$$

$$\psi_{II} = a'\psi_{10^00} + b'\psi_{02^00}$$

Since orthogonality relation has to be satisfied

$$a' = b \qquad b' = -a$$

So

$$\psi_I = a\psi_{10^00} + b\psi_{02^00}$$
$$\psi_{II} = b\psi_{10^00} - a\psi_{02^00}$$

f) <u>Electrostatic Phenomena in a Dielectric</u>

While deriving the expression relating the integrated intensity and polar property, it is assumed that the applied electromagnetic field and the field at the molecule absorbing radiation are the same or it is as if the molecule is in vacuum. This assumption is reasonable when the matrix is gas, since their refractive index does not differ very much from 1. But it is not valid when the molecule is in a denser

medium like liquid or solid. The applied field and the local field, i.e., the field at the molecule, are different in liquid and solid phase and consequently the expression relating integrated intensity and polar property has to be modified.

The molecule absorbing the radiation is assumed to be in a sphere surrounded by a continuous dielectric, which has a cubic crystal structure. The internal field is divided into three parts

$$\vec{E}_i = \vec{E} + \vec{E}_1 + \vec{E}_2$$

$\vec{E}$ is due to apparent charges on the outer surface of the dielectric and the charge on the condenser plate. $\vec{E}_1$ is due to apparent surface charges on the sphere surrounding the molecule. $\vec{E}_2$ is the field caused by the molecule inside the sphere.

The field $\vec{E}_1$, which is essentially due to polarization charges, is computed as follows. If θ is the polar angle referred to the polarization direction axis and $\vec{P}$ is the density of electric polarization

$$\vec{E}_1 = \int_0^{\pi} \frac{\vec{P}\cos^2\theta}{2} \, 2\pi r^2 \sin\theta \, d\theta$$

$$= \frac{4\pi \vec{P}}{3}$$

E is related to electric polarization by the relation

$$\vec{E} = \vec{D} - 4\pi\vec{P}$$

where $\vec{D}$ is the field due to displacement of charges. $\vec{D}$ and $\vec{E}$ are related by the equation $\vec{D} = \epsilon\vec{E}$. E_2 in a cubic lattice and can be shown to be equal to zero.

$$E_i = E + \frac{4\pi P}{3}$$

$$= E + \frac{1}{3}(\epsilon - 1) E$$

$$= E\,\frac{\epsilon + 2}{3} = E\,\frac{n^2 + 2}{3}$$

$$E_i^2 = \left(\frac{n^2 + 2}{3}\right)^2 E^2$$

It is clear from these considerations that E is not the applied field, i.e., the field in vacuum.

Passing from vacuum to the dielectric medium, the flux of electromagnetic vector or the magnitude of Poynting vector remains constant

$$\vec{S}_{vacuum} = \vec{S}_{dielectric}$$

$$S = \frac{v}{4\pi}\; E \times D$$

where v is the velocity of electromagnetic radiation in the medium under consideration. So

$$S_{vacuum} = \frac{c}{4\pi}\left[E_o^{\,2}\right]$$

$$S_{dielectric} = \frac{c}{4\pi n}\left[E^2 \cdot \epsilon\right]$$

$$\epsilon = n^2$$

$$n = \text{refractive index}$$

$$E_o^{\,2} = E^2 \cdot n$$

$$E_i^{\,2} = \left(\frac{n^2+2}{3}\right)^2 \frac{1}{n} E_o^{\,2}$$

The intensity in gas phase is proportional to $E_o^{\,2}$ and that in condensed phase is propoertional to $E_i^{\,2}$.

$$A_c = \left(\frac{n^2+2}{3}\right)^2 \frac{1}{n} A_g$$

So the expression to be used relating condensed phase intensities and polar properties is

$$A_c' = \frac{N\pi}{3c\nu_{ij}} \cdot \left(\frac{n^2+2}{3}\right)^2 \cdot \frac{1}{n}\left(\frac{\partial u}{\partial Q}\right)^2 \qquad (22)$$

All the intensity data reported in Chapter V are calculated according to this equation.

A similar equation has been derived by Polo and Wilson (30). The experimental verification of this equation has met with little success. The reasons are

many. In deriving this equation, the field due to the permanent and induced dipole moment of the molecule has been taken to be zero, which may not be true in all cases. The experimental data available on liquids are inaccurate precluding a reasonable verification of this equation. In addition, in the case of liquids, other intermolecular forces like hydrogen bonding influence the intensity.

Equation (22) is applicable in the case of a pure liquid and Onsager's equation (27 , p. 1488) for the internal field is more appropriate for a solution.

$$F = \left(1 + \frac{n^2(\epsilon - 1)}{(2\epsilon + n^2)}\right) E + \frac{2(\epsilon - 1)}{(2\epsilon + 1)} \frac{\mu}{a^3} \vec{u}$$

n is the 'internal refractive index', i.e., the refractive index of the molecule while ϵ is the dielectric constant of the medium, u is the actual electric moment of the molecule and 'a' is cavity radius. The second term has the direction of the permanent dipole moment of the molecule which can be taken to be fixed during oscillation for frequencies in infrared.

So

$$\frac{F}{E} = 1 + \frac{n^2(\epsilon - 1)}{(2\epsilon + n^2)}$$

By a procedure similar to that given above, a relationship between condensed phase and gas phase intensities can be derived, which is

$$\frac{A_c}{A_g} = \frac{1}{n_o} \left\{ 1 + \frac{n^2(n_o^2 - 1)}{2n_o^2 + n^2} \right\} \qquad (23)$$

where n_o is the refractive index of the medium. Person (28), using the data of Welsh et al. (reference 7 in 28) on the pressure induced absorption of methane fundamentals, has compared the merits of equations (22) and (23) and has found that the latter gives better agreeing results with experimental value than equation (22).

The subject matter is not developed further, since it is in a state of flux. Equation (22) has been used in this work to apply correction for the observed intensity.

III. PREVIOUS INTENSITY WORK

The survey of previous work has not been done chronologically, but with the object of bringing out the various facets of this subject.

It was mentioned in the introduction that a few papers on this subject appeared during 1927-1928. These were by Bourgin, Matheson and Barthalome. Bourgin (3) studied the line intensity of the hydrogen chloride fundamental band at 3.5 μ. The experiment consisted of studying HCl at different path lengths and extrapolating the integrated area to zero path length to arrive at the absolute value. Similar work was carried out by Matheson (24) with CO, while Barthalome (1) studied hydrogen halides. The result of these investigations are unreliable since they have been obtained using low resolution instrument and are of purely historical interest.

Immediately after the publication of Wilson-Wells Extrapolation Theorem, to which reference has already been made, several papers appeared on gas phase intensities. Three of them, being of special importance to this work, are considered here. Two are by Thorndike and the other is by Eggers and Crawford. Thorndike et al. (42) studied nitrous oxide and have carried out

a complete analysis of the molecule. Since interaction force constant was not available to them, they assumed values ranging from +1 to +10 millidynes/Å and computed $\left(\frac{\partial \mu}{\partial r}\right)_{NO}$ and $\left(\frac{\partial \mu}{\partial r}\right)_{NN}$. Since then the interaction constant has been determined using the isotopic molecule to be 1.43 millidynes/Å (37) and so reasonable values for $\left(\frac{\partial \mu}{\partial r}\right)_{NN}$ and $\left(\frac{\partial \mu}{\partial r}\right)_{NO}$ are -3.45×10^{-10} and -7.1×10^{-10} (cgs units), respectively. Calloman *et al.* (4) have assigned to these parameters values of -3.3×10^{-10} and $+6.5 \times 10^{-10}$ (cgs units), respectively. Thorndike (41) has also studied carbon dioxide by a similar procedure and has obtained a value of ± 1.17 d for its dipole moment. Taking into consideration the three resonating structures of carbon dioxide and also the bond moments assigned to single and double bonds, he has concluded that the triple bond has low bond moment.

Work on carbon dioxide and nitrous oxide has been repeated by Eggers and Crawford (6), but their interest has been the computation of higher terms in the Taylor series expansion of dipole moment. In addition to these, other works on carbon dioxide have been published by Weber *et al.* and by Kaplan and Eggers and on nitrous oxide by Calloman *et al.* Accurate data

on the intensity of 15 u band of CO_2 is important since it helps to determine the thermal balance in the atmosphere. Weber and Penner (45) have studied this and their data are not very much different from that already reported. But the value obtained by Kaplan and Eggers (19) is higher. The latter authors are of the opinion that Wilson-Wells extrapolation method, though an improvement over that of Bourgin and others, is not suited to the study of intensity of a band with a narrow intense Q branch, as in the case 15 μ band of CO_2. Half the intensity of perpendicular band of CO_2 occurs in the Q branch whose width is small compared to the total band width. The absorption of Q branch will be linear if the intensity of P and R branches are low, in which case the measurements will be inaccurate. A high resolution instrument is an answer to the problem of measuring such narrow bands. The curve of growth method, though not novel, is not extensively used in preference to the extrapolation method, which is less tedious. The method used by Kaplan and Eggers consisted of calculating absorption theoretically as a function of path length, pressure, peak intensity and line widths. The latter two parameters are varied until a best fit between the observed and theoretical values is obtained. Then from these values the integrated intensity is computed.

Calloman et al. have studied nitrous oxide by the usual method. Data obtained by these authors on CO_2 and N_2O (which are isoelectronic with OCN^-) are tabulated in Tables 1 and 2.

CS_2 and OCS have been studied by Robinson (35). The intensity of the anti-symmetric mode, 7900 x 10^{10} cycle cm^{-1}, is comparable to that of carbon dioxide and $\frac{\partial u}{\partial Q_3}$ is ± 288. Since the symmetric mode is inactive in the infrared spectrum, further analysis has been carried out in terms of internal coordinates instead of in normal coordinate and a value of -5.6×10^{-10} esu has been obtained for $\frac{\partial u}{\partial r}$.

A complete analysis of the OCS molecule has been carried out. In addition, $\frac{\partial u}{\partial r}$ values have been plotted vs f_{12} and it is noticed that they are not so sensitive to change in f_{12} as the normal modes. A change of 0.5 in f_{12} value brings about only 10% in $\frac{\partial u}{\partial r}$. The data on the OCS molecule are tabulated in Table 3.

Compounds containing a CN group, like cyanogen, cyanogen chloride, HCN and DCN, have been studied. Nixon and Cross (26) studied C_2N_2 and ClCN. Cyanogen has a fundamental at 2150 cm^{-1} which is of moderate intensity. In the case of cyanogen chloride the ν_1 and ν_3 modes are at 714 and 2214 cm^{-1} respectively,

Table 1

$\frac{\partial \mu}{\partial Q}$ in esu $g^{-1/2}$ for CO_2 and N_2O

Band	Eggers and Crawford[a]	Dispersion[b]	Thorndike *et al.*[c]	Kaplan and Eggers[d]	Calloman *et al.*[e]
CO_2					
667 cm^{-1}	± 50.77	±53.55	± 54.65	±61.96	
2349 cm^{-1}	±293.66				
N_2O					
589 cm^{-1}	± 18.20	±24.0	± 25.18		
1285 cm^{-1}	± 88.47	±92.7	±110.8		±103
2224 cm^{-1}	±229.6				±226

[a]Reference (6)
[b]Reference (6)
[c]Reference (41, 42)
[d]Reference (19)
[e]Reference (4)

Table 2

Dipole Moment Coefficients of
CO_2 and N_2O in Debyes

	Band	Eggers and Crawford[a]	Dispersion[b]
CO_2 upper state			
01'0	667 cm^{-1}	$d_2 = \pm 0.150 \pm 0.007$	$+0.074 \pm 0.004$
N_2O upper state			
01'0	589 cm^{-1}	$d_2 = \pm 0.058$	

[a]Reference (6)
[b]Reference (6)

Table 3

Polar Parameters for OCS

$\frac{\partial \mu}{\partial Q_1}$	$\frac{\partial \mu}{\partial Q_3}$	$\left(\frac{\partial \mu}{\partial r}\right)_{CO} \times 10^{10}$	$\left(\frac{\partial \mu}{\partial r}\right)_{CS} \times 10^{10}$
± 33.2 esu $g^{-1/2}$	± 28.8 esu $g^{-1/2}$	-6.7 ± 0.5 esu	-4.3 ± 0.5 esu

while the bending mode is at 390 cm^{-1}. This has been observed by these authors using a Thallium Bromoiodide prism but the intensities have not been analysed due to the presence of considerable amount of stray light. The intensity data are summarized in Table 4. They have obtained for $\left(\frac{\partial \mu}{\partial r}\right)_{CN}$ in C_2N_2 a value of $\pm 0.72 \times 10^{-10}$ esu while in ClCN, the same derivative has a value of $\sim 1.8 \times 10^{-10}$ esu. The difference indicates that the C-Cl band is more polarizable than the C-C band.

Hyde and Hornig have studied HCN and DCN (13). The interesting feature of this work is that the study of isotopic molecules has enabled them to derive μ_{CH} and μ_{CN} which are, respectively, 1.14 d and 1.75 d resulting in 2.89 d for the molecule. The intensities of HCN and DCN are tabulated in Table 5 which indicates the fundamentals of these molecules are of medium intensity, except ν_1 which is weak compared to other triatomic molecules like CO_2, CS_2, OCS, and N_2O and OCN^-. $\left(\frac{\partial \mu}{\partial r}\right)_{CN}$ found by them is 0.66 d/A, similar to that in cyanogen but less than that in cyanogen chloride. But the value for $\left(\frac{\partial \mu}{\partial r}\right)_{CH}$ is considerably larger than in methane. This is explained as due to the use of Sp orbital in CH band formation. As hybridization changes from Sp^3 to Sp, the polarity of hydrogen is increased.

Table 4

Intensity of C_2N_2 and ClCN

C_2N_2	A (cycles cm^{-1})
2150 cm^{-1}	90×10^{10}
ClCN	
714 cm^{-1}	17×10^{10}
2214 cm^{-1}	220×10^{10}

Table 5

$\partial\mu/\partial Q$ Values for HCN and DCN in esu $g^{-1/2}$

Band	HCN $\pm \frac{\partial\mu}{\partial Q}$	DCN $\pm \frac{\partial\mu}{\partial Q}$
ν_1	4.5	20
ν_2	57	31
ν_3	88	66

$\partial\mu/\partial r$ values of some of the compounds which are of interest to this work are tabulated in Table 6.

In recent years considerable amount of work is being done in the liquid phase. Unlike the gas phase work the object of these investigations is not so much the study of polar properties of the molecules, but other aspects connected with liquid phase. In these studies pure liquids are not used, since this would necessitate the use of an inconveniently small absorption cell length, making the intensity data unreliable.

When the study in liquid phase is done in solution, it is natural to expect solvent effects on the intensity. This will be in the form of solvent-solute interaction due to orientation forces and electric polarizability of the solvent. Both theoretical and experimental studies have been carried out to assess the role of solvent and at the same time to compare the gas phase intensity with the liquid phase intensity.

Two equations have been derived relating the gas phase and liquid phase intensities. One is based on Debye's theory of dielectric polarization and the other on Onsager's theory of dielectric polarization.

Table 6

$\frac{\partial \mu}{\partial r}$ Values for CO_2, N_2O, HCN, DCN, C_2N_2 and ClCN in Debye/Å

Compound	$\left(\frac{\partial \mu}{\partial r}\right)_{CO}$	$\left(\frac{\partial \mu}{\partial r}\right)_{NN}$	$\left(\frac{\partial \mu}{\partial r}\right)_{NO}$	$\left(\frac{\partial \mu}{\partial r}\right)_{CN}$
CO_2	-6.0 ±0.6			
N_2O		-3.3	+6.5	
HCN DCN				±0.66
C_2N_2				±0.72
ClCN				1.80

$$\frac{A_l}{A_g} = \frac{1}{n}\left(\frac{n^2 + 2}{3}\right)^2 \qquad (24)$$

$$\frac{A_l}{A_g} = \frac{1}{n}\left(\frac{3n^2}{2n^2 + 1}\right)^2 \qquad (25)$$

where A_l and A_g are liquid and gas phase intensities and n is the refractive index of the medium at the frequency of absorption band. Assuming n = 1.5000, a 30% increase in intensity is expected according to Debye's theory, going from gas to liquid while Onsager's theory predicts no change. But careful consideration by Polo and Wilson (30) has shown that Onsager's theory yields the same results as Debye's and so equation (24) can be used to compare gas and liquid phase intensities.

A number of investigations have been carried out to test the validity of equation (24) and some results are in consonance with it and some are not. If the same molecule is studied in different solvents the intensities should be in the ratio

$$\frac{1}{n_1}\left(\frac{n_1^2 + 2}{3}\right)^2 : \frac{1}{n_2}\left(\frac{n_2^2 + 2}{3}\right)^2 : \ldots\ldots$$

Jaffe and Imel (16) have studied n-hexane in the 3 μ region in Fluorolube, CCl_4 and CS_2 and the ratio

found experimentally is in good agreement, within experimental error, with that expected.

Working with methyl formate in various solvents, Russel and Thompson (36) have noticed that there is no difference between gas phase and liquid phase intensities. Their results indicate that an appreciable change in intensity can only be expected when the refractive index is high.

After much is said and done, it is obvious that both a better theoretical knowledge of liquid phase and more accurate experimental work is necessary to say anything intelligible about the correlation between gas phase and liquid phase intensities.

Intensity of solute can also be modified due to solute solvent interaction. Lord et al. (21) have found a 10-20 fold change in the intensity of C-D stretching vibration band of deuterochloroform in different solvents. They explained this change in terms of the hydrogen bond between CD_3Cl and the solvent, like -C-D....O or C-D....N resulting in a change in the polar properties of C-D bond. Similar work has been carried out by Thompson and Steel (43). Substituted benzonitriles have been studied in $CHCl_3$ and CCl_4 and difference in intensity has been noticed, which is explained on the basis of a hydrogen band between the

C≡N group and $CHCl_3$. But similar interaction cannot be expected in the case of CCl_4 and as the authors themselves have admitted, studies with other solvents are desirable.

Studies with benzonitrile have led these authors to another interesting aspect of this field. It has been observed that a regularity exists between -C≡N frequency in substituted benzonitrile and the Hammett σ value (17) which is a measure of the reactivity of C≡N group, which obviously depends on the nature of the substituent. The square root of the integrated absorption coefficient is a measure of the polar property of the band and it is natural to expect that it should be related to the reactivity. A linear relationship has been observed by these authors between log A and σ for different substituted compounds, which can be expressed in the form

$$\text{Log } A - \log A_o = \rho'\sigma$$

which is similar to Hammett relation

$$\log k - \log k_o = \rho\sigma$$

IV. SPECTRUM OF CYANATE ION

Cyanate ion being a linear triatomic molecule has four fundamental modes of vibrations which are depicted below.

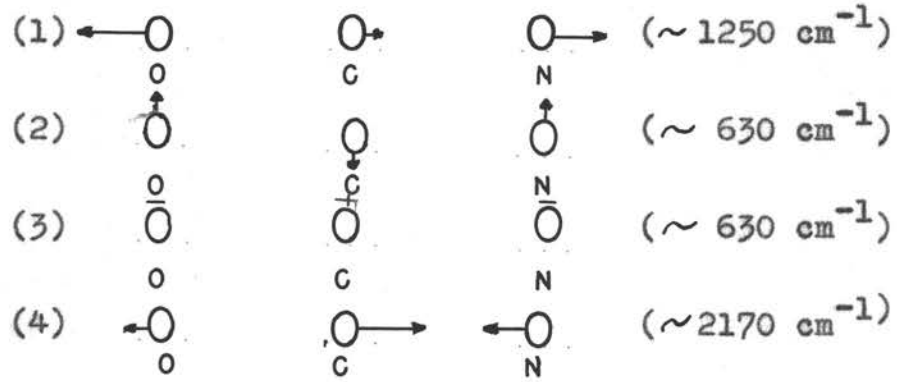

Thus the spectrum of cyanate ion should consist of three strong bands, but actually four are observed. The band at 630 cm^{-1} is due to the bending mode and that at 2170 cm^{-1} is due principally to the CN stretching mode. Since ν_3 has a frequency of the same order as the antisymmetric stretch in CO_2, it is sometimes referred to as the "antisymmetric stretch". The remaining fundamental frequency which arises principally from a stretch of the CO bond would presumably occur near 1250 cm^{-1}, but owing to Fermi resonance with $2\nu_2$ is split into two components near 1210 and 1290 cm^{-1}. The spectrum of cyanate ion in a KBr host lattice is shown in Figures 2, 3, 4 and 5. The spectrum has been extensively studied by Maki and Decius (23) in solid

solution and Table 7 gives the frequencies observed by them of the fundamentals and those of other transitions relevant to this work in KCl, KBr and KI lattices.

Table 7

Frequencies of NCO^- in KCl, KBr and KI

Host Lattice	Lower State	Upper State	Frequency (in cm^{-1})	Remarks
	0 0° 0	0 1' 0	631.0	
	0 0° 0	1 0° 0	1210.7	
	0 0° 0	0 2° 0	1297.3	
KCl	0 0° 0	0 0° 1	2181.8	
	0 0° 0	0 0° 1	2124.7	C^{13}
	0 1' 0	1 1' 0	1193.0	
	0 1' 0	0 3' 0	1314.4	
	0 0° 0	0 1' 0	629.4	
	0 0° 0	1 0° 0	1205.5	
	0 0° 0	0 2° 0	1292.6	
KBr	0 0° 0	0 0° 1	2169.6	
	0 0° 0	0 0° 1	2112.8	C^{13}
	0 1' 0	1 1' 0	1188.1	
	0 1' 0	1 3' 0	1309.1	
	0 0° 0	0 1' 0	628.0	
	0 0° 0	1 0° 0	1200.8	
	0 0° 0	0 2° 0	1288.0	
KI	0 0° 0	0 0° 1	2155.8	
	0 0° 0	0 0° 1	2099.0	C^{13}
	0 1' 0	1 1' 0	1183.0	
	0 1' 0	1 3' 0	1304.2	

V. EXPERIMENTAL PROCEDURE AND RESULTS

a) Spectrophotometry

All spectra were recorded on a Perkin Elmer Spectrometer Model 21, which is a double beam single pass instrument. To record the Fermi doublet and $\sim 2170\ cm^{-1}$ band the NaCl prism was used, while to record the bending mode, a KBr prism was used. Single crystals of alkali halide containing cyanate, made according to the procedure described by Maki (22, p. 158-161), were cut into suitable size and were mounted in a holder made out of cork and placed close to the slit. The spectrum was scanned at the slowest possible drum speed and slow pen speed so that the detector, amplifier and recorder faithfully followed the radiation flux transmitted by the specimen. For reasons which will be obvious later, the Fermi doublet and bending mode of OCN^- in KBr were recorded at different slit widths. The slit width that would give best resolution at the desired frequency was roughly estimated with the slit control on programme. Then holding the slit width constant at this value the spectrum was scanned. Slit widths lower than this were tried and the one that gave the best resolution was used as the starting point. The slit widths that

have been used are given in tables giving intensity data. Unlike in the case of KI and KCl, while studying the bending mode of OCN^- in KBr different slit widths have been used for different crystals. This is perfectly reasonable since these slit widths gave the best resolution, subject to the condition of the instrument. But while studying the same mode in KCl and KI crystals the same slit width in each case gave the best resolution. The same is true in the study of the CN stretching mode and Fermi doublet.

The spectrum thus obtained was analyzed in the following manner. A suitable base line was drawn to represent 100% transmission. This was drawn such that it coincided with the zero absorption line on either side of the band. At an interval of 1 or 2 cm^{-1} depending on the situation, the incident and transmitted intensity were read and their ratio computed. This ratio and the corresponding frequency were tabulated. The logarithms to the base 10 of these two quantities were taken. Then the logarithm of T_o/T was plotted against the logarithm of ω. Examples of the resulting plots are shown in Figures 2, 3, 4 and 5.

It is to be mentioned at this stage that this procedure is slightly different from the method commonly adopted. In most of the works so far reported the

logarithm of T_o/T is plotted against ω. But according to the definition of absolute integrated intensity given earlier (Chapter II, equation 1), it is necessary to plot the logarithm of T_o/T against the logarithm of ω. This procedure has been suggested by Crawford (5) and it is claimed by him that it has certain advantages over the other method. A', unlike A, is invariant under changes of quantum mechanical representation and its units are lucid (moles^{-1} cm^2), which is a sort of cross section and it comes out expressed in this way in convenient numbers.

The area of the plot thus made was then determined using a planimeter. The planimeter reading with suitable conversion factor gave the area as a dimensionless quantity. The apparent integrated intensity for each case was obtained by dividing the area by the concentration of cyanate in the crystal expressed as moles/cm^2. In the next section the quantitative analysis of the crystal is considered.

b) <u>Analysis of Crystals</u>

Analysis of the crystals for the concentration of cyanate ion, whose amount is about 1 micromole, was one of the problems to contend with in this investigation. Cyanate ion in acid solution undergoes

hydrolysis as follows giving NH_4^+ and $CO_3^=$.

$$OCN^- + 2H^+ + 2H_2O \rightarrow NH_4^+ + H_2CO_3$$

This hydrolysis is complete within 10-15 minutes if the cyanate to acid mole ratio is 1 to 150. To analyze for the cyanate content, it was decided to use this reaction and to determine the NH_4^+ formed by Nessler's reagent, thus obtaining the concentration of OCN^-. In the early stages of this work the method suggested by Shaw and Bordeaux (38) with suitable modification was tried. The method which is suited for the estimation of cyanate in the presence of excess interfering ions consists of passing a buffered solution of the crystal through a column of cation exchanger which retains the cations in solution. The effluent is treated with suitable amount of 0.1N H_2SO_4 and kept aside for 10-15 minutes to complete the hydrolysis. Meanwhile, the column is washed with KOH solution to remove the trapped cations and then washed. Then the hydrolyzed solution is passed through the column when NH_4^+ is retained, while neutral molecules and anions are discarded. The column is then eluted with KOH solution and the effluent is made up to 100 ml and treated with Nessler's reagent and the absorbance of the yellow solution formed was determined on a Beckman spectrophotometer.

Since it was expected that the cyanate content of crystal would be 5-6 micromoles, it was thought that this method would succeed. It was possible to construct a decent calibration curve, but when the crystals were analyzed, except in one case which was highly concentrated, hardly any perceptible yellow color was developed. The method which is suited for 40-100 micromoles in a litre of Nesslerized solution was not useful in this case where the crystals contain 10 or less micromoles per litre of Nesslerized solution.

Since this analytical method was not a success, it was decided to try synthetic solid solutions of KCNO and alkali halides. There are various methods by which a solid solution can be made. The best method is to pull out a crystal from a molten mixture of cyanate and alkali halide and KCNO. Though a known amount of cyanate could be added to the melt, due to thermal decomposition of cyanate and due to the existence of a concentration gradient in the melt, it is not possible to grow crystals with controlled amounts of cyanate.

The other method by which a solid solution can be made is by freeze drying. Known amounts of potassium halide and KCNO, weighed from a microbalance, are placed in a flask and the aqueous solution of the mixture is suddenly chilled in an acetone-dry ice bath until the

whole solution is completely frozen. Then the flask is connected to a pump through two cold traps cooled in acetone-dry ice and a drying tower containing calcium chloride and pumped till the mixture is dry. Then the powder, which comes out in a fluffy form, is ground into a fine powder in a mortar and evenly distributed in a die and pressed into a clear pellet using a pressure of 89,000 lbs/sq in. The pellet is placed in the path of the beam by means of a cork holder and the spectrum scanned.

With the pellets the Fermi doublet was first studied and lines were not sharp in contrast to the spectrum of single crystal, from which it could have been concluded that complete solution was not formed. However, the spectrum was analyzed and area computed. The results were in complete contradiction to what is expected. The slope of B' vs nl was positive. But when the 2170 cm^{-1} band was studied, surprisingly enough a strong band at 2142 cm^{-1} was noticed, not observed by Maki (22). It was first thought that it may be due to antisymmetric stretch of CNO^- in a different environment like NaBr in NaNCO lattice due to impurities either in KBr and KCNO used. But the study of Nujol emulsion spectrum revealed that the 2142 cm^{-1} band was due to undissolved cyanate. The Nujol spectrum had a strong

peak at 2142 cm^{-1} and a weak one at 2170 cm^{-1}. When cyanate was ground between KBr windows with Nujol, exchange of anions took place and a very dilute solid solution of cyanate in alkali halide was formed. This explains the weak absorption at 2170 cm^{-1} and it was also observed that grinding for a longer period increased its intensity. Due to limited solubility of KCNO in alkali halides and due to limitations of the freeze drying technique, it was realized that this procedure is not well suited for making solid solutions in this case. Experience with NH_4Cl has shown that if the ion dissolved has approximately the same size as that of the ion which it displaces, this technique could be adapted to make solid solutions.

Solid solutions can also be prepared by fusing a mixture in a crucible and rapidly chilling it. In the case of cyanate a metallic crucible is undesirable since a metal catalyzes its decomposition. Though a porcelain or quartz crucible is preferable, during rapid chilling due to expansion of the melt of solidification, the crucible breaks and the coolant enters into the solid and spoils the mixture. Though this may be a convenient general method for making solid solution, it is obviously not suited for making solid solution of cyanate with controlled amount.

After these failures it was decided to use single crystals for obtaining the spectrum and to work out a suitable method for the analysis. It has been pointed out that cyanate ion hydrolyzes to $CO_3^=$ and NH_4^+. Various courses are open by which either NH_4^+ or $CO_3^=$ could be estimated. By the isotopic dilution method, $CO_3^=$ could be estimated as $BaCO_3$ with a mass spectrometer. It is to be remembered that the cyanate concentration is in the 1-10 micromole range and hydrolysis never proceeds to completion in a neutral medium. Acid hydrolysis has to be avoided since $CO_3^=$ will be decomposed and alkaline hydrolysis is not suited since slight exposure to atmosphere brings in more carbonate into solution than what is produced from cyanate. Because of these difficulties, the idea of analyzing the crystal by mass spectrometry was given up.

The only alternative remaining involves the analysis of NH_4^+. Two methods were possible, either polarographical or spectrophotometric. The decision was in favor of the latter.

Ammonium salts form complete solid solution in alkali halide since the size of NH_4^+ and K^+ are comparable, and NH_4^+ gives a fairly sharp and pure absorption band at 1400 cm^{-1} and this band has been used to

construct calibration curves for NH_4^+ in different alkali halides. Since the intensity of a band depends on the environment in which the absorbing material is present, it was necessary to construct calibration curves for each of the alkali halides.

A mixture containing known amounts of potassium halide and NH_4Cl was made by weighing on a microbalance and the solution of the mixture was freeze dried. The dried sample was made into a pellet and the spectrum was run. The original mixture was made intentionally more concentrated and other concentrations were obtained by diluting the original mixture with corresponding potassium halide. The calibration plots are shown in Figure 6. They clearly indicate that the intensity of NH_4^+ band decreases from KI-KBr-KCl, since dielectric constant of these alkali halides decrease from KI-KBr-KCl.

To make sure that this procedure would be suitable for the analysis of the crystals, synthetic mixtures of KBr and KNCO were made and were treated with 5 ml of 0.035N hydrobromic acid and kept aside for half an hour for complete hydrolysis. Then the solution was freeze dried. The dried sample was made into a pellet and its spectrum scanned from 4000 cm^{-1} to 600 cm^{-1}. The complete absence of the most intense 2170 cm^{-1} band of cyanate was a clear indication that the hydrolysis was

complete. The spectrum had one intense peak around 3000 cm^{-1} and the other at 1400 cm^{-1} which are due to NH_4^+ (25, p. 1291). The absence of any other peak indicates that no other products have been formed due to hydrolysis. The optical density of 1400 cm^{-1} band agreed well within experimental error with the calibration curve for NH_4^+ in KBr. This is also shown in Figure 6.

The crystals were analyzed in the following manner. First its length, width and height were measured and then weighed into a flask. Depending on its weight it was diluted with corresponding alkali halide so that the total weight was about 0.4 gm. It was then treated with 5 ml of 0.034N HBr (HCl was used while analyzing KCl crystal while HBr was used while analyzing KI crystal) and kept aside for half an hour. It was then freeze dried and most of the dried sample was recovered and made into a pellet. The spectrum of the pellet was scanned rapidly in some cases from 4000-600 cm^{-1} and in some other cases from 2600-1200 cm^{-1}. One such spectrum is shown in Figure 7. These have indicated that hydrolysis is complete and no impurities have been formed. Then it was scanned from 1700-1200 cm^{-1}, at slow pen and drum speed, to get the intensity of 1400 cm^{-1} band of

NH_4^+. The optical density was read and with the aid of calibration charts and other data that has been collected the concentration of KCNO in the crystal was computed and was expressed as micromoles/cm^2. The complete data on the analysis of the crystals are given in Table 8.

c) Integrated Intensity

The information that has been collected so far are the integrated area of each band and the concentration of OCN^- in the crystals used. In addition in some cases the peak intensity and half intensity width have also been measured and in some other cases the integrated area has been obtained at different slit widths. It is possible at this stage to compute the absolute integrated intensity. But due to finite resolving power of the instrument the data that have been obtained give only the apparent integrated intensity. Since the aim of this work is to calculate the objective polar properties of the molecule, it is necessary to consider methods which eliminate this subjective feature and give the true value. Different methods are available to arrive at the absolute integrated intensity from apparent integrated intensity or from apparent peak intensity and half intensity width or from apparent integrated area. Three methods have been tried in this work and they are

Table 8

Experimental Data on the Analysis of OCN^- in KCl, KBr and KI

Host Lattice		Thickness (cm)	Mass (gm)	Mass of alkali halide added (gm)	Volume ($10^{-2}cm^3$)	Mass of Pellet (gm)	$Log(T_o/T)_{max}$ from NH_4^+ spectrum	OCN^- concentration (micro-moles)	nl Micro-moles/cm^2
	I	0.367	0.2965	0.1137	14.94	0.3396	0.152	0.81	1.99
	II	0.353	0.2374	0.0977	11.96	0.1930	0.124	0.94	2.76
	III	0.335	0.2475	0.1662	12.47	0.3340	0.267	1.45	3.89
KCl	IV	0.351	0.2441	0.0986	13.31	0.3059	0.355	1.74	4.66
	V	0.441	0.2874	0.1021	14.48	0.1915	0.266	2.37	7.23
	VI	0.417	0.2831	0.2130	14.27	0.4037	0.466	2.49	7.29
	VII	0.317	0.1287	0.1508	6.48	0.2275	0.277	1.50	7.33
	I	0.153	0.1556	0.1980	5.65	0.2781	0.180	0.77	2.10
	II	0.210	0.1024	0.2127	3.72	0.2527	0.151	0.61	3.49
	III	0.144	0.0869	0.3021	3.16	0.2834	0.256	1.16	5.27
KBr	IV	0.198	0.2094	0.2159	7.61	0.2645	0.410	2.15	5.61
	V	0.272	0.1751	0.2423	6.37	0.3326	0.340	1.44	6.16
	VI	0.175	0.2207	0.2391	8.02	0.3523	0.712	3.17	6.91

Table 8 - Cont.

Host Lattice		Thickness (cm)	Mass (gm)	Mass of alkali halide added (gm)	Volume ($10^{-2}cm^3$)	Mass of Pellet (gm)	$Log(T_o/T)_{max}$ from NH_4^+ spectrum	OCN^- concentration (micro-moles)	nl Micro-moles/cm^2
KBr	VII	0.253	0.2012	0.2887	7.31	0.3082	0.428	2.22	7.70
	VIII	0.112	0.0813	0.3279	2.95	0.3296	0.505	2.13	8.12
	IX	0.130	0.0504	0.4095	1.83	0.3508	0.307	1.36	9.66
	X	0.164	0.1496	0.3033	5.44	0.3690	0.853	3.51	10.59
	XI	0.292	0.1802	0.4540	6.54	0.3651	0.585	3.32	14.77
	XII	0.138	0.1416	0.2612	5.14	0.1735	0.834	6.70	18.00
KI	I	0.105	0.0480	0.3639	1.53	0.3567	0.118	0.40	2.73
	II	0.096	0.0580	0.3252	1.85	0.3123	0.181	0.65	3.41
	III	0.184	0.0902	0.3768	2.88	0.3939	0.182	0.63	4.02
	IV	0.190	0.1499	0.3044	4.79	0.3663	0.299	1.08	4.27
	V	0.131	0.0944	0.3686	3.01	0.4156	0.316	1.03	4.46
	VI	0.148	0.0912	0.3504	2.91	0.3607	0.280	0.99	5.09
	VII	0.192	0.1315	0.2870	4.20	0.3189	0.314	1.19	5.47
	VIII	0.178	0.0881	0.3460	2.81	0.3560	0.296	1.06	6.70

discussed below.

i) Wilson-Wells Extrapolation Method.

This method is discussed in detail in Appendix I. Only the essential details are mentioned here. The absolute integrated intensity A' and apparent integrated intensity B' differ from each other due to finite slit width . But B' → A' as nl (moles/cm^2) → 0. So the value of B', which can be obtained by dividing the area by nl, is computed at different values of nl for each band. Then B' is plotted against nl. The points are fitted into a straight line by the least square method and the line is extrapolated to zero nl. The intercept gives the value of A'. Then the standard deviation in the intercept is calculated by the method suggested by Beers (2 , p. 41).

ii) Triangular Slit Transform Method.

In the course of the discussion of line shape and intensity (Chapter II, Section c) it was mentioned that the true Lorentian line shape can be corrected for finite slit width, i.e., the true line and the apparent line are related through a slit function, which has been assumed to be triangular in this work. The relationship is

$$\frac{T}{T_o} = \frac{\int e^{-L} f(\omega\omega')\, d\omega}{\int f(\omega\omega')\, d\omega} \tag{26}$$

where

$$L = \ln \frac{I_o}{I} = \frac{a}{(\omega - \omega_o)^2 + b^2} \tag{27}$$

This equation gives the shape of a true line. It can be readily seen that

$$\ln (I_o/I)_{max} = a/b^2 \tag{28}$$

and

$$\Delta\nu^t_{1/2} = 2b \tag{29}$$

To transform an apparent line to true line it is necessary to know the spectral slit width (s) at which the band is recorded, its peak intensity ($\ln (T_o/T)_{max}$) and half intensity width ($\Delta\nu^a_{1/2}$). So the line has three characteristic variables, $s/\Delta\nu^a_{1/2}$, $\ln (T_o/T)_{max}$ and $\Delta\nu^a_{1/2}$. Knowing these and referring to Ramsay's tables (34 , p. 75), it is possible to get to $\ln (I_o/I)_{max}$ and $\Delta\nu^t_{1/2}$. These give the values of 'a' and 'b' according to equations (28) and (29). It is

shown in Appendix I that integrated intensity is

$$A' = \frac{1}{nl} \cdot \pi \cdot \frac{a}{b} \cdot \frac{1}{\omega_o}$$

So this affords another method by which absolute integrated intensity could be obtained. But this method can be adopted only if the experimental absorption curve is Lorentian in shape. Casual examination shows that the bending mode and Fermi doublet of OCN^- are Lorentian in shape while the $\sim$ 2170 cm^{-1} band is not, due to the overlapping hot band. The components of the Fermi doublet are too narrow, having values for $s/\Delta\nu^a_{1/2}$ almost equal to 1, while this value for the bending mode is between 0.67 and 0.85, which fall beyond Ramsay's table. So it was necessary to extend Ramsay's table which was carried out as follows. The values of $\ln (I_o/I)_{max}/\ln (T_o/T)_{max}$ and that of $\Delta\nu^a_{1/2}/\Delta\nu^t_{1/2}$ read from Ramsay's table for a given value of $\log (T_o/T)_{max}$ were plotted against $s/\Delta\nu^a_{1/2}$ and extrapolated over a short range to get an approximate value of these ratios for $s/\Delta\nu^a_{1/2}$ = 0.7. From these values 'a' and 'b' were calculated. Choosing ω_o = 630 cm^{-1} the value of L is computed (equation 27) at different values of ω. The value of e^{-L} was read from an exponential table (29, p. 281-530) and tabulated against the corresponding value of ω.

A suitable value was chosen for s and was divided into 10 equal divisions and at these points the slit function was computed, multiplied by e^{-L} and integration carried out using Simpson's rule (15 , p. 341). This gives the numerator in equation (26). Since a triangular slit function has been assumed the denominator is nothing but the area of the triangle which is equal to s. Dividing one by the other gives the value of T_o/T at a particular slit setting and this was repeated until the band was covered. From the resulting plot $\ln (T_o/T)_{max}$ and $\Delta\nu^a_{1/2}$ were read. Since 'a' and 'b' were assumed, the ratio of $\ln (I_o/I)_{max}$ to $\ln (T_o/T)_{max}$ and that of $\Delta\nu^a_{1/2}$ to $\Delta\nu^t_{1/2}$, for this particular value of $s/\Delta\nu^a_{1/2}$, were computed. This was repeated for other values of $s/\Delta\nu^a_{1/2}$ and $\ln (T_o/T)_{max}$. The results are given in Appendix III.

Using these results the experimental ν_2 band of OCN^- has been compared with Lorentz line shape modified by finite resolving power. Experimental and theoretical data are shown in Figure 12 and the agreement is quite close. In addition the absolute integrated intensities of 630 cm^{-1} band in KCl, KBr and KI have also been obtained and they are given in Table 9.

Table 9

Integrated Intensity of ν_2 Band of OCN^-
in KCl, KBr and KI by Triangular Slit Transform Method

Host Lattice	nl (micromoles/cm^2)	$s/\Delta\nu^a_{1/2}$	$\frac{\Delta\nu^a_{1/2}}{\Delta\nu^t_{1/2}}$	$\frac{\log (I_o/I)_{max}}{\log (T_o/T)_{max}}$	a	b	$A' \times 10^{-2}$
KCl	1.99	0.77	2.62	2.28	0.52	0.68	19.09
	4.67	0.73	1.92	1.90	2.06	0.99	22.27
	7.23	0.79	2.50	3.00	1.92	0.70	18.82
	7.33	0.79	2.50	3.00	1.93	0.70	18.72
						Ave.	19.7±1.4
KBr	3.49	0.77	2.56	2.35	1.13	0.84	18.34
	5.61	0.74	2.04	1.97	1.91	0.86	19.74
	7.70	0.73	1.93	2.09	2.43	0.90	17.44
	14.77	0.78	2.33	2.33	5.54	1.10	16.99
						Ave.	18.1±1.1
KI	2.73	0.77	2.44	2.38	1.29	0.84	28.16
	3.41	0.78	2.42	2.72	1.67	0.83	29.59
	4.27	0.70	1.86	1.95	2.71	1.21	26.23
	5.09	0.67	1.68	1.62	3.53	1.40	24.77

Table 9 - Cont.

Host Lattice	(micromoles/cm^2)	$s/\Delta\nu^a_{1/2}$	$\frac{\Delta\nu^a_{1/2}}{\Delta\nu t_{1/2}}$	$\frac{\log (I_o/I)_{max}}{\log (T_o/T)_{max}}$	a	b	$A' x 10^{-2}$
KI	5.47	0.70	1.80	1.62	2.95	1.25	21.58
	6.7	0.66	1.53	1.59	4.52	1.56	21.63
						Ave.	25.3±3.0

iii) Zero Slit Extrapolation Method.

Another possible method by which absolute integrated intensity could be obtained is by extrapolating the apparent integrated area to zero slit width. The true integrated area (L_a)* and apparent integrated area (L_b)* differ because of finite slit width. So it is to be expected that $L_b \rightarrow L_a$ as $s \rightarrow 0$. So the integrated area is plotted against spectral slit width and extrapolated to zero width and the intercept gives the true integrated area, L_a. This divided by nl gives the absolute integrated intensity. This method has been tried in this work with reasonable success. The spectrum of Fermi doublet and bending mode were recorded at different fixed slit widths. The lowest of these chosen was the one which gave the best resolution. Then the slit was increased in increments of 20 μ which recording the components Fermi doublet, and 50 μ while recording the bending mode and the integrated area was obtained as described earlier.

---

* The definition of L_a and L_b

$$L_a = \int \log_{10} I_o/I \;\; d \log_{10}\omega$$

$$L_b = \int \log_{10} T_o/T \;\; d \log_{10}\omega$$

The data obtained are presented graphically in Figures 13-15 and also in Table 10. Absolute integrated intensities thereby obtained are given in Table 11.

The three methods used in this work to arrive at absolute integrated intensity have been described above in general terms. Next, the detailed results for the individual bands are considered below.

d) Bending Mode.

This band of cyanate is free from overlapping bands and shape is Lorentian. The integrated intensity of this band has been obtained by all the three methods and relevant data are tabulated in Table 12.

e) CO Stretch (Fermi Doublet).

For a complete analysis of polar properties of cyanate ion, the intensity of ν_1 band is required. But actually it is not observed, but transitions from 0 0° 0 to levels which are mixtures of ν_1 and $2\nu_2^{\circ}$ are observed at 1205 cm^{-1} and 1292.6 cm^{-1} in KBr lattice. These are components of Fermi doublet. They are accompanied by less intense bands at 1193 cm^{-1} and 1314 cm^{-1}. These are transitions to Fermi levels formed due to resonance between 1 1' 0 and 0 3' 0. Fermi triplets due to $2\nu 1$, $\nu_1+2\nu_2^{\circ}$ and $4\nu_2^{\circ}$ at 2392 cm^{-1}, 2487 cm^{-1}, 2602 cm^{-1}

Table 10

Spectral Slit Width and Integrated Area of Bending Mode of OCN^{-1} in KBr

Frequency	Mechanical Slit Width (μ)	Spectral Slit Width (cm^{-1})	Integrated Area, $L_b \times 10^4$			
			nl = 2.10 (I)	nl = 3.49 (II)	nl = 5.27 (III)	nl = 7.70 (VII)
	150	2.62				20.57
	190	3.04			14.30	
	200	3.15	8.72			20.39
	210	3.32		10.82		
	250	3.68	8.02	10.50	13.72	20.00
630 cm^{-1}	300	4.21	7.67	10.84	13.90	19.60
	350	4.75	8.00	10.20	13.42	18.63
	400	5.28	8.20	10.38	13.10	18.31
	450	5.81	7.70	9.82	13.12	18.00
	500	6.35	7.45	9.72	13.00	17.40
	550	6.88	7.65	10.03	12.77	17.90

Table 10 - Cont.

Frequency (cm^{-1})	Mechanical Slit Width (μ)	Spectral Slit Width (cm^{-1})	Integrated Area, $L_b \times 10^4$		
			nl = 5.26 (III)	nl = 5.59 (IV)	nl = 7.65 (VII)
1205.5	80	4.40	10.56	13.30	15.91
	100	5.10	10.39	13.13	15.68
	130	6.10	9.75	12.45	14.91
	160	7.20	9.72	12.01	14.16
	180	7.90	9.17	11.51	13.54
	200	8.60	8.89	11.14	13.72
1292.6	80	5.58	13.05	16.03	18.96
	100	6.48	12.67	15.90	18.98
	130	7.83	11.84	14.66	18.07
	160	9.18	12.01	14.17	17.04
	180	10.08	11.03	13.72	16.33
	200	10.98	11.01	13.68	

Table 11

Integrated Intensity of OCN^- in KBr Lattice
by Slit Extrapolation Method

Band Frequency (cm^{-1})	nl (micromoles/cm^2)	$L_a \times 10^4 \times (2.303)^2$	A' (in 10^2 $mole^{-1}cm^2$)	
630				
	2.10	47.67	22.7	
	3.49	61.07	17.5	
	5.27	77.99	14.8	
	7.70	122.43	15.9	Ave. 17.7±3.0
1205.5				
	5.26	66.80	12.7	
	5.59	84.40	15.1	
	7.65	100.90	13.2	Ave. 13.7±1.0
1292.6				
	5.26	94.68	18.0	
	5.59	97.82	17.5	
	7.67	111.98	14.6	Ave. 16.7±1.5

Table 12

Intensity Data for ν_2 (Bending Fundamental 620-640 cm^{-1})

Host Lattice and Sample		Mechanical Slit Width (μ)	Spectral Slit Width (cm^{-1})	$\Delta\nu^a_{1/2}$ (cm^{-1})	$\ln(T_o/T)_{max}$	$\frac{B' \times 10^{-2}}{(2.303)^2}$ ($mole^{-1}cm^2$)	$A' \times 10^{-2}$ ($mole^{-1}cm^2$) Method a	Method b	Method c
KCl	I			3.6	0.49	3.56		19.09	
	IV			3.2	1.10	3.40		22.27	
	V			3.2	1.30	2.50		18.82	
	VII	160	2.785	3.8	1.31	2.40	21.5±1.1	18.72	
	III			3.2	0.52	3.14		Ave. 19.7±1.4	
	VI			3.8	1.09	2.09			
KBr	I	210	3.32	4.3	0.65	3.3			22.7
	II	150	2.61	3.5	1.31	3.3		21.00	17.5
	IV	150	2.61	3.5	1.43	2.8		19.74	
	XI	250	3.68	4.7	1.71	2.1	19.1±0.9	17.44	15.9
	III	190	3.04	3.6	0.44	2.8		16.99	
	XII	250	3.68	6.2	1.60	2.3		Ave. 18.8±1.6	14.8
									Ave. 17.7±3.0

Table 12 - Cont.

Host Lattice and Sample	Mechanical Slit Width (μ)	Spectral Slit Width (cm^{-1})	$\Delta\nu^{a}_{1/2}$ (cm^{-1})	$\ln(T_o/T)_{max}$	$\frac{B' \times 10^{-2}}{(2.303)^2}$ ($mole^{-1}cm^2$)	$A' \times 10^{-2}$ ($mole^{-1}cm^2$) Method a	Method b	Method c
I					4.56			28.16
II					4.09			29.59
IV					3.76			26.33
KI VI	200	3.15			3.80	27.6±2.4		24.77
VII					4.09			21.58
VIII								21.63
III					4.56			Ave. 25.32±3.0

Method a is Wilson-Wells Method.
Method b is Triangular Slit Transform Method.
Method c is Zero Slit Extrapolation Method.

and $2\nu_1+\nu_3$, $\nu_1+2\nu_2^{\circ}+\nu_3$ and $4\nu_2^{\circ}+\nu_3$ at 4524.7, 4623.0 and 4737.5 cm^{-1} have been observed and transition to Fermi triplets is from the ground state (23 , p. 774). It is clear from these considerations that to compute the intensity of ν_1 band it is only the area under 1205.5 cm^{-1} and 1296.6 cm^{-1} band which should be taken into account. The intensity of these bands have been obtained by Wilson's extrapolation method and by the slit extrapolation method only in KBr lattice and data are given together in Table 13 for purposes of comparison. Additional details are found in Table 10.

f) <u>CN Stretch</u>.

To study the intensity of a band, the concentration of the absorbing molecule should be such that the maximum percent absorption is between 30 and 70. This ensures accurate results. Unfortunately, this band being too intense, 70% absorption corresponds to very low concentration which cannot be analyzed by the method adopted. So it was imperative to choose crystals of high concentration and % absorption of crystals chosen was between 80-95%. Since concentrated crystals were chosen it was possible to observe the C^{13} peak, which has an absorption of 15-20%. While scanning this band, suitable gear ratio was used such that the two bands were well separated,

Table 13

Intensity Data for ν_1 and $2\nu_2$ (CO Stretch, Bend Overtone (1200-1300 cm^{-1})

Host Lattice and Sample	Frequency (cm^{-1})	nl umoles/cm^2	Mechanical Slit Width (μ)	Spectral Slit Width (cm^{-1})	$\frac{B' \times 10^{-2}}{(2.303)^2}$ $mole^{-1}cm^2$	$A' \times 10^{-2}$ ($mole^{-1}cm^2$) Method a	Method b
KCl I	1210.7	1.980	60	3.7	1.87	10.9±0.3	
KCl III		3.87			1.90		
KCl IV		4.64			1.87		
KCl V		7.19			1.68		
KCl VI		7.29			1.64		
KCl I	1297.3	1.985	60	4.68	2.92	17.2±0.4	
KCl III		3.88			2.73		
KCl IV		4.65			2.71		
KCl V		7.21			2.30		
KCl VI		7.27			2.05		
KCl VII		7.31			2.18		

Table 13 - Cont.

Host Lattice and Sample	Frequency (cm^{-1})	nl umoles/cm^2	Mechanical Slit Width (μ)	Spectral Slit Width (cm^{-1})	$\frac{B' \times 10^{-2}}{(2.303)^2}$ $mole^{-1}cm^2$	$A' \times 10^{-2}$ ($mole^{-1}cm^2$) Method a	Method b
II		3.47			2.35		
III		5.26			2.01		12.7
IV		5.59			2.37		15.1
VI	1205.5	6.68	80	4.4	2.14	13.5±0.6	
VII		7.65			2.08		13.2
XI		14.72			1.62		Ave. 13.7±1.0
KBr							
II		3.47			2.87		
III		5.26			2.48		18.0
IV		5.59			2.86		17.5
VI	1292.6	6.68	80	5.58	2.78	16.7±1.6	
VII		7.65			2.47		14.6
XI		14.72			2.02		Ave. 16.7±1.5

Table 13 - Cont.

Host Lattice and Sample		Frequency (cm^{-1})	nl umoles/cm^2	Mechanical Slit Width (μ)	Spectral Slit Width (cm^{-1})	$\frac{B' \times 10^{-2}}{(2.303)^2}$ $mole^{-1}cm^2$	$A' \times 10^{-2}$ ($mole^{-1}cm^2$) Method a	Method b
	I		2.71			3.34		
	II		3.99			3.25		
	V		4.43			3.03		
	VI	1200.8	5.06	60	3.7	2.89	20.9±1.4	
	VII		5.44			3.13		
	VIII		6.66			2.44		
KI	I		2.72			4.28		
	II		3.39			3.37		
	III		4.00			4.28		
	IV		4.26			3.71		
	V	1288	4.45	60	4.68	3.64	24.92±2.5	
	VI		5.07			3.16		
	VII		5.45			3.76		
	VIII		6.67			3.10		

Method a is Wilson-Wells Method
Method b is Slit Extrapolation Method

indicated in Figure 2. Still there is a region in which the intensity is shared. To apportion the intensity between these two, the two bands are symmetrically extended on the lower and higher frequency side as the case may be and the area under the symmetric band is computed. This procedure is quite reasonable when the intensity of one of the bands is low compared to the other. The error introduced is 2% in the case of the stronger band and 10% in the case of the weaker band. So the error in the area of the stronger band is within experimental error. The experimentally measured intensity of this band in KCl, KBr and KI is shown in Figure 8. The absolute integrated intensity of this band has been obtained only by the Wilson-Wells method. Triangular slit transform method could not be adopted since the shape of this band is not Lorentian due to overlapping bands. Though this band was recorded at different slit widths, the particular crystals used could not be analyzed for their cyanate concentration since they were too dilute. Hence the integrated intensity of this band has not been obtained by slit extrapolation method. The intensity obtained by Wilson-Wells method is tabulated in Table 14.

To study this band it was imperative to chose crystals of high concentration and consequently it was possible to observe the C^{13} peak. The natural abundance

Table 14

Intensity Data for ν_3 (CN Stretch 2100-2200 cm^{-1})

Host Lattice and Specimen		nl umoles/cm^2	Mechanical Slit Width (u)	Spectral Slit Width (cm^{-1})	$\frac{B' \times 10^{-2}}{(2.303)^2}$ ($mole^{-1}$ cm^2)	$A' \times 10^{-2}$ $mole^{-1}$ cm^2
	I	1.99			8.77	
	III	3.89			9.22	
KCl	IV	4.66	30	15.17	9.48	48.00±10.28
	V	7.23			8.93	
	VII	7.33			7.35	
	V	6.16			9.36	
	VI	6.91			9.00	
KBr	VIII	8.12	30	15.17	8.40	55.37±2.6
	IX	9.66			8.60	
	X	10.59			8.33	
	III	4.02			16.33	
	IV	4.27			13.59	
KI	V	4.46	30	15.17	15.13	81.94±14.05
	VII	5.47			15.71	
	II	3.40			14.88	

of C^{13} is 1.1% and so it is to be expected that the intensities of C^{12} and C^{13} should be in this ratio. But the actual value are very much different. The explanation for the discrepancy is that the absorption of C^{13} is low which has varied between 10-25% and under such circumstances the intensity measurement may not be accurate. On the other hand, it may be true that the area under C^{12} peak is not accurate, since its absorption is too large. Since the absorption of C^{13} peak is maximum in the KI crystals, the area under it has been computed in this case only and the $(\partial\mu/\partial Q)$ value has been calculated by the usual procedure and the data are given in Table 15. It is to be pointed out, though embarassing, that there is wide difference between the value thus obtained and the value obtained from the area under C^{12}, though they have to be the same and it is comparable to those of CO_2 and N_2O which are isoelectronic with OCN^-. Similar calculations could not be done with KCl and KBr since it was noticed that apparent integrated intensity varied between extremes, indicating that the measurement of area under C^{12} peak is inaccurate because of low absorption.

Table 15

Intensity Data for ν_3 of $OC^{13}N$
(CN Stretch 2099 cm^{-1}) in KI

nl in 10^{-8} moles/cm^2	$\frac{B' \times 10^3}{(2.303)^2}$ ($mole^{-1}cm^2$)	$A' \times 10^{-3}$ $mole^{-1}cm^2$	$\pm \partial\mu/\partial Q$ esu $g^{-1/2}$
2.99	7.02		
3.75	6.56		
4.42	8.00		
4.70	6.70	41.26	±289.
4.90	6.40		
5.60	5.39		
6.01	7.01		

g) Dipole Moment and its Derivatives.

The main object of this work is to compute $\partial\mu/\partial Q$, $\partial\mu/\partial r$ and μ values for OCN^-. ($\partial\mu/\partial Q$) values have been calculated using the relation (22) which involves a correction for the polarizability of the solvent. The refractive index used is that of the alkali halide at band frequency. Dipole moment and its derivatives computed have ambiguity in sign. They are presented as such in this section and taken up later to decide their sign. As usual each band of OCN^- has its own peculiarity and so is considered individually.

i) Dipole moment Derivative with Respect to Q_3.

The computation of this is straight forward and the values obtained are tabulated in Table 16.

Table 16

$(\partial\mu/\partial Q_3)$ Values for OCN^- in KCl, KBr and KI

Host Lattice	$\pm(\partial\mu/\partial Q_3)$ esu $g^{-1/2}$
KCl	106.7
KBr	111.7
KI	130.6

ii) Dipole Moment Derivative with Respect to Q_1.

It has been pointed out that the intensity of ν_1 band can be arrived at from the intensity of Fermi doublet, which means that $\partial\mu/\partial Q_1$ value can be obtained from the intensities of Fermi doublet. In harmonic oscillator approximation the intensity of a band is the sum of all intensities due to transitions differing in quantum number by 1. This has been taken into consideration in deriving the expression (5). A brief discussion given earlier indicates that Fermi doublets are due to single transitions and there is no overlapping of intensity on them due to transitions from excited states.

Consequently, equation (5) is not valid in this case and has to be suitably modified. To make the treatment less ambiguous, the transition moment matrix elements have been computed first and then the $\partial\mu/\partial Q$ values. Recalling an earlier step that led to equation (5)

$$\int \alpha(\nu)\,\frac{d\nu}{\nu} = \frac{8\pi^3}{3hc}\,|u_{oj}|^2\,(N_o - N_j)$$

$$= \frac{8\pi^3}{3hc}\,|u_{oj}|^2\,\frac{N}{2}\left\{1 - \mathrm{Exp}\,\frac{-hc\,\omega_{oj}}{kT}\right\}$$

$$= \frac{8\pi^3}{3hc}\,|u_{oj}|^2\,N\left\{1 - \mathrm{Exp}\,\frac{-hc\,\omega_{oj}}{kT}\right\}^2$$

$$= \frac{8\pi^3}{3hc}\,|u_{oj}|^2\,N'$$

where

$$N' = N\left\{1 - \mathrm{Exp}\,\frac{-hc\,\omega_{oj}}{kT}\right\}^2$$

Since N and ω_{oj} are known, N' can be computed.

$$A' = \frac{1}{N'l}\int \alpha(\nu)\,\frac{d\nu}{\nu} = \frac{8\pi^3}{3hc}\,|u_{oj}|^2\left(\frac{n^2+2}{3}\right)^2\frac{1}{n}$$

After correcting for refractive index of the medium. The wave function for higher and lower Fermi levels are respectively

$$\psi_I = a\psi_{10^\circ 0} - b\psi_{02^\circ 0}$$

$$\psi_{II} = b\psi_{10^\circ 0} + b\psi_{02^\circ 0}$$

For ω_{oj} = 1292.6 (in KBr)

$$A' = \frac{8\pi^3}{3hcn} \cdot \left(\frac{n^2+2}{3}\right)^2 \left[\psi_o \mu (a\psi_{10^\circ 0} - b\psi_{02^\circ 0}) d\tau\right]^2$$

$$= \frac{8\pi^3}{3hcn} \cdot \left(\frac{n^2+2}{3}\right)^2 \left[aM_+ - bM_-\right]^2$$

where

$$M_+ = \int \psi_o \mu \psi_{10^\circ 0} d\tau$$

and

$$M_- = \int \psi_o \mu \psi_{02^\circ 0} d\tau$$

$$aM_+ - bM_- = \pm\sqrt{\frac{3hcA'n}{8\pi^3}} \left(\frac{3}{n^2+2}\right)$$

For ω_{oj} = 1205.5 (in KBr)

$$A' = \frac{8\pi^3}{3hcn} \cdot \left(\frac{n^2+2}{3}\right)^2 \left[\int \psi_o \mu (b\psi_{10^\circ 0} + a\psi_{02^\circ 0}) d\tau\right]^2$$

So

$$bM_+ + aM_- = \pm \sqrt{\frac{3hcA'n}{8\pi^3}} \left(\frac{3}{n^2+2}\right)$$

It has been shown in an earlier section (Chapter II, section e) that 'a' and 'b' can be expressed in terms of Δ, the difference between the perturbed levels, and Δ_o, the difference between the unperturbed levels. Δ is practically the same in all the three cases and it is assumed Δ_o is also the same. a = 0.7337, b = 0.6663. Since each of the simultaneous equations to be solved to arrive at M_+ and M_- have two possible values, each of the transition moment matrix elements has four possible values. They are tabulated in Table 17. The values with * mark cannot be accepted, since they indicate that overtone is stronger than the fundamental which is unreasonable. From the accepted values of M_+ and M_-, $\partial\mu/\partial Q_1$ and $\partial^2\mu_z/\partial Q^2_2$ are computed.

$$M_+ = \int \psi_o \mu \psi_{10^\circ 0} d\tau = \left(\frac{h}{8\pi^2 \nu_{10^\circ 0}}\right)^{1/2} \frac{\partial \mu}{\partial Q_1}$$

$$M_- = \int \psi_o \mu \psi_{02^\circ 0} d\tau$$

Since in this transition an overtone level is involved,

Table 17

Possible Values for M_+ and M_-

Host Lattice	Possible Signs of Simultaneous Equations	$M_+ \times 10^{20}$	$M_- \times 10^{20}$
KCl	$\begin{matrix} + & + \\ - & - \end{matrix}$	± 9.26	∓ 0.54
	$\begin{matrix} + & - \\ - & + \end{matrix}$	± 1.57	$\mp 9.14^*$
KBr	$\begin{matrix} + & + \\ - & - \end{matrix}$	± 9.38	± 0.03
	$\begin{matrix} + & - \\ - & + \end{matrix}$	± 1.02	$\mp 11.1^*$
KI	$\begin{matrix} + & + \\ - & - \end{matrix}$	± 11.16	∓ 0.15
	$\begin{matrix} + & - \\ - & + \end{matrix}$	± 1.092	$\mp 11.11^*$

the quadratic terms in Taylor series expansion of dipole moment have to be included.

$$\mu = \mu_o + \left(\frac{\partial \mu}{\partial Q_2}\right)_o Q_2 + \frac{1}{2}\left(\frac{\partial^2 \mu}{\partial Q_2^2}\right)_o Q_2^2 + \ldots.$$

$$M_- = \int \psi_o \left(\mu_o + \left(\frac{\partial \mu}{\partial Q_2}\right)_o Q_2 + \frac{1}{2}\left(\frac{\partial^2 \mu}{\partial Q_2^2}\right)_o Q_2^2\right)$$

$$\psi_{02^\circ 0} d\tau$$

The integrand involving Q_2^2 is nonvanishing while the other two are zero (50, p. 290). So

$$M_- = 1/\sqrt{2} \cdot \frac{h}{8\pi^2 \nu_{02^\circ 0}} \cdot \frac{\partial^2 \mu}{\partial Q_2^2}$$

$\nu_{00^\circ 0 - 02^\circ 0}$ are computed from anharmonicity constants given by Maki (22, p. 131). Since no accurate data are available for the KCl lattice, the second derivative of the dipole moment is not computed in this case. Table 18 includes values of $\partial\mu/\partial Q_1$ and $\partial^2\mu/\partial Q_2^2$.

Table 18

$(\partial\mu/\partial Q_1)$ and $(\partial^2\mu/\partial Q_2^2)$ Values for OCN^- in KCl, KBr and KI Lattices

Host Lattice	$\pm(\partial\mu/\partial Q_1)$ esu $g^{-1/2}$	$\pm(\partial^2\mu/\partial Q_2^2)$ esu $cm^{-1}g^{-1}$
KCl	61.86	
KBr	62.28	1.89×10^{20}
KI	74.58	9.44×10^{20}

iii) Dipole Moment Derivative with Respect to Internal Coordinates.

At this stage it is necessary to calculate normal coordinates of OCN^- ion so that $(\partial\mu/\partial Q)$ values can be

transformed into $(\partial \mu / \partial r)$ values. The potential function for the harmonic motion of cyanate ion is

$$2V = F_{11}r_1^2 + F_{22}r_2^2 + F_{12}r_1r_2$$

where r_1 is O-C distance and r_2 is C-N distance and F_{11} and F_{22} are the corresponding force constants and F_{12} is interaction force constant. The bending coordinate is ignored in the above expression since it does not interact with stretching modes. Assuming such a potential function the force constant for OCN^- in KBr and KI lattices have been calculated by Maki (22 , p. 135). For KCl lattice force constant similar to that in KBr has been assumed. They are given in Table 19.

Table 19

Force Constant in mdynes/Å for OCN^- in KCl, KBr and KI Lattices

Host Lattice	F_{11}	F_{22}	F_{12}
KCl	11.003	15.879	1.422
KBr	11.003	15.879	1.422
KI	11.028	15.512	1.352

It has been shown that

$$(FG - E\lambda)(L^{-1})'_k = 0$$

$\lambda = 4\pi^2\omega_o^2$ where ω_o is equilibrium frequency. The elements of L^{-1} matrix are needed to transform dipole moment derivative with respect to normal coordinate to dipole moment derivative with respect to internal coordinate. The calculation is shown in detail for the case of potassium iodide. Since force constant in this lattice is known, the equilibrium frequencies are calculated with the aid of equation

$$(FG - E\lambda_k) = 0$$

If force constant is in mdynes/Å and masses in AMU.

$$\lambda = \left(\frac{\omega_o}{1303.2}\right)^2$$

The elements of G matrix are

$$G_{11} = \mu_o + \mu_C$$

$$G_{22} = \mu_C + \mu_N$$

$$G_{12} = G_{21} = -\mu_C$$

where u's are reciprocal AMU

$$\left| FG - E\lambda_1 \right| \begin{vmatrix} 0.57039 & -0.70949 \\ -1.09502 & +1.36206 \end{vmatrix} = 0$$

These simultaneous equations give

$$\frac{L_{11}^{-1}}{L_{12}^{-1}} = 1.24386 \text{ (Average)}$$

$$\left| FG - E\lambda_2 \right| \begin{vmatrix} -1.36206 & -0.70949 \\ -1.09502 & -0.57039 \end{vmatrix} = 0$$

These simultaneous equations give

$$\frac{L_{21}^{-1}}{L_{22}^{-1}} = -0.52089 \text{ (Average)}$$

To determine the values of elements of L^{-1} elements uniquely, the following normalizing condition is used

$$(L^{-1})'(L^{-1}) = G^{-1}$$

The inverse G elements are computed from the following condition

$$\sum_{t'} G_{tt'} \, G_{t't''}^{-1} = \quad {}_{tt''}$$

where ${}_{tt''} = 1$ if $t = t''$, otherwise zero. The inverse G elements are

$$G_{11}^{-1} = 16.4412 \times 10^{-24}$$

$$G_{22}^{-1} = 15.49650 \times 10^{-24}$$

$$G_{12} = 8.85363 \times 10^{-24} = G_{21}^{-1}$$

From the ratio of L^{-1} elements and the equations that relate L^{-1} elements to G^{-1} elements, L^{-1} elements are solved. They are given below.

$$L_{11}^{-1} = \pm 3.85213 \ (+)$$

$$L_{12}^{-1} = \pm 3.09692 \ (+)$$

$$L_{21}^{-1} = \pm 1.26583 \ (+) \qquad (\text{in } 10^{-12})$$

$$L_{22}^{-1} = \pm 2.43014 \ (-)$$

$$Q_k = \sum_{t} (L^{-1})_{kt} \, rt$$

When normal coordinate Q_1 changes in positive sense both r_1 and r_2 increase while the change in normal coordinate Q_1 increases r_1 and decreases r_2. Based on this, the sign for L^{-1} elements are decided and they are indicated beside the corresponding values. Using the following two equations $\partial\mu/\partial r_1$ and $\partial\mu/\partial r_2$ are calculated.

$$\frac{\partial\mu}{\partial r_1} = \frac{\partial\mu}{\partial Q_1} L_{11}^{-1} + \frac{\partial\mu}{\partial Q_2} L_{21}^{-1}$$

$$\frac{\partial\mu}{\partial r_2} = \frac{\partial\mu}{\partial Q_1} L_{12}^{-1} + \frac{\partial\mu}{\partial Q_2} L_{22}^{-1}$$

Similar calculations are carried out for KBr and KCl lattices and results are given in Table 20.

iv) <u>Dipole Moment</u>.

Intensity of the bending mode of cyanate ion gives the dipole moment of the molecule.

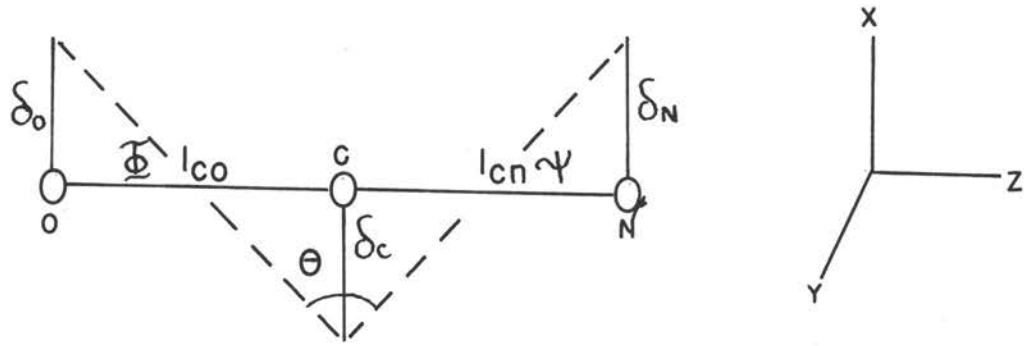

* The normal coordinate 3 is represented by Q_2 for the sake of convenience while in other places it is represented by Q_3.

Table 20

$(\partial\mu/\partial r)$ Values for OCN^-
in KCl, KBr and KI Lattices

Host Lattice	$(\partial\mu/\partial Q_1)$ / $(\partial\mu/\partial Q_2)$	$(\partial\mu/\partial r_1)$ (in 10^{-10} esu)	$(\partial\mu/\partial r_2)$ (in 10^{-10} esu)
KCl	+	± 3.69	± 0.73
	−	± 1.08	± 4.52
KBr	+	± 3.77	± 0.84
	−	± 1.04	± 4.65
KI	+	± 4.52	± 0.86
	−	± 1.22	± 5.48

$$\Phi = \frac{\delta_o - \delta_c}{l_{CO}} \qquad \psi = \frac{\delta_N - \delta_C}{l_{CN}} \qquad \theta = \Phi + \psi$$

$$\mu_z = \mu_{CN} \cos\psi - \mu_p \cos\Phi$$

$$\mu_x = \mu_{CN} \sin\psi + \mu_p \sin\Phi$$

$\mu_p = \mu_{CO}$

$$\left(\frac{\partial^2 u_z}{\partial\theta^2}\right)_o = -\mu_{CN}\left(\frac{\partial\psi}{\partial\theta}\right)^2 + \mu_p\left(\frac{\partial\Phi}{\partial\theta}\right)^2$$

$$\left(\frac{\partial\mu_x}{\partial\theta}\right)_o = \mu_{CN}\frac{\partial\psi}{\partial\theta} + \mu_p\frac{\partial\Phi}{\partial\theta}$$

If C_α is the equilibrium distance from center of gravity

$$m_o C_o + m_C C_C + m_N C_N = 0 \qquad (1)$$

$$m_O C_O \;\; {}_O + m_C C_C \;\; {}_C + m_N C_N \;\; {}_N = 0$$

$$m_O C_O \frac{\partial \delta_O}{\partial \theta} + m_C C_C \frac{\partial \delta_C}{\partial \theta} + m_N C_N \frac{\partial \delta_N}{\partial \theta} = 0 \qquad (2)$$

$$l_{CO} \frac{\partial \Phi}{\partial \theta} = \frac{\partial \delta_O}{\partial \theta} - \frac{\partial \delta_C}{\partial \theta} \qquad (3)$$

$$l_{CN} \frac{\partial \Psi}{\partial \theta} = \frac{\partial \delta_N}{\partial \theta} - \frac{\partial \delta_C}{\partial \theta} \qquad (4)$$

Using (1), expressions for C_α's in terms of masses and interatomic distance can be derived. Using these and (2), (3) and (4) it can be shown that

$$\frac{\partial \Phi}{\partial \theta} \quad \frac{\partial \Psi}{\partial \theta} = \frac{l_{CN} m_N \left[(m_O + m_C)\, l_{CN} + m_O l_{CO} \right]}{l_{CO} m_O \left[(m_C + m_N)\, l_{CO} + m_N l_{CN} \right]}$$

Using this and the other relation that

$$\partial \Psi / \partial \theta + \partial \Phi / \partial \theta = 1$$

the absolute values of $\partial \Phi / \partial \theta$ and $\partial \Psi / \partial \theta$ can be obtained.

$$\partial \Phi / \partial \theta = 0.481$$

$$\partial \Psi / \partial \theta = 0.519$$

$$\frac{\partial \mu_x}{\partial \theta} = \frac{\partial \mu_x}{\partial Q_3} \cdot \frac{\partial Q_3}{\partial \theta} = \frac{\partial \mu}{\partial Q_3} L_{33}^{-1}$$

$$(L^{-1})_{33} (L^{-1})_{33} = G_{33}^{-1} = 1/G_{33}$$

$$L^{-1}_{33} = \sqrt{\frac{1}{G_{33}}}$$

$$G_{33} = \frac{\mu_O}{l_{CO}^2} + \frac{\mu_{CN}}{l_{CN}^2} + \mu_C \left[\frac{1}{l_{CO}^2} + \frac{1}{l_{CN}^2} + \frac{2}{l_{CO} l_{CN}} \right]$$

$$= 2.000 \times 10^{39}$$

$$G_{33}^{-1} = 5.000 \times 10^{-40}$$

$$L_{33}^{-1} = 2.24 \times 10^{-20}$$

Since the second derivative of the dipole moment could not be accurately obtained in KCl, due to reasons mentioned earlier, the dipole moment of CNO^-, only in KBr and KI lattices have been computed.

	KBr	KI
$\partial \mu_x / \partial \theta$	$\pm 56.53 \times 10^{-20}$	$\pm 65.31 \times 10^{-20}$
$\partial^2 \mu_z / \partial \theta^2$	$\pm 9.45 \times 10^{-20}$	$\pm 47.20 \times 10^{-20}$

Solving the following two simultaneous equations, the individual band moments are obtained and they are tabulated in Table 21.

$$\frac{\partial^2 \mu_z}{\partial \theta^2} = -\mu_{CN}\left(\frac{\partial \psi}{\partial \theta}\right)^2 + u_{CO}\left(\frac{\partial \Phi}{\partial \theta}\right)^2$$

$$\frac{\partial \mu_x}{\partial \theta} = \mu_{CN}\ \frac{\partial \psi}{\partial \theta} + \mu_{CO}\ \frac{\partial \Phi}{\partial \theta}$$

Table 21

Bond Moments of OCN in KBr and KI in Debyes

	$\frac{(\partial \mu_x/\partial \theta)}{(\partial^2 \mu_z/\partial \theta^2)}$	u_{CO}	u_{CN}
KBr	+	±0.81	±0.34
	-	±0.41	±0.70
KI	+	±1.69	±0.30
	-	±0.27	±1.51

VI. DISCUSSION

Up to the present time, the intensity investigations carried out have been concerned with the gas phase or the liquid phase. The solid phase intensity work appears to be at its infancy.

In the work involving the gas phase, the lines of rotational fine structure accompanying the vibrational-rotational bands in a gas are too narrow to carry out absolute intensity measurements. This is a consequence of the limited resolving power of the instrument. To overcome this difficulty and make it possible to apply the Wilson-Wells extrapolation theorem for absolute intensity measurements, the lines are broadened by increasing the pressure. But the absence of rotational lines in the spectrum of a molecule in the solid phase gives rise to narrow bands and it is but natural to question whether reliable intensity data could be obtained under such circumstances. In addition, other problems to be faced in solid phase intensity work are scattering and reflection at the solid surface. These phenomena are dependent on the particle size. These points have to be borne in mind while considering the results that are obtained in solid phase work. The analytical method used in this work, though proven to

be quite satisfactory, is perhaps responsible to a large extent in introducing error in the results. In preparing calibration curves for the three alkali halides, the ammonium salt used was NH_4Cl. It may be argued that NH_4^+ in the pellet is surrounded by ions of different polarizability, which affect the intensity of NH_4^+ peak. The corresponding ammonium halide could have been used; however, it may be argued that the very low concentration (in the ratio of 1:2000) of chloride ion would not alter the situation very much.

The solid solution of NH_4Cl and alkali halide were made by freeze drying an aqueous solution. A similar procedure was adopted in analyzing the crystal. To ensure uniform distribution of the NH_4^+ or OCN^-, as the case may be, the solution was swirled in the flask a large number of times. Different portions of the freeze dried sample were taken and spectrum was run and the peak intensity differed by 1%. In addition, the pellet was mounted in different positions and spectrum scanned. There was hardly any difference between different scans, thus indicating that there is uniform distribution both in the freeze dried sample and in the pellet.

Particle size in the pellet could vitiate the results to a considerable extent due to scattering losses. It has been observed by Stewart (39, p. 43)

that transmittance is not considerably altered over a wide range of particle radii (from 10-30 μ) provided the absorption coefficient is low. The latter condition is true in this work. Though no attempt has been made to measure the particle size in the pellets, it can be taken that it is within reasonable limit, since a good Beer's law plot has been obtained in NH_4^+ calibration. The analysis of the crystal has been carried out under identical conditions and so it can be taken for granted that no sizable error has been introduced due to particle size in the quantitative analysis of the crystal.

Another source of error is due to inhomogeneous distribution of cyanate in single crystal. When a single crystal is pulled out from the melt, a concentration gradient exists in the crystal. An attempt is made here to estimate the error by considering extreme cases, which may not be true in an actual situation. The concentration gradient may be across the length of the crystal or may be along the height, as shown in Figure 17. The two cases are considered separately.

Considering the case where the concentration gradient exists along the length, the crystal is portioned to a number of blocks differing in thickness and concentration. If I_o is the intensity of incident radiation and I_1, I_2 .... I_{n-1} are the intensities of

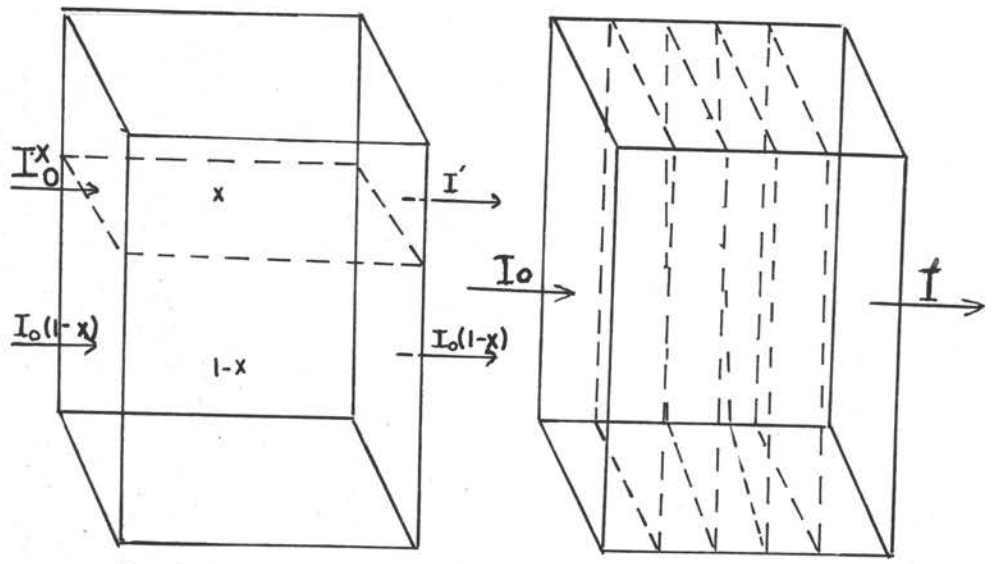

Figure 17

radiation entering blocks 2, 3 .... n and I the intensity of transmitted radiation, the following relations hold good.

$$c_1 l_1 \alpha_1 = \ln I_o/I_1$$

$$c_2 l_2 \alpha_2 = \ln I_1/I_2$$

$$c_n l_n \alpha_n = \ln I_{n-1}/I$$

So

$$\ln I_o/I = (\alpha_1 c_1 l_1 + \alpha_2 c_2 l_2 + \ldots\ldots \alpha_n c_n l_n)$$

The experimentally measured absorption coefficient is

given by the relation

$$\ln I_o/I = \alpha_x cl$$

where n and l are the total concentration and total length of the crystal, respectively, and α_x is the experimentally measured absorption coefficient. If each block is assumed to be infinitesimally small, the distribution of molecule is uniform and absorption coefficient would be the same. This would be the absorption coefficient in the crystal if the distribution is uniform. Representing this by α_t

$$\alpha_x/\alpha_t = \frac{c_1l_1 + c_2l_2 + c_3l_3 + \ldots . c_nl_n}{cl}$$

In a situation like this it is hard to estimate the error in the experimental value of α_x in the absence of definite values of c_i's and n_i's. But certain cases can be considered. For example, the crystal can be divided into two equal blocks, one of which is completely free from absorbing material while in the other all the molecules are concentrated. This introduces 100% error in the experimentally measured value which is highly unreasonable. In the absence of reliable data it is difficult to estimate error due to inhomogeneous distribution of cyanate ion in the crystal. In the other

case, as shown in Figure 17, a simple situation is envisaged in which a part of the crystal is free from absorbing molecule and it is concentrated entirely in one part. The following relations can be readily written down.

$$\alpha_t = (x/cl)\ (\ln xI_o/I)$$

$$\alpha_x = \frac{1}{cl} \ln \frac{I_o}{I' + (1-x)I_o}$$

where α_t and α_x are true and experimentally measured absorption coefficient. Using these two equations a relation between α_t and α_x can be derived which is

$$e^{-\alpha_x \cdot cl} = (1-x) + xe^{-\alpha_t \cdot cl/x}$$

A similar equation has been derived by Norman Jones ([18]) and it has been estimated by him that for a 10% freely transmitting space and for a true optical density of 1.5, the error in experimentally measured absorption coefficient could be as high as 39%. The error that has been computed in these two cases is for the absorption coefficient and not for integrated intensity. But it has been observed in this work that a change in peak intensity results in a corresponding change in integrated area. So a 39% error in absorption coefficient may introduce a similar error in integrated intensity. In the absence

of any precise data on the fraction of freely transmitting space, it is not possible to estimate the error due to inhomogeneous distribution. The object of this consideration is to explain the scattering in points in the intensity measurements. In most cases the error is within ±10% which is within experimental error and it can be safely said that error due to inhomogeneous distribution is not significant. The scattering is due to 1) limitations of the analytical method, 2) lack of correspondence between integrated intensity and concentration. The scattering is much in the case of intensity measurement of antisymmetric stretch mode. Due to limitations of the analytical method, it was necessary to choose crystals of high concentration and consequently intensity measurements are not very accurate. The error in this case has been estimated to be ±20% while in other cases it is within ±10% which is quite reasonable.

In the case of the ν_2 band of OCN^- in KBr and KCl, the area under the band was computed up to 10 cm^{-1} on either side of the band maximum and wing correction was applied by the method suggested by Ramsay (34 , p. 78), which amounted to 4-5% in most cases. The residual area was also obtained by counting squares and it also amounted to 4-5%, indicating that there was no necessity for wing correction. This situation indicates that

infrared bands of molecules in solids, which are sharp and do not extend over a wide range as in the case of liquids, could be profitably used to settle some controversial questions like temperature dependence of peak intensity and integrated intensity.

It was pointed out earlier that the absorption band of a molecule in solid solution is narrow compared to the resolving power of the instrument. Under such circumstances it is claimed that the intensity data is not reliable. The results that have been obtained for dipole moment derivative with respect to C-O distance is of the same order of magnitude as in CO_2, though it is less. CO bond in OCN^- has a different bond order and force constant from that in CO_2. Though there is no definite correlation between bond order and bond intensity, a different value for this in OCN^- from that in CO_2 seems plausible or it may be that the $\partial\mu/\partial Q_1$ value that has been obtained is unreliable. The question can be only settled by working with enriched $OC^{13}N^-$. The intensity of ν_2 band and that of the components of Fermi doublet are reliable since agreeing values have been obtained by independent methods. So it can be said that though the solid phase intensity work has to be done under adverse circumstances, reliable results can be obtained. But the situation can be improved by using

high resolving power instrument, preferably a grating instrument. But nothing definite can be said in the absence of experimental data.

Due to ambiguity in the sign of $\partial\mu/\partial Q$ values, two pairs of values, each equal in magnitude but opposite in sign, for dipole moment and its derivative with respect to internal coordinate have been obtained. To choose between these values, it is necessary to consider the electronic structure of OCN^-. The following two resonance forms are possible for OCN^-

1) $O{=}C{=}N^-$

2) $^-O{-}C{\equiv}N$

The structure (2) is more probable than (1), as pointed out by Maki and Decius (23 , p. 780).

Two possible values, depending on whether $(\partial\mu/\partial Q_1)/(\partial\mu/\partial Q_3)$ is positive or negative, differing in sign have been obtained for $(\partial\mu/\partial r)_{CO}$ and $(\partial\mu/\partial r)_{CN}$. The higher of the two values, i.e., 3.69×10^{-10} esu, has been accepted for $(\partial\mu/\partial r)_{CO}$ since it is closer to the similar value in CO_2 and this decides the value of $(\partial\mu/\partial r)_{CN}$ to be ± 0.73 in KCl. But the values are still left with ambiguity in sign. The choice can be made considering the electronic

structure. The stretching of CO bond favors structure (2) giving a dipole directed to the right while stretching of CN bond favors structure (1) giving a dipole directed to the left. This indicates that $(\partial\mu/\partial r)_{CO}$ and $(\partial\mu/\partial r)_{CN}$ should have opposite sign. Since oxygen is more electronegative than carbon $(\partial\mu/\partial r)_{CO}$ is negative which means that both $\partial\mu/\partial Q_1$ and $\partial\mu/\partial Q_3$ are negative. This gives a positive value for $(\partial\mu/\partial r)_{CN}$ which is reasonable.

Different possible values have been obtained for dipole moment and a choice has to be made among them. But it is to be pointed out that the method that has been adopted to derive bond moment is not rigorous. In arriving at $(\partial^2\mu/\partial Q^2)$ values it has been assumed that the wave functions are harmonic. Since a transition to an overtone level is involved here, the assumption is not legitimate. But considering the values obtained for KBr lattice, they seem to be within reasonable limits. The accepted value for C-O (single bond) moment is 0.7 debye in gaseous medium; the triple bond moment is considered to be very low (41, p. 870). Since the resonating form (2) is dominant, the C-O bond is essentially a single bond and consequently the value ± 0.81 debye can be accepted. Nothing definite can be said about the corresponding value of μ_{CN}, which is ± 0.34 debye.

Strangely enough, though a sharp increase in the dipole and its derivative of CO bond is noticed in changing the host lattice from KBr to KI, the corresponding values for CN bond are practically constant.

A gradation is noticed in the values of dipole moment and its derivatives in the three alkali halides. This can be explained on the basis of reaction field. The oscillating dipole induces moment in the surrounding dielectric, which contributes to the internal field. This contribution is called reaction field. The reaction field magnitude depends on the polarizability of ions in the dielectric. The polarizability of halogen ions increase from Cl^- to I^-, the values being Cl^- = 3.6×10^{-24} cc, Br^- = 5.0×10^{-24} cc and I^- = 7.6×10^{-24} (40 , p. 198). The difference in the polarizability of Cl^- and Br^- is less than that between Br^- and I^-. The intensity values have followed this pattern.* Though the applied field has been corrected for its behaviour in the dielectric, there is still difference between $(\partial\mu/\partial Q)$ values in the three alkali halides, indicating that the equation (21) is not satisfactory. It is as

---

* Mention must be made of a single exception. The u/ Q_2 value in KBr is less than KCl and in all probability this is due to experimental error.

expected since this equation does not take into account the field at the dipole. This is only a first order correction. But still it is instructive to compare the intensities with and without this correction. In Table 22 are given the values of $(\partial \mu / \partial Q_1)$ in the two cases. A 5% increase from KCl to KBr is reduced to

Table 22

Values of $(\partial \mu / \partial Q_1)$

Host Lattice	According to (6)	According to (21)
KCl	69.71	61.86
KBr	73.31	62.68
KI	90.48	74.58

1% after correction. But the difference in intensity in KBr and KI is still appreciable. This may be due to the higher polarizability of the iodide ion. These observations are more or less true in regard to the intensity of the other two modes.

Though an equation has been derived taking into consideration "cavity refractive index", it could not be tested due to unavailability of suitable data in the literature.

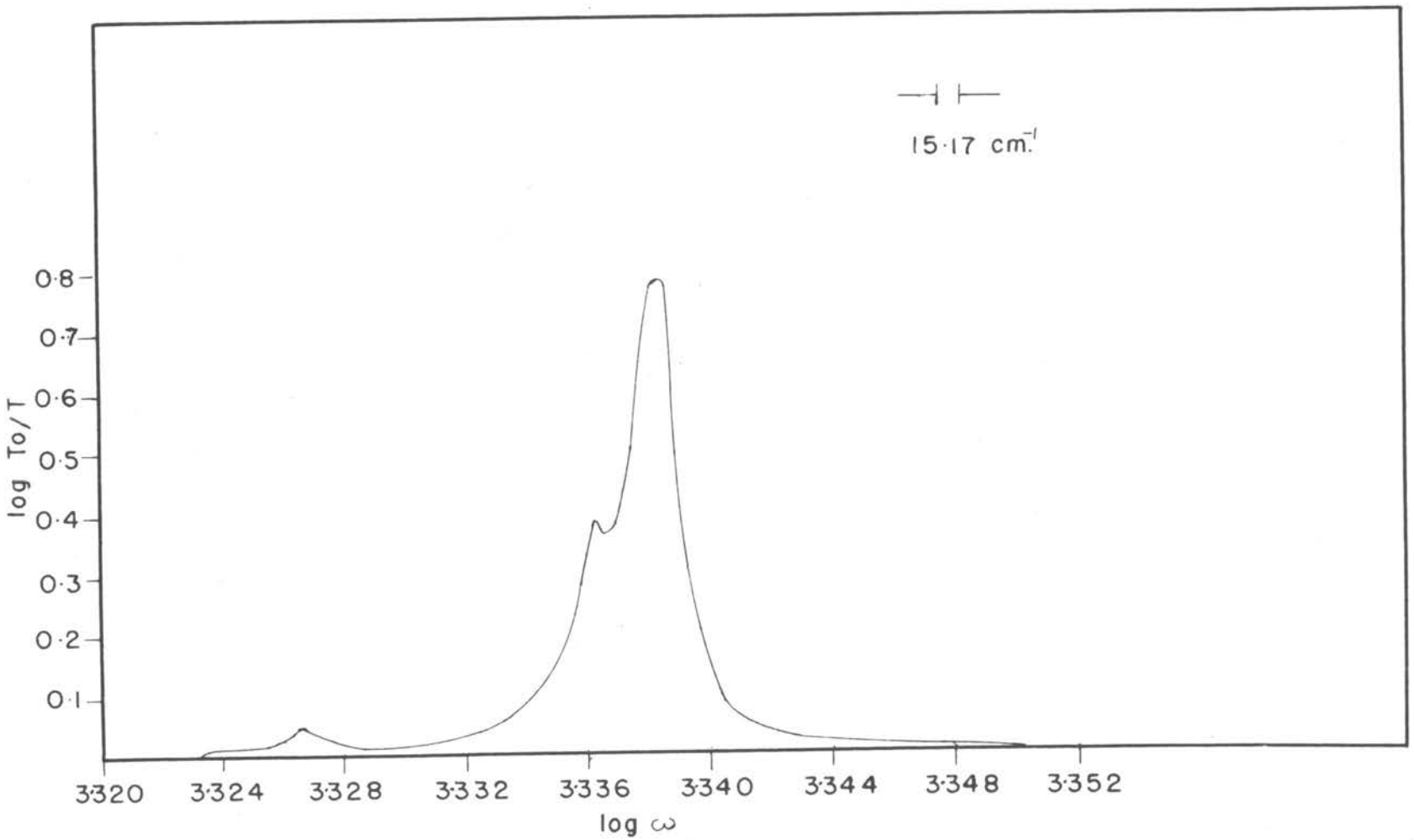

Figure 2

Spectrum of OCN^- in the Region 2240-2060 cm^{-1}

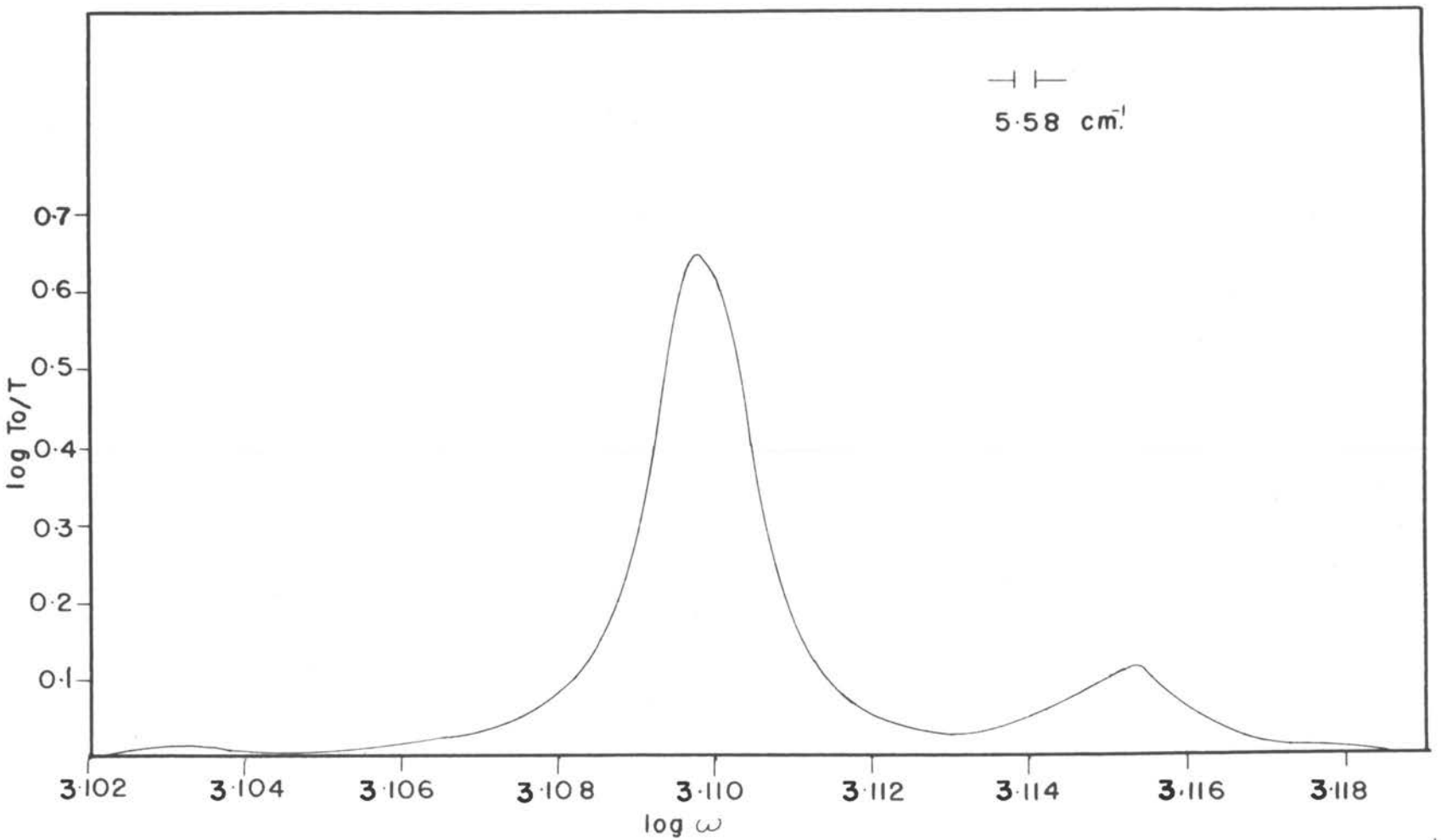

Figure 3. - Spectrum of OCN^- in KBr in the Region 1300-1200 cm^{-1}.

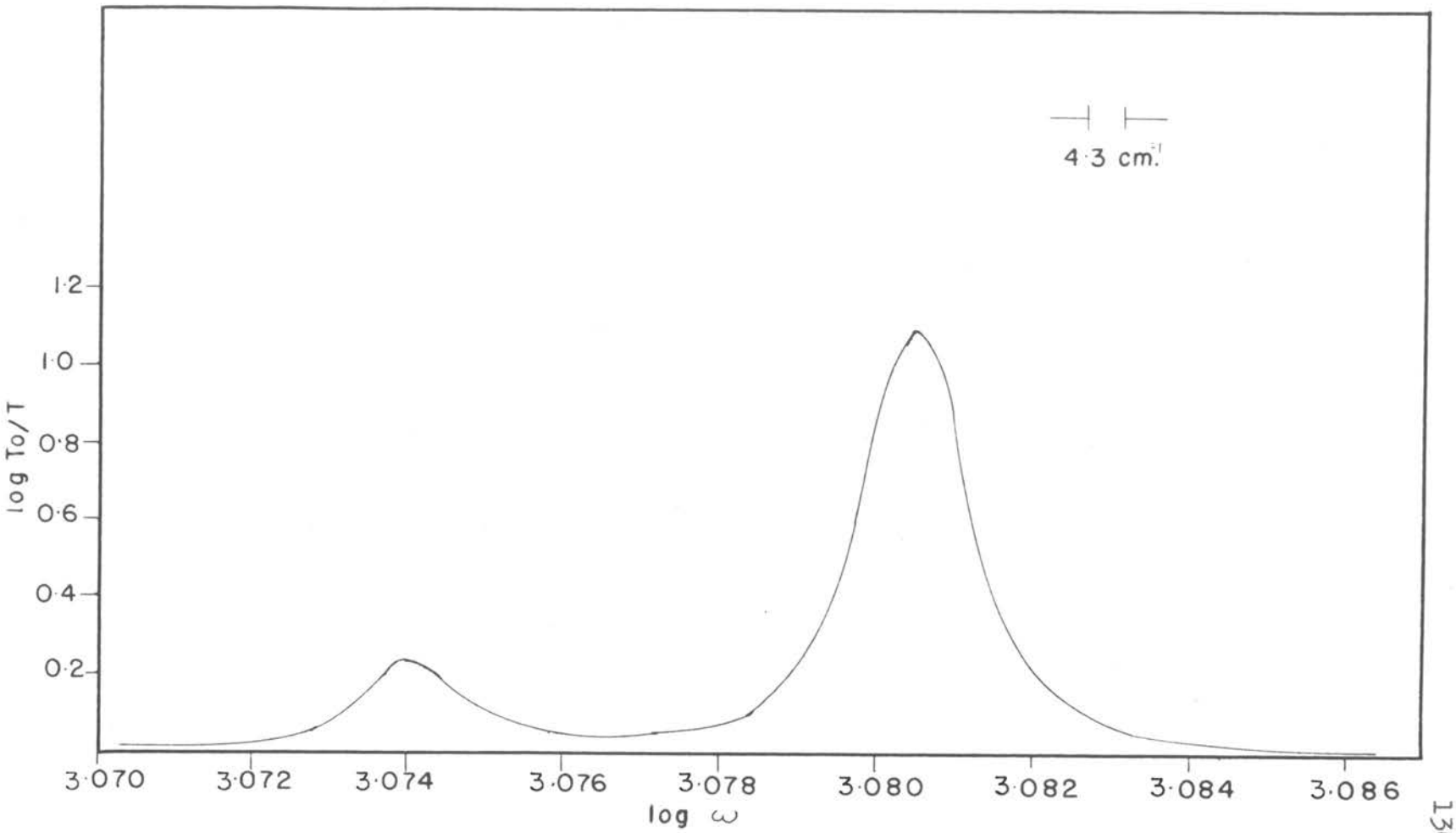

Figure 4. - Spectrum of OCN^- in the Region 1220-1160 cm^{-1}.

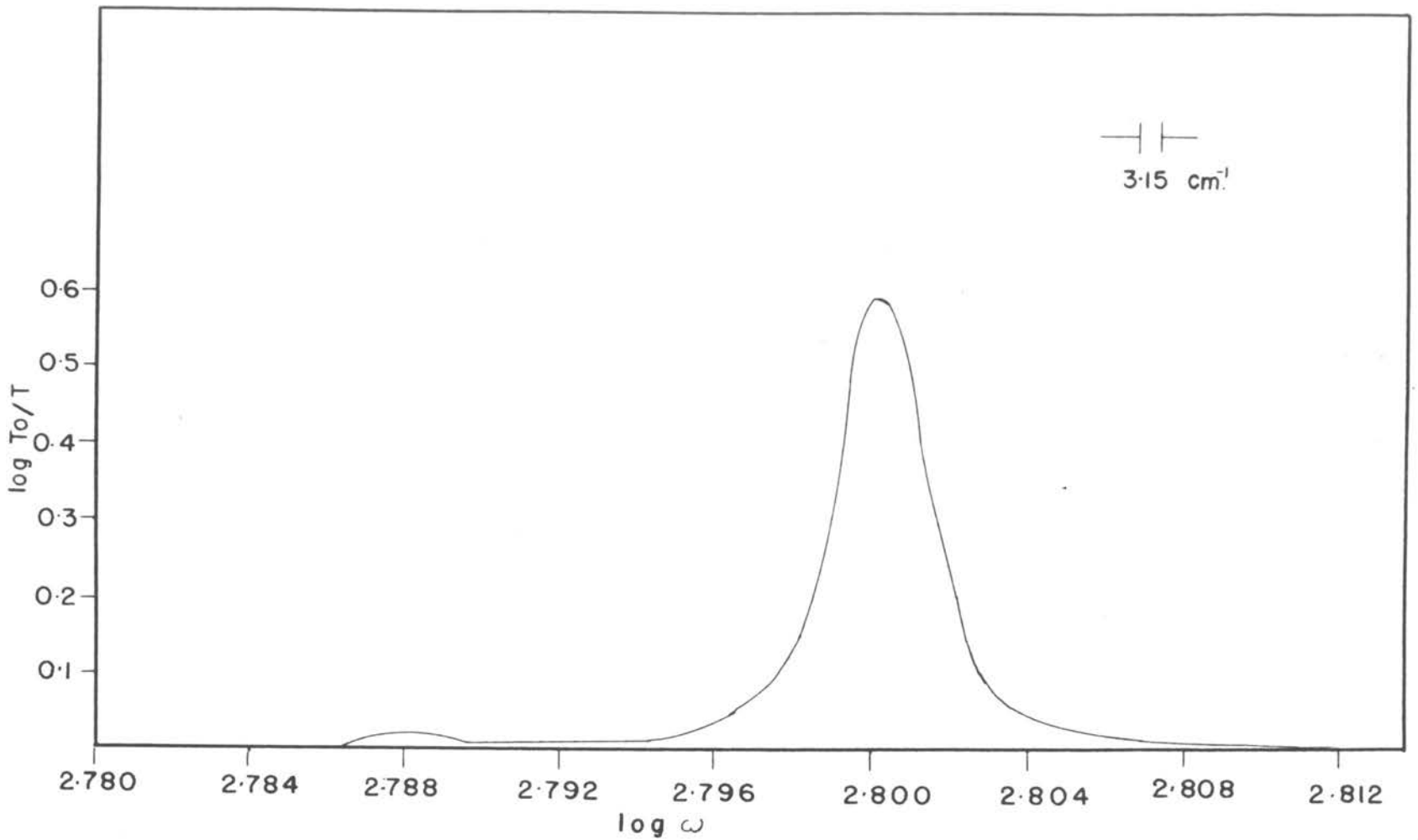

Figure 5

Spectrum of OCN^- in the Region 660-600 cm^{-1}

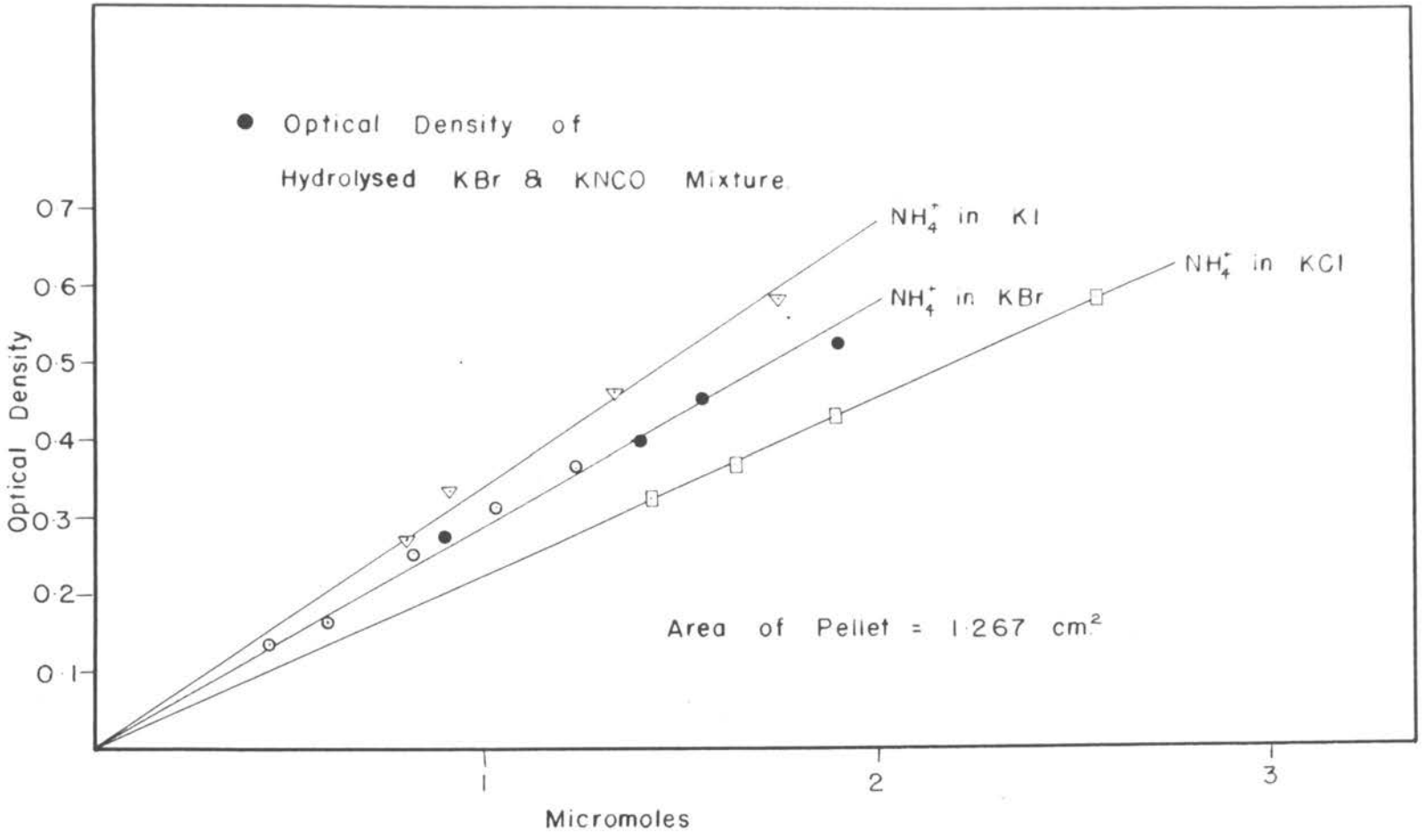

Figure 6. - Calibration Curve for NH_4^+ in KCl, KBr, KI Lattices and Comparison with Data Obtained from Hydrolyzed KBr-KNCO Mixtures.

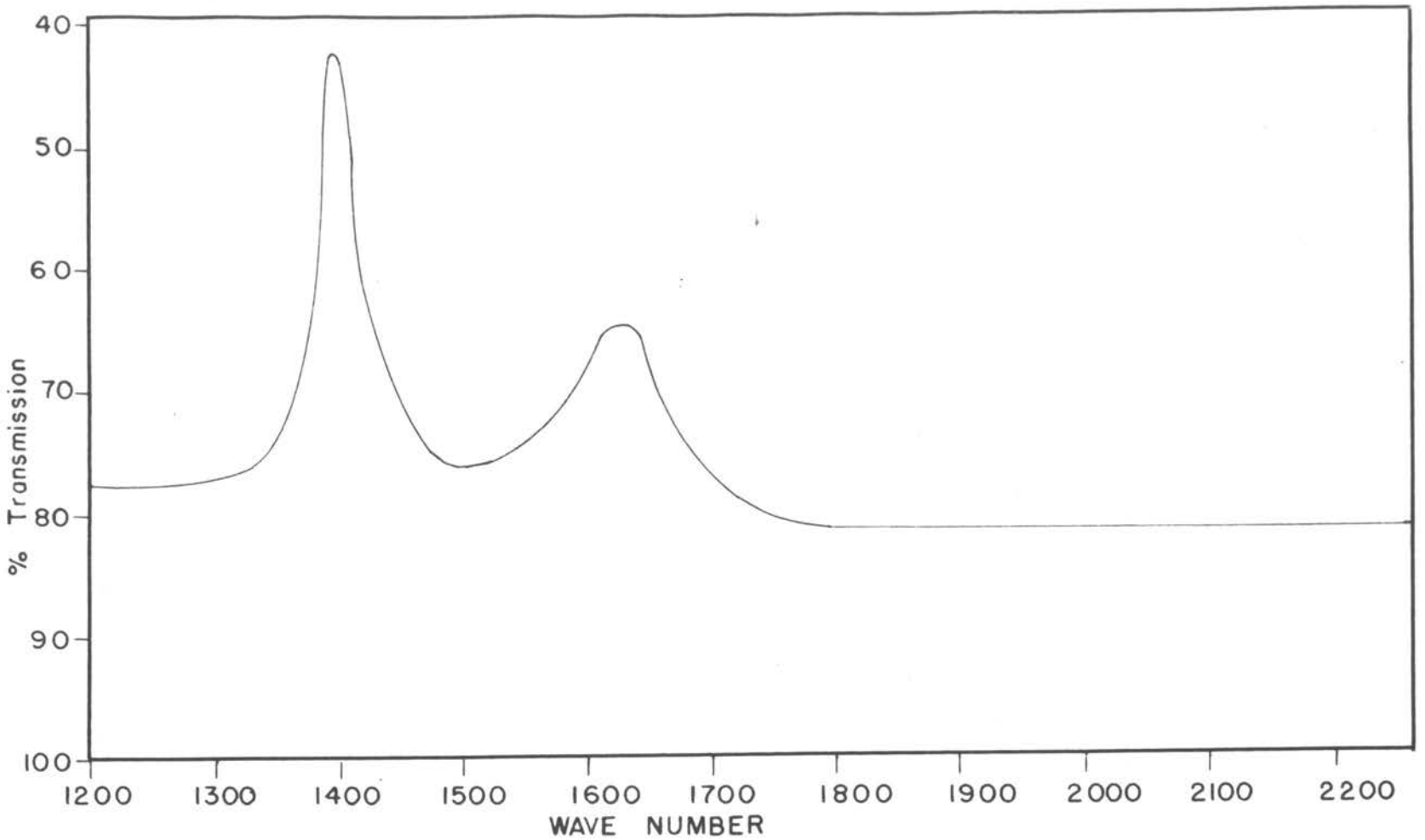

Figure 7. - Spectrum of Hydrolyzed KCl-KNCO Single Crystal.

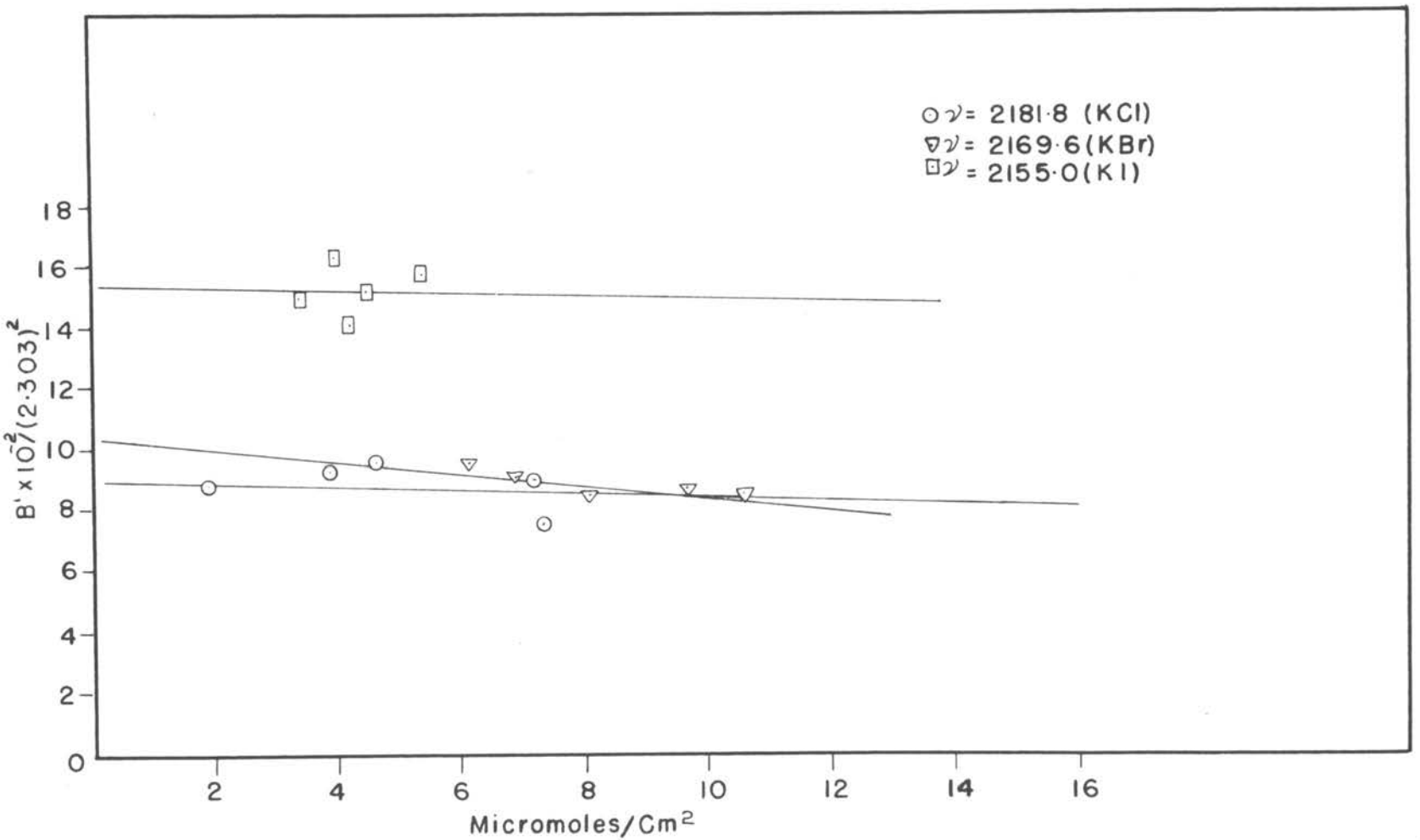

Figure 8. - Intensity Measurement for ν_1 Band of OCN^- in KCl, KBr and KI Lattices.

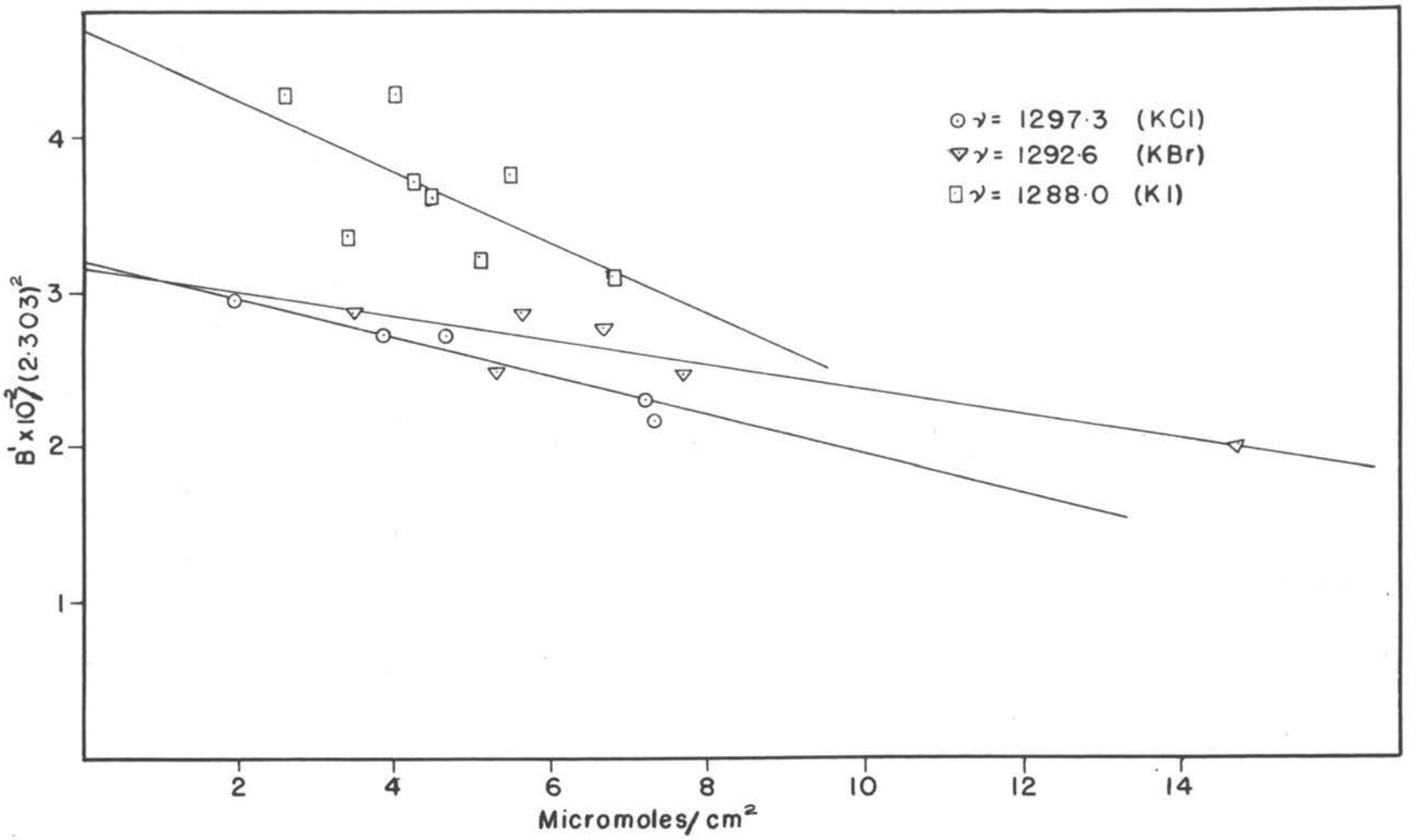

Figure 9. - Intensity Measurement for Higher Frequency Component of Fermi Doublet of OCN^- in KCl, KBr and KI Lattices.

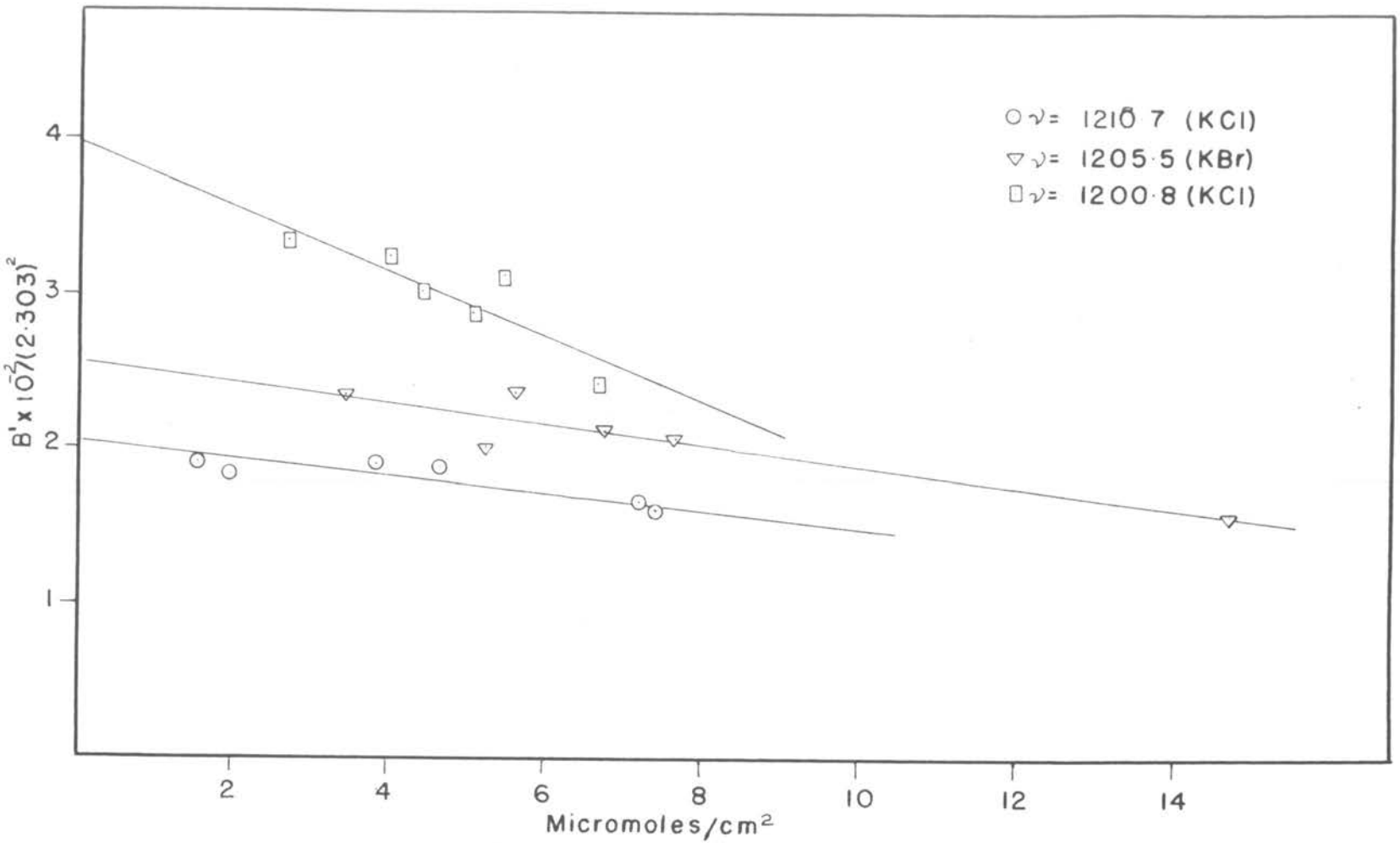

Figure 10. - Intensity Measurement for Lower Frequency Component of Fermi Doublet of OCN^- in KCl, KBr and KI Lattices.

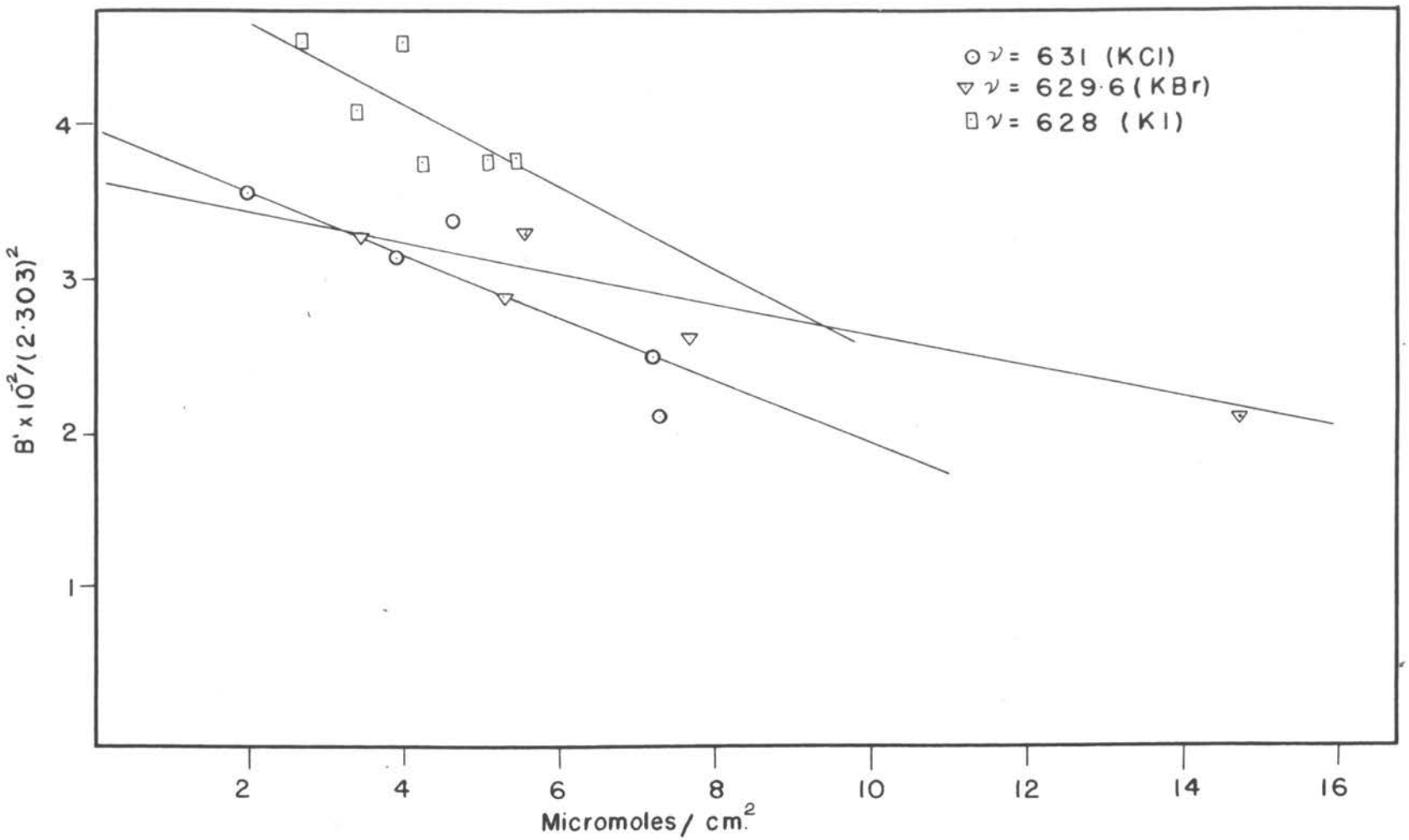

Figure 11. - Intensity Measurement for Bending Mode of OCN^- in KCl, KBr and KI Lattices.

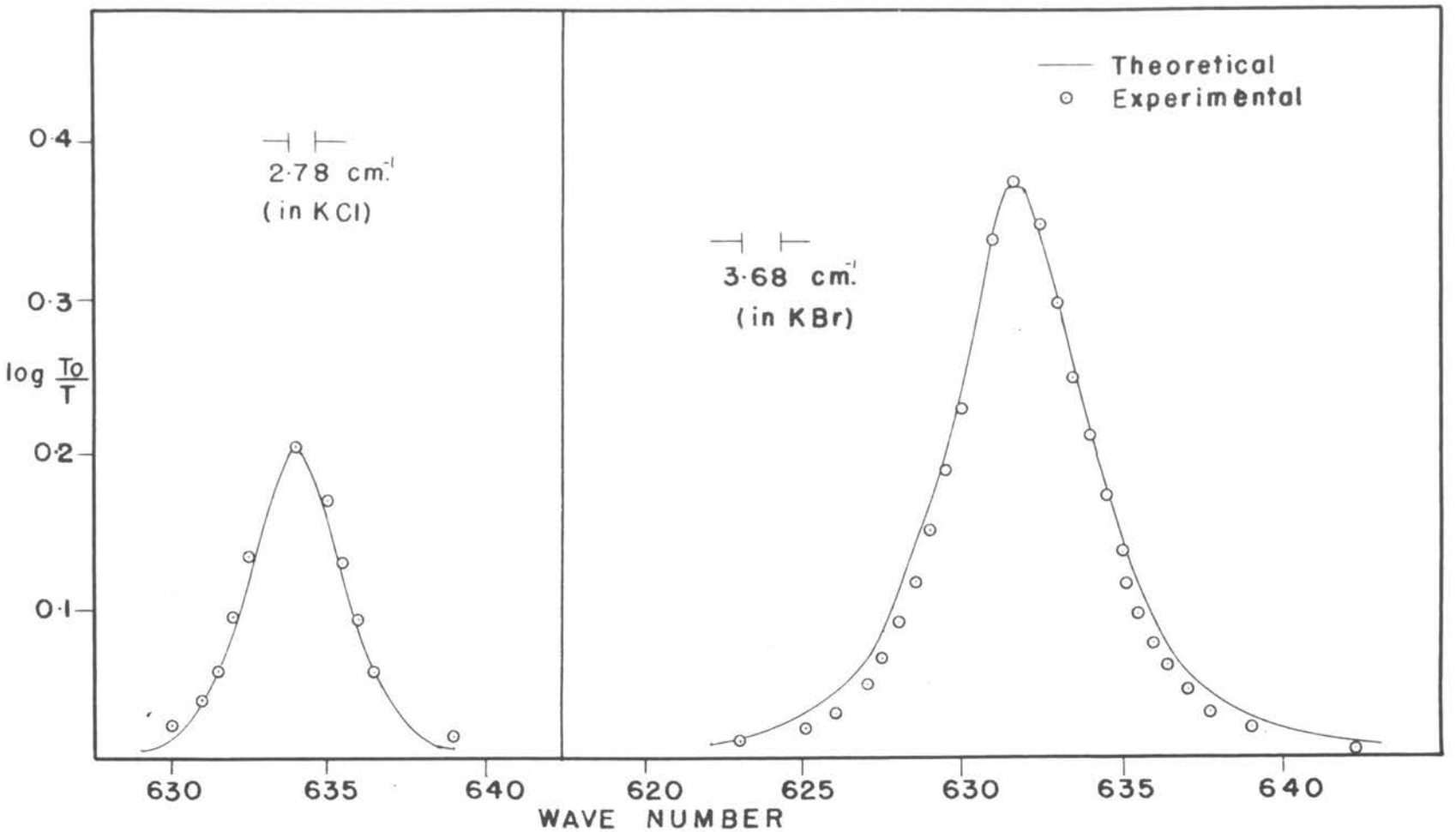

Figure 12. - Comparison of Experimental ν_2 Band of OCN^- with Lorentz Line Shape Modified by Finite Slit Width.

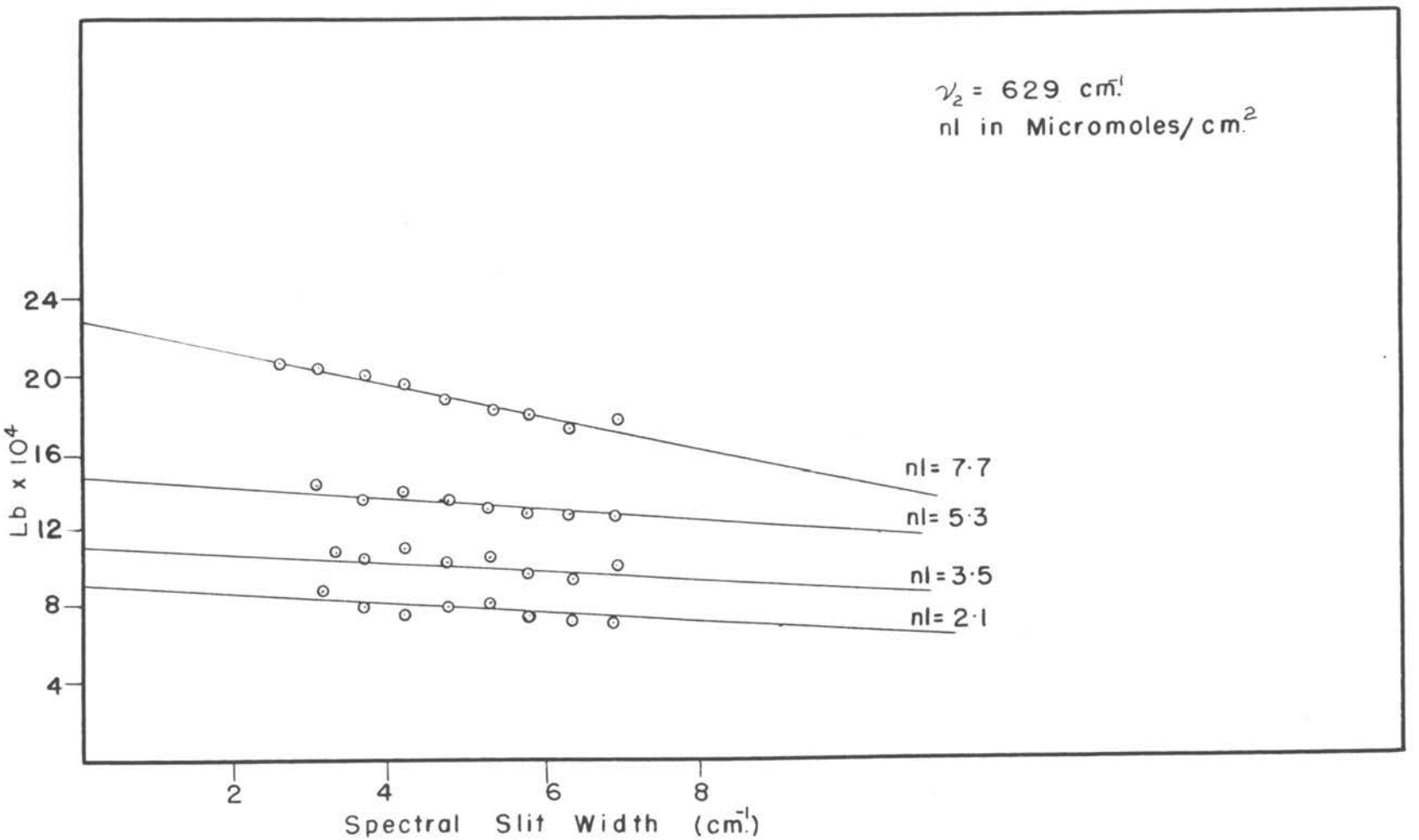

Figure 13. - Integrated Area at Different Slit Widths of Bending Mode of OCN^- in KBr.

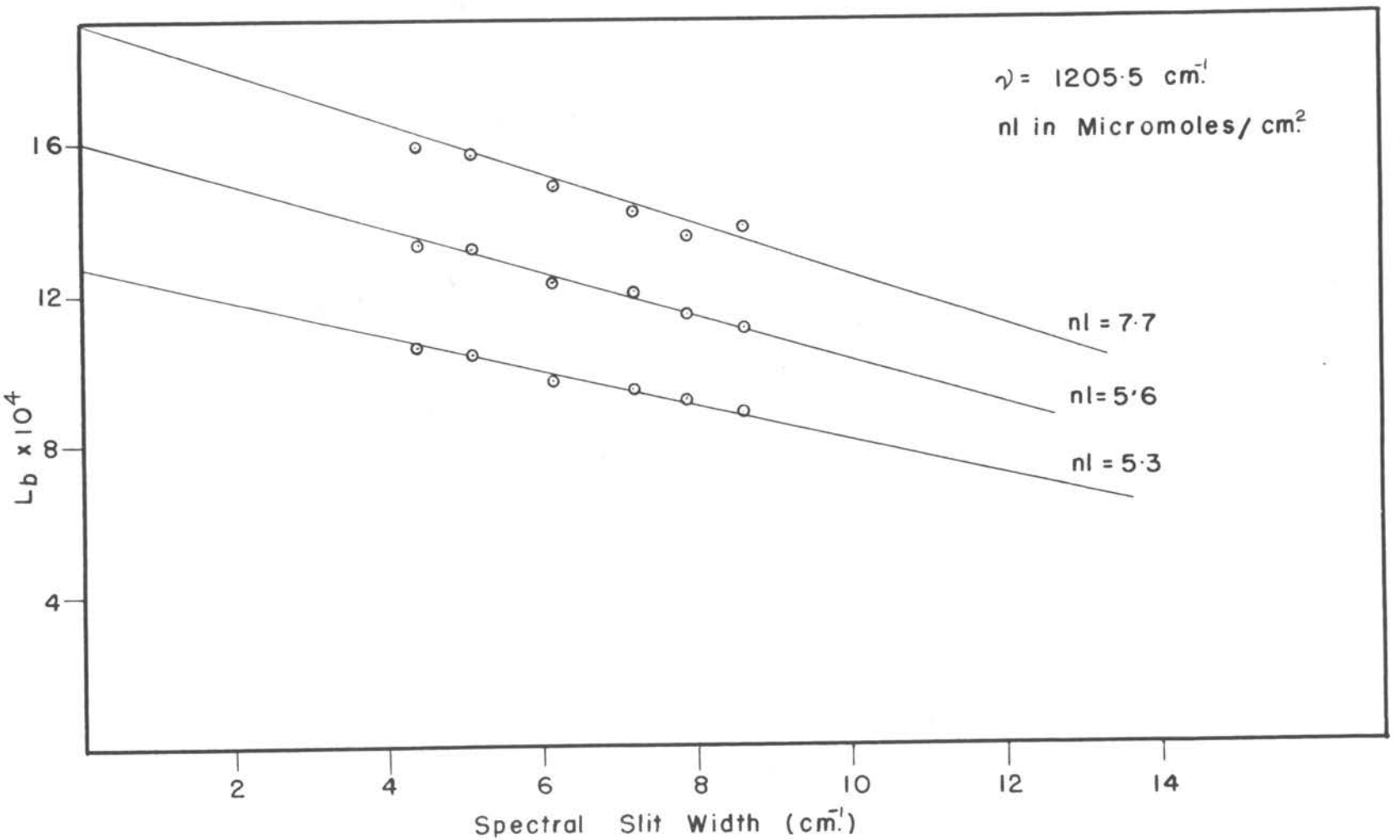

Figure 14. - Integrated Area at Different Slit Widths of Lower Frequency Component of Fermi Doublet of OCN^- in KBr.

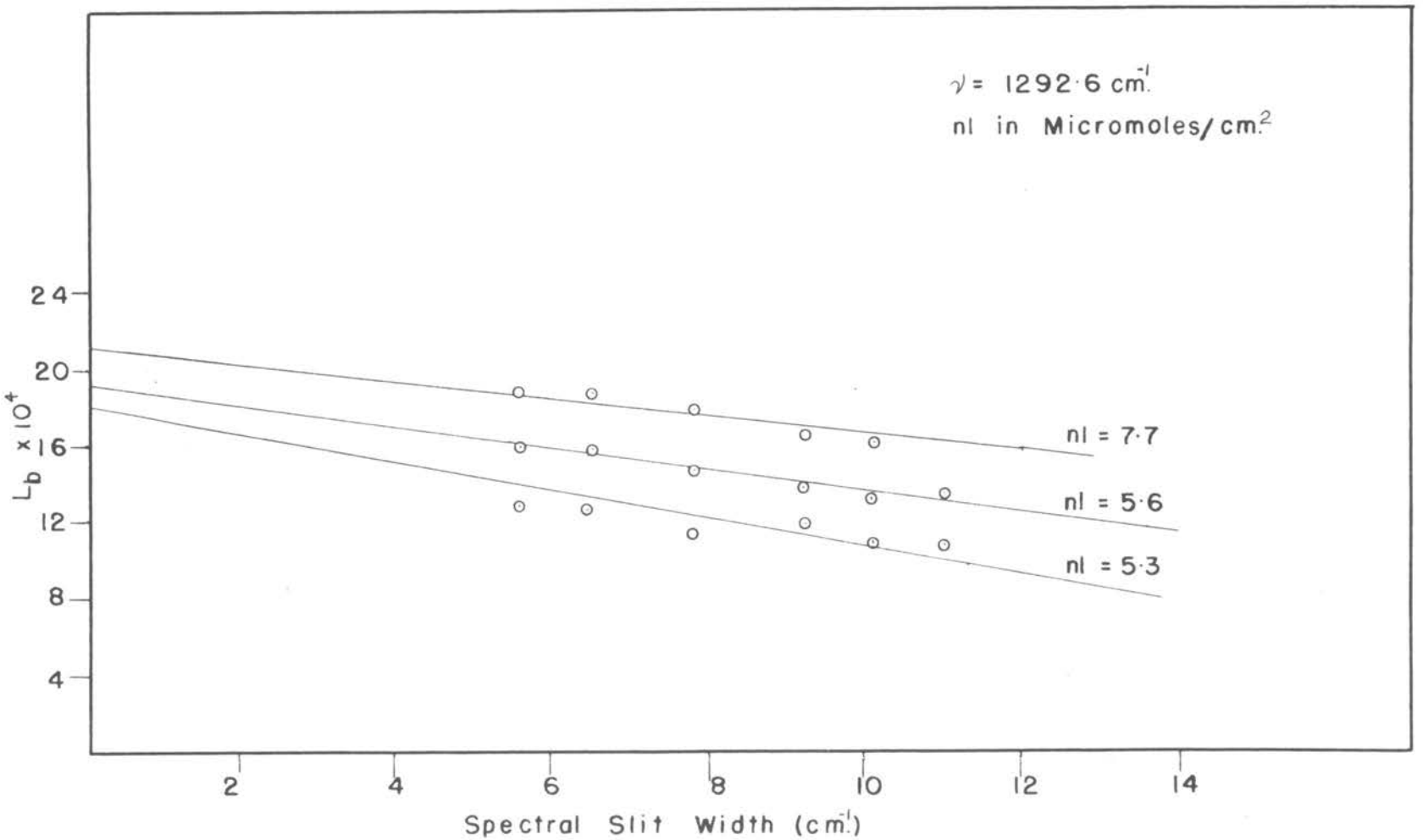

Figure 15. - Integrated Area at Different Slit Widths of Higher Frequency Component of Fermi Doublet of OCN^- in KBr.

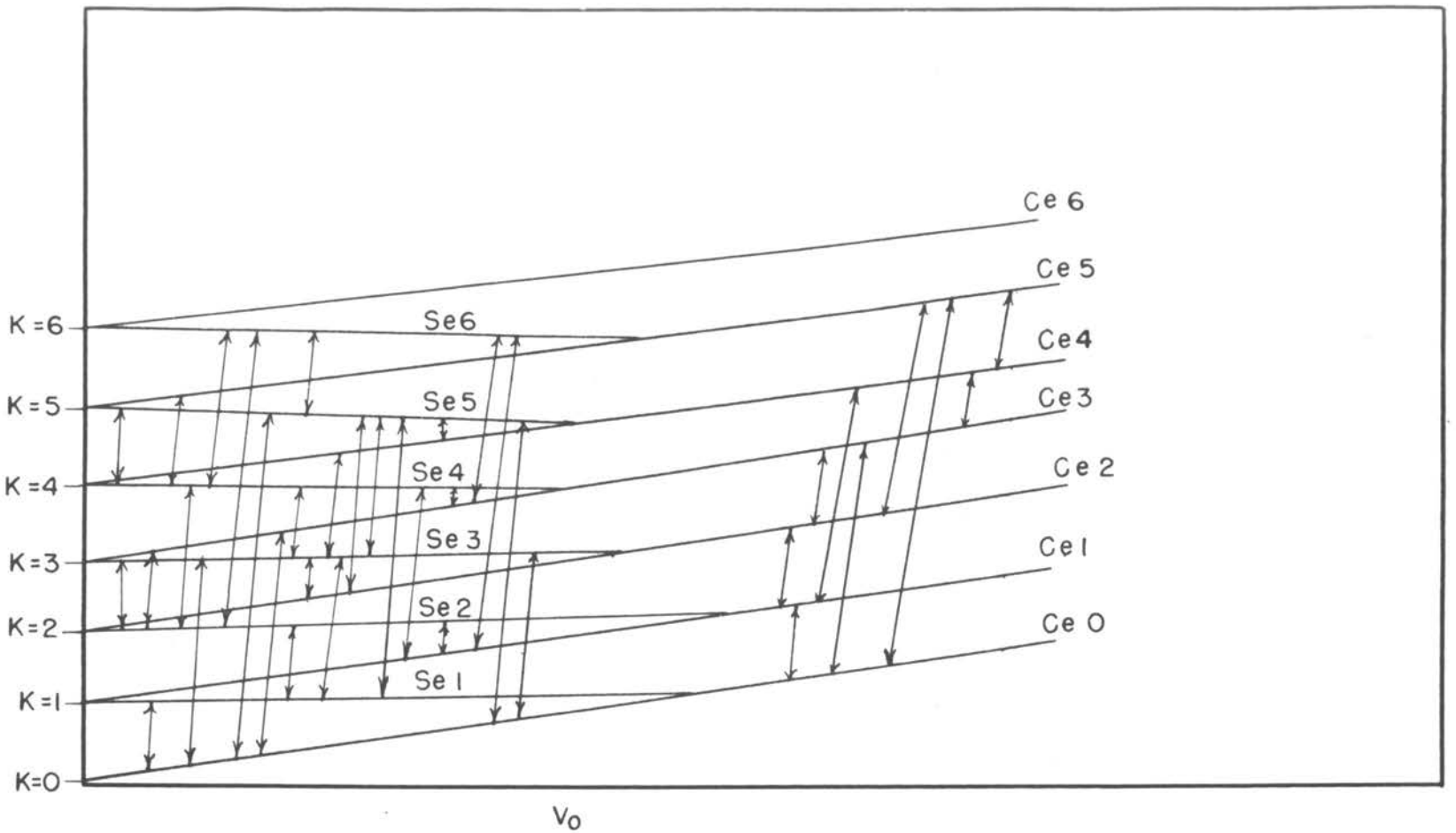

Figure 16. - Correlation Diagram of the Energy Levels of Hindered Rotation in a Crystal for a Diatomic Molecule.

BIBLIOGRAPHY

1. Barthlome, E. Über den Bindungscharakter in den Halogenwasserstoffen auf grund absoluter Intensitathmessungen der ultraroten grundschwingungsbanden. Zeitschrift für Physikalische Chemie Abt B 23:131-151. 1933.

2. Beers, Yardley. Theory of error. Cambridge, Mass., Addison-Wesley, 1953. 64 p.

3. Bourgin, D. G. Line intensities in the hydrogen chloride fundamental band. Physical Review. 29:794-816. 1927.

4. Callomon, H. J., D. C. McKean, and H. W. Thompson. Intensity of vibrational bands. III. Nitrous oxide. Proceedings of the Royal Society of London, ser. A, 208:332-341. 1951.

5. Crawford, Bryce, Jr. Vibrational intensities. X. Integration theorem. Journal of Chemical Physics 29:1042-1045. 1958.

6. Eggers, David F., Jr. and Bryce Crawford, Jr. Vibrational intensities. III. Carbon dioxide and nitrous oxide. Journal of Chemical Physics 19:1554-1561. 1951.

7. Fermi, E. Über den Ramaneffect des Kohlendioxides. Zeitschrift für Physik 71:250-259. 1931.

8. Goldberg, Leo, Orren C. Mohler, and Russel E. Donovan. Experimental determination of absolute f values of methane. Journal of the Optical Society of America 42:1-6. 1952.

9. Goldstein, S. Mathieu functions. Transactions of the Cambridge Philosophical Society 23(11):303-336. 1927.

10. Goody, R. M. and T. W. Wormell. The quantitative determination of atmospheric gases by infrared. I. Laboratory determination of the absorption of the 7.8 and 8.6 μ bands of nitrous oxide with dry air as foreign gas. Proceedings of the Royal Society of London, ser. A, 209:178-196. 1951.

11. Hornig, Donald F. Vibrational spectrum in crystals. Journal of Chemical Physics 16:1063-1076. 1948.

12. Hexter, R. M. and D. A. Dows. Low frequency libration and vibrational spectra of molecular crystals. Journal of Chemical Physics 25:504-509. 1956.

13. Hyde, G. E. and D. F. Hornig. The measurement of bond moments and their derivatives in HCN and DCN from infrared intensities. Journal of Chemical Physics 20:647-652. 1952.

14. Hirschfelder, Joseph O., Charles F. Curtiss, and R. Byron Bird. Molecular theory of gases and liquids. New York, Wiley, 1954. 1219 p.

15. Hodgmann, Charles D., ed. Standard mathematical tables. 10th ed. Cleveland, Ohio, Chemical Rubber Publishing Co., 1956. 441 p.

16. Jaffe, Joseph H. and S. Kimel. Infrared intensities in liquids. Journal of Chemical Physics 25: 374-375. 1956.

17. Jaffe, H. H. A reexamination of the Hammett equation. Chemical Reviews 53:191-261. 1953.

18. Jones, Norman R. The absorption of radiation by inhomogeneously dispersed system. Journal of the American Chemical Society 74:2681-2683. 1952.

19. Kaplan, D. Lewis and David F. Eggers, Jr. Intensity and line width of the 15 μ CO_2 band determined by a curve of growth method. Journal of Chemical Physics 25:876-883. 1956.

20. Lorentz, H. A. Theory of electrons. 2nd ed. New York, Dover, 1952. 343 p.

21. Lord, R. C., B. Nolin, and H. D. Stidham. Quantitative study of the bonding of chloroform-d in various solvents by infrared spectrometry. Journal of the American Chemical Society 77: 1365-1368. 1955.

22. Maki, Arthur George, Jr. The infrared spectrum of cyanate ion in different environment. Ph.D. thesis. Corvallis, Oregon State College, 1960. 151 numb. leaves.

23. Maki, Arthur and J. C. Decius. Vibrational spectrum of cyanate ion in various alkali halide lattices. Journal of Chemical Physics 31:772-782. 1959.

24. Matheson, Lorne A. The intensity of infrared absorption bands. Physical Review 40:813-828. 1932.

25. Miller, F. A. and C. H. Wilkins. Infrared spectrum and characteristic frequencies of inorganic ions. Analytical Chemistry 24:1253-1294. 1952.

26. Nixon, Eugene R. and Paul C. Cross. The intensities of several of the infrared absorption bands of cyanogen and cyanogen chloride. Journal of Chemical Physics 18:1316-1319. 1950.

27. Onsager, Lars. Electric moment of molecules in liquids. Journal of the American Chemical Society 58:1486-1493. 1936.

28. Person, Willis B. Liquid-gas infrared intensities, pressure induced absorption, and the temperature dependence of infrared intensities in liquids. Journal of Chemical Physics 28:319-322. 1958.

29. Project for the computation of mathematical tables. Table of the exponential function e^x. Federal Works Agency, Work Projects Administration for the City of New York. Conducted under the sponsorship of the National Bureau of Standards, 1939. 535 p.

30. Polo, S. R. and M. K. Wilson. Infrared intensities in liquids and gas phase. Journal of Chemical Physics 22:2376-2377. 1955.

31. Perkin-Elmer Corporation. Instructional manual. Glenbrook, Connecticut, 1950. 45 numb. leaves.

32. Pauling, Linus. The rotational motion of molecules in a crystal. Physical Review 36:430-443. 1930.

33. Pauling, Linus and E. Bright Wilson. Introduction to quantum mechanics. New York, McGraw-Hill, 1935. 468 p.

34. Ramsay, D. A. Intensities and shapes of infrared absorption bands of substances in liquid phase. Journal of the American Chemical Society 74:72-80. 1952.

35. Robinson, David Z. The experimental determination of the intensities of infrared absorption bands. IV. Measurement of stretching vibrations of OCS and CS_2. Journal of Chemical Physics 19:881-886. 1951.

36. Russel, R. A. and H. W. Thompson, Intensity of vibration bands. Part VI. Alkyl esters. Journal of the Chemical Society 479-482. 1955.

37. Richards, W. S. and E. Bright Wilson, Jr. The infrared spectrum of $N^{15}N^{14}O$ and the force constant of nitrous oxide. Journal of Chemical Physics 18:694-697. 1950.

38. Shaw, William H. R. and Boredeaux, John T. Semimicro method for determination of cyanate ion in presence of interfering substances. Analytical Chemistry 27:136-138. 1955.

39. Stewart, James E. Absorption of radiant energy by solid particles in suspension. Journal of Research of the National Bureau of Standards 54: 41-46. 1955.

40. Syrrin, Y. K. and M. E. Dyatkina. Structure of molecules and the chemical bond. London, Butterworths, 1950. 509 p.

41. Thorndike, A. M. The experimental determination of the intensities of infrared absorption bands. III. CO_2, methane and ethane. Journal of Chemical Physics 15:868-874. 1947.

42. Thorndike, A. M., A. J. Wells and E. Bright Wilson, Jr. The experimental determination of the intensities of infrared absorption bands. II. Measurement on ethylene and nitrous oxide. Journal of Chemical Physics 15:157-165. 1947.

43. Thompson, H. W. and G. Steel. The correlation of vibrational band intensities with reactivity: the CN group. Transactions of the Faraday Society 52:1451-1457. 1956.

44. Van Vleck, J. R. and V. F. Weisskopf. On the shape of collision broadened line. Reviews of Modern Physics 17:227-236. 1945.

45. Weber, D., R. J. Holm and S. S. Penner. Integrated absorption of vibrational rotational bands of CO_2. Journal of Chemical Physics 20:1820. 1952.

46. White, Harvey Elliot. Introduction to atomic spectra. New York, McGraw-Hill, 1934. 457 p.

47. Williams, Van Zandt. Infrared instrumentation and techniques. Review of Scientific Instruments 19:135-180. 1948.

48. Wilson, E. Bright. A method of obtaining the expanded secular equations for the vibration frequencies of a molecule. Journal of Chemical Physics 7:1047-1052. 1939.

49. Wilson, E. Bright, Jr. and A. J. Wells. The experimental determination of the intensities of infrared absorption bands. I. Theory of the method. Journal of Chemical Physics 14:578-580. 1946.

50. Wilson, E. Bright, Jr., J. C. Decius and P. C. Cross. Molecular vibrations. New York, McGraw-Hill, 1955. 388 p.

APPENDIX I

Wilson-Wells Extrapolation Theorem

Absolute molar integrated intensity is defined by Wilson and Wells (49) as

$$A = \frac{1}{nl} \int_{band} \ln \frac{I_o}{I} \, d\nu$$

Due to the limitations of a spectrograph like finite slit width, it does not record the true incident and transmitted intensity, but something less. Corresponding to actual intensity of incident and transmitted radiation, the apparent molar integrated intensity is defined as

$$B = \frac{1}{nl} \int_{band} \ln \frac{T_o}{T} \, d\nu$$

If $g(\nu, \nu')$ is the fraction of light transmitted by the instrument when it is set at a frequency ν'

$$T = \int_{slit} I \, g(\nu \; \nu') \, d\nu$$

$$T_o = \int_{slit} I_o \, g(\lambda \lambda') \, d\lambda$$

(A-B) is

$$A-B = \frac{1}{nl} \int_{band} \ln \frac{I_o}{I} \frac{\int_{slit} I \, g(\lambda \lambda') \, d\lambda}{\int_{slit} I_o \, g(\lambda \lambda') \, d\lambda} \, d\lambda'$$

It is assumed that I_o is constant over the slit, which is perfectly legitimate, which reduces the above expression to

$$= \frac{1}{nl} \int_{band} \ln \frac{\int_{slit} f(\lambda \lambda') \, g(\lambda \lambda') \, d\lambda}{f(\lambda \lambda') \int_{slit} g(\lambda \lambda') \, d\lambda} \, d\lambda'$$

where

$$f(\lambda \lambda') = e^{-\alpha nl} = \frac{I}{I_o}$$

Now the behaviour of (A-B) as $nl \to 0$ is examined with the help of L' Hospital Rule.

$$\lim_{nl \to 0} (A-B) = \int_{band} \alpha - \frac{\int_{slit} \alpha\, f(\nu\nu')\, g(\nu\nu')\, d\nu}{\int_{slit} f(\nu\nu')\, g(\nu\nu')\, d\nu}\, d\nu'$$

If α is assumed to be constant over the slit which is a reasonable assumption, it can be readily seen that

$$\lim_{nl \to 0} (A-B) = 0$$

i.e., $B \to A$ as $nl \to 0$

So by plotting B against nl and extrapolating to zero nl, should give A. Other methods of extrapolating have been adopted, but in this work the above procedure was found convenient.

It can be easily seen that Wilson-Wells method holds good even when both absolute integrated intensity and apparent integrated intensity are defined according to the equations

$$A' = \frac{1}{nl} \int \ln (I_o/I)\, d\ln \omega$$

$$B' = \frac{1}{nl} \int \ln (T_o/T)\, d\ln \omega$$

Absolute Integrated Intensity from Peak Intensity and Half Intensity Width.

It was mentioned earlier that if the band shape is assumed Lorentian or Van-Vleck-Weiskopfian, the true integrated intensity can be obtained without resorting to extrapolation methods. If Lorentian

$$\ln I_o/I = a/(\omega - \omega_o)^2 + b^2$$

$$A = 1/nl \int \ln I_o/I \quad d\omega = 1/nl \int_{-\infty}^{+\infty} a/(\omega - \omega_o^2) + b^2$$

$$= \frac{\pi}{nl} \cdot \frac{a}{b}$$

If Van-Vleck-Weiskopfian

$$A' = \frac{1}{nl} \int \ln \frac{I_o}{I} \frac{d\omega}{\omega} = \frac{1}{nl} \int \frac{a}{\omega_o(\omega_o - \omega)^2 + b^2}$$

Since most of the contribution to the area comes near about the central frequency

$$A = \frac{\pi}{nl} \cdot \frac{a}{b} \cdot \frac{1}{\omega_o}$$

APPENDIX II

Libration and Restricted Rotation

It is a common experience that the individual lines in rotational fine structure of infrared band of a gas become broader as the pressure is increased and at considerably high pressure the fine structure is smoothened out. This is due to increased collision between molecules. This should be true in the case of liquids, where the molecules are close together and infrared bands of liquids in general do not show any fine structure. But there are cases in which P, Q and R branches have been observed.

In the case of solids under ordinary conditions the quantization of rotatory motion is not spectroscopically observed. This does not mean that rotation is completely frozen, but it is only restricted. It may be highly restricted or may be slightly restricted. When rotation is highly restricted the motion of the molecule will be vibratory, but the vibration is not within the molecule, but will be with reference to an axial system and to distinguish such motion from true vibration, they are called libration.

When the rotation is slightly restricted the relation will be non-uniform. Due to the environment a

potential barrier is set up to rotatory motion of the molecule. When the molecule passes the potential barrier it is slowed down and as it approaches the equilibrium position it is speeded up. The spectrum of a molecule in a crystal has to be analyzed in the light of these two situations.

In addition to molecular motion, there are also lattice motions. Interaction between lattice vibrations and molecular vibrations can be expected provided that certain symmetry conditions are satisfied. Lattice vibrations have frequency lower than 200 cm^{-1} and pure lattice vibrations are hardly observed, but are usually observed in combinations. This results in converting a sharp line to a band. Since numerous lattice modes are permitted, their combination with a fundamental may considerably increase the intensity of the latter. In some cases the forbidden fundamental becomes active due to combination with lattice modes. This results in a band in the vicinity of forbidden fundamental and in some cases with fine structure. The 5.7 μ band of NH_4^+ in NH_4Cl and NH_4Br, though forbidden appears (11, p. 1072).

Working at low temperature, Maki and Decius (23) have observed fine structure around CN stretching mode. Some of them have been attributed by them to libration and lattice modes. Since the present study was made at

room temperature such fine structure have not been observed. But they will be a part of vibration band that is observed and the intensity computed is the sum of librational and vibrational transitions.

A general consideration of highly restricted and slightly restricted rotation is given below. The object is to justify that the equation derived for a gas relating integrated intensity and $\frac{\partial \mu}{\partial Q}$ is valid in the case of a solid too. The work reported below on slightly restricted rotor was carried out in collaboration with Mr. J. V. Martinez under the guidance of Dr. J. C. Decius. First, the librational motion is considered.

If V stands for vibrational quantum number and n for librational quantum number, the intensity of a band will be the sum of all transitions (V, n) → (V + 1, n) (12). The partition function for a doubly degenerate librator is

$$Q_1^{(2)} = \left[1 - \exp(-hc\omega/kT)\right]^2$$

and consequently the fraction of the molecule in a librational state is

$$\frac{N_n}{\sum_n N_n} = \left[1 - \exp - \frac{hc\omega}{kT}\right]^2 (n+1) \exp\left(-\frac{nhc\omega}{kT}\right)$$

So the vibrational transition v, n → V + 1, n is thus composed of series of lines due to thermal distribution in the librational levels as given by the above equation. But, as in the case of a spectrum of free molecule, the changes due to departure from rigid rotor and harmonic oscillator approximation has to be considered. They are changes in the moment of inertia between the upper and lower vibrational states and anharmonicity in the upper vibrational states. Because of these two it is to be expected, analogous to the situation in free molecule, that the transition v, n → V + 1, n should have higher frequency than v, n + 1 → V + 1, n + 1. Consequently, the main band will shade towards lower frequency. Another change that can be expected is that librational force constant may change with vibrational level and this causes a change in librational frequency in upper and lower level. This may shade the band in either on the lower or higher frequency side.

In addition to the bands (v, n) → (v+1, n) there may be other bands of the type v, n → V+1, n±1, n±2, etc. So the selection rules are less restrictive than in the case of rotor and so in addition to the P Q R branches there will be other bands like .... N O P Q R S T ....

The libration motion is of rotatory origin and the dipole moment matrix element has a similar form as

in the case of a free molecule, which is

$$\int \psi_{v''} \mu_z \psi_{v'} \, d\tau_v \sum_n \int \psi_{n''} \Phi_{Fg} \psi_{n'} \, d\tau_n$$

The terms involved in this expression are familiar and it is similar to the equation

$$(u_F)_{v'R'v''R''} = \sum_F \sum_g \int \psi_{v'} \mu_g \psi_{v''} \, d\tau_v$$

$$\int \psi_{R'} \Phi_{Fg} \psi_{R''} \, d\tau_R$$

Though the molecule in the crystal is not free as in gas phase, the spectrum is essentially similar with additional features peculiar to solid phase. Though P and R branches are not usually resolved, under ordinary conditions, the librations give rise to these branches whose intensity is included in the vibrational band. So the expression derived for a gas relating integrated intensity and $\frac{\partial \mu}{\partial Q}$ holds good for solid too, with correction mentioned in Chapter II, section f.

The other possibility for the motion of a molecule in a crystal is restricted rotation, otherwise

called hindered rotation, first treated by Pauling (32). The molecule subjected to a potential barrier has two equilibrium positions, one at $\theta = 0$ and the other at $\theta = \pi$. The wave equation is

$$- \frac{h^2}{8\pi^2 I} \nabla^2 \psi + V\psi = E\psi$$

The potential function is dependent on θ, which represents the averaged interaction of the molecule with the surrounding.

$$V = \frac{V_o}{2} (1 - \cos 2\theta)$$

The potential is zero when $\theta = 0, \pi , 2\pi$ .... and has a maximum value, V_o, when $\theta = \pi/2, 3\pi/2$ .... If the motion of the molecule is restricted to a plane, which is a good approximation, the wave equation will be

$$- \frac{h^2}{8\pi^2 I} \frac{\partial^2 \psi}{\partial \theta^2} + \frac{V_o}{2} (1 - \cos 2\theta) = E\psi$$

The first part of this expression is kinetic energy, while the second part is potential energy. Two extreme cases can be envisaged, one when $V_o = 0$, in which case the molecule functions as pure rotor and another V_o is large when molecule executes pure vibratory motion. The energy corresponding to these positions are, respectively

$$E = \frac{h^2}{8\pi^2 I} K^2$$

K is rotation quantum number

$$E = V_o \theta_o^{\ 2}$$

The eigenfunction which forms a solution of this differential equation should be periodic in θ with a period of 2π. They are known as Mathieu functions, which have been worked by Goldstein (9). They are usually represented by C_{eo}, S_{e1}, C_{e1}, S_{e2}, etc., and they have been evaluated in terms of total energy and the potential barrier.

For the purpose of illustration a linear diatomic molecule like OH^- is taken and since it can have two equivalent orientation and consequently all energy levels other than K = O are split into two. When $V_o = O$, the spectrum that should be expected is pure rotational spectrum, which would consist of equally spaced lines, the intensity of which being determined by Boltzman distribution factor. When V_o is large, the motion of the molecule is harmonic vibration and eigenfunction is a linear combination of Hermite orthoganal functions which are $\psi_n(\theta/\theta_o)$ and $\psi_n(\theta - \pi/\theta_o)$ where θ_o is given by

$$E = \frac{h\nu_o}{2} = V_o\theta_o^{\,2}$$

and

$$\nu_o = \sqrt{\frac{V_o}{2I}}$$

In between these extreme cases the wave function changes over to Mathieu functions and this change over takes place at values of q where the separation of adjacent levels become appreciable. In the language of Mathieu functions, the eigenfunction for the degenerate levels corresponding to K = 0, 1, 2 .... are given below.

o	C_{eo}	since nondegenerate
1	S_{e1}	
	C_{e1}	
2	S_{e2}	
	C_{e2}	
K	S_{eK}	
	C_{eK}	

By considering the transition moment probability the selection rules and intensities of lines in the spectrum due to the perturbation of potential barrier can be arrived at.

$$(u)^{n''n'} = \int \psi_{n''} \mu \psi_{n'} \, d\tau$$

where $\psi_{n''}$ and $\psi_{n'}$ are the total wave function of the molecule which can be separated into vibrational and rotational wave functions. The dipole moment of the molecule has two components, one along the x axis and the other along the y axis. The selection rules are derived below.

$$\mu_x = \mu \cos \theta \qquad \mu_y = \mu \sin \theta$$

$$(u_x)^{n''n'} = \int \psi_{v''} \mu_x \psi_{v'} \, d\tau_v \int_0^{2\pi} \psi_{R''} \cos \theta \, \psi_{R'} \, d\theta$$

$$= (u_x)^{v''v'} \int_0^{2\pi} \psi_{R''} \cos \theta \, \psi_{R'} \, d\theta$$

where $\psi_{R''}$ and $\psi_{R'}$ are the Mathieu functions.

$$C_{en} = \sum_m A_m^n \cos m\theta$$

$$S_{en} = \sum_m B_m^n \sin m\theta$$

$C_{en} \rightarrow C_{en'}$

$$\int \psi_{R''} \cos\theta \, \psi_{R'} \, d\theta = \sum_{m} \sum_{m'} A_m^{\,n} A_{m'}^{\,n'}$$

$$\int_0^{2\pi} \cos m\theta \cos\theta \cos m'\theta \, d\theta$$

$$= \frac{1}{2} \sum_{m} \sum_{m'} A_m^{\,n} A_{m'}^{\,n'}$$

$$\int_0^{2\pi} \left\{ \cos (m+1)\theta + \cos (m-1)\theta \right\} \cos m'\theta \, d\theta$$

The integrand is non-vanishing under the condition

$$m+1 = m' \pm 0 \qquad \text{and} \qquad m-1 = m' \pm 0$$

So the selection rules for this transition are $\Delta m = \pm 1$.

$$(u_x)^{n''n'} = (u_x)^{v''v'} \; \frac{\pi}{2} \cdot \sum_{m} A_m^{\,n} \left(A_{m+1}^{\,n'} + A_{m-1}^{\,n'}\right)$$

$S_{en} \rightarrow S_{en'}$

$$\int_0 \psi_{R''} \cos\theta \, \psi_{R'} \, d\theta = \sum_m \sum_{m'} B_m^{\,n} B_{m'}^{\,n'}$$

$$\int_0^{2\pi} \sin m\theta \cos\theta \sin m'\theta \, d\theta$$

$$= \frac{1}{2} \sum_m \sum_{m'} B_m^{\,n} B_{m'}^{\,n'}$$

$$\int_0^{2\pi} \left\{ \sin (m+1)\theta + \sin (m-1)\theta \right\} \sin m'\theta \, d\theta$$

The integrand is non-vanishing when

$$m+1 = m' \pm 0 \qquad \text{and} \qquad m-1 = m' \pm 0$$

So the selection rule is $\Delta m = \pm 1$.

$$\int \psi_{R''} \sin\theta \, \psi_{R'} \, d\theta = \frac{1}{2}\pi \sum_m B_m^{\,n} \left(B_{m+1}^{\,n'} + B_{m-1}^{\,n'}\right)$$

$C_{en} \rightarrow S_{en'}$

$$\int \psi_{R''} \sin\theta\, \psi_{R'}\, d\theta = \sum_{m} \sum_{m'} A_m^n B_{m'}^{n'}$$

$$\int_0^{2\pi} \cos m\theta \sin\theta \sin m'\theta\, d\theta$$

$$= \frac{1}{2} \sum_{m} \sum_{m'} B_m^{\,n} A_{m'}^{\,n'}$$

$$\int_0^{2\pi} \left\{ \sin (m+1)\theta - \sin (m-1)\theta \right\} \sin m'\theta\, d\theta$$

The integrand is non-vanishing if $m+1 = m'$ and $m-1 = m'$. So the selection rule is $\Delta m = \pm 1$.

$$\int \psi_{R''} \sin\theta\, \psi_{R'}\, d\theta = \frac{1}{2}\pi \sum_{m} A_m^{\,n} \left(B_{m+1}^{\,n'} - B_{m-1}^{\,n'}\right)$$

$S_{en} \rightarrow C_{en'}$

$$\int \psi_{R''} \sin\theta \, \psi_{R'} \, d\theta = \sum_{m} \sum_{m'} B_m A_{m'}^{n'}$$

$$\int_0^{2\pi} \sin m\theta \sin\theta \cos m'\theta \, d\theta$$

$$= \frac{1}{2} \sum_{m} \sum_{m'} B_m A_{m'}^{n'}$$

$$\int_0^{2\pi} \left\{ \cos (m-1)\theta - \cos (m+1)\theta \right\} \cos m'\theta \, d\theta$$

The selection rules are $m-1 = m'$ and $m+1 = m'$

$$m = \pm 1$$

$$\int \psi_{R''} \sin\theta \, \psi_{R'} \, d\theta = \frac{1}{2}\pi \sum_{m} B_m \left(A_{m-1}^{n'} - A_{m+1}^{n'}\right)$$

The other transitions like $C_{en} \rightarrow S_{en'}$ and $S_{en} \rightarrow C_{en'}$ when x component of the dipole is considered and $C_{en} \rightarrow C_{en'}$ and $S_{en} \rightarrow S_{en'}$ when y component of the dipole is

considered are not allowed. The other permitted transitions are pictorially represented in Figure 16.

The line intensity will be the square of the dipole moment matrix element and a presentative case is

$$\left|(\mu_x)^{n''n'}\right|^2 = \left|(\mu_x)^{v''v'}\right|^2 \left\{ \frac{\pi}{2} \sum_m A_m{}^n (A_{m+1}{}^{n'} - A_{m-1}{}^{n'}) \right\}^2$$

The quantity within the parenthesis was computed on Alwac computer for all transition represented in Figure 16 with corresponding energy values, for different values of barrier. The sum of them for different barriers is tabulated in Table 23.

Table 23

Potential Barrier and Sum of Line Intensity

V_o	Sum of Line Intensities
2B	18.99800 $\lvert\mu\rvert^2_{v''v'}$
8B	18.998142 $\lvert\mu\rvert^2_{v''v'}$
16B	19.017926 $\lvert\mu\rvert^2_{v''v'}$
32B	19.068243 $\lvert\mu\rvert^2_{v''v'}$
80B	19.580203 $\lvert\mu^2\rvert_{v''v'}$

It is noticed as the barrier is increased the intensity gets piled up at the Q branch and in addition that the sum of all intensities is constant independent of the barrier. From this it can be concluded that as the barrier is further increased the entire intensity will be found at the Q branch. This state of affairs is a proof for the equation

$$\sum_{R}\sum_{R'}\sum_{F}\sum_{g}\sum_{g'} (\mu_g)^*_{v'v''} \, (\mu_g)_{v'v''} \, (\Phi_{Fg})^*_{R'R''}$$

$$(\Phi_{Fg})_{R'R''} = \sum_{g}\sum_{g'} (\mu_g)^*_{v'v''} \, (\mu_g)_{v'v''}$$

So the above theoretical calculation justifies that expression (5) could be used to analyze the spectrum of a molecule in solid state.

APPENDIX III

Table 24

Values of $\ln (I_o/I)_{max}/\ln (T_o/T)_{max}$ and $\Delta\nu^a_{1/2}/\Delta\nu^t_{1/2}$ in terms of $S/\Delta\nu^a_{1/2}$ and $\ln (T_o/T)_{max}$

$S/\Delta\nu^a_{1/2}$	$\ln (T_o/T)_{max}$	$\frac{\ln (I_o/I)_{max}}{\ln (T_o/T)_{max}}$	$\Delta\nu^a_{1/2}/\Delta\nu^t_{1/2}$
0.69	0.3888	1.72	1.99
0.755	0.4101	2.13	2.45
0.800	0.3848	2.65	3.04
0.842	0.3724	3.69	4.04
0.909	0.4168	4.67	4.95
0.923	0.3758	7.09	6.50
0.727	0.6050	1.98	2.21
0.754	0.6033	2.11	2.31
0.792	0.6070	2.52	2.69
0.822	0.5620	3.11	3.07
0.833	0.5836	3.31	3.47
0.740	0.8097	2.12	2.25
0.777	0.7450	2.15	2.34
0.784	0.8129	2.66	2.70
0.870	0.8217	3.80	3.44
0.687	1.010	1.68	1.85
0.755	0.9825	1.90	2.04
0.788	0.9700	2.12	2.26
0.852	0.9550	2.67	2.71
0.887	1.0800	3.44	3.10
0.900	1.0200	4.11	3.54

Table 24 - Cont.

$S/\Delta\nu^{a}_{1/2}$	$\ln (T_o/T)_{max}$	$\frac{\ln (I_o/I)_{max}}{\ln (T_o/T)_{max}}$	$\Delta\nu^{a}_{1/2}/\Delta\nu^{t}_{1/2}$
0.714	1.2075	1.72	1.76
0.752	1.1850	2.24	2.14
0.796	1.1600	2.34	2.36
0.833	1.1411	4.52	3.47
0.740	1.3887	2.12	2.00
0.784	1.4287	2.54	2.27
0.800	1.4200	3.35	2.72
0.819	1.4025	4.59	3.27
0.833	1.3679	6.52	4.051
0.695	1.5580	1.85	1.76
0.747	1.5950	2.20	2.05
0.785	1.5473	2.89	2.39
0.816	1.600	4.7	3.16
0.690	1.7920	1.86	1.72
0.750	1.8178	2.24	1.95
0.790	1.845	2.93	2.26
0.833	1.8202	6.235	3.468